2017

# Analysis of the ABC transporter CG31731 in engulfment during programmed cell death in the Drosophila melanogaster ovary

BOSTON UNIVERSITY

GRADUATE SCHOOL OF ARTS AND SCIENCES

Thesis

# ANALYSIS OF THE ABC TRANSPORTER CG31731 IN ENGULFMENT DURING PROGRAMMED CELL DEATH IN THE *DROSOPHILA MELANOGASTER* OVARY

by

**CLARISSA S. SANTOSO**

B.S., College of William and Mary, 2015

Submitted in partial fulfillment of the

requirements for the degree of

Master of Arts

2017

Approved by

First Reader _____

Kim McCall, Ph.D.

Professor of Biology

Second Reader _____

John L. Celenza, Ph.D.

Associate Professor of Biology

Third Reader _____

Francisco J. Naya, Ph.D.

Associate Professor of Biology

## ACKNOWLEDGMENTS

The research presented in this thesis was conducted in the laboratory of Dr. Kim McCall at Boston University. Foremost, I would like to thank Dr. Kim McCall for her support and guidance throughout my Master's education. Your mentorship was instrumental in my growth and success thus far as a scientist.

I am also incredibly grateful to members of the McCall lab. To Dr. Jeanne Peterson, I feel honored to have worked with you. Your wisdom and compassion have helped me grow professionally and personally. To Alla Yalonetskaya, Albert Mondragon, Johnny Elguero, and Alice Chirn, I truly appreciate all the help you have given me in lab and in life. I will cherish all the unforgettable memories we've shared. To Victoria Jenkins, Sandy Serizier, and Diane Lebo, thank you for your advice and assistance during my project. A special thank you to Dr. Tracy Meehan and Christopher Turlo, who performed the preliminary work which identified *CG31731* and *CG1718* as putative *ced-7* orthologs. To the undergraduates, thank you for your tireless effort in the lab.

This work would not have been possible without the help of several BU faculty members. Thank you to Dr. Todd Blute for help with microscopy and imaging. Thank you also to Dennis Batista and Peter Castellano. An immense thank you to Christina Honeycutt for handling all the administrative work.

Finally, I would like to thank my family. To Mama and Papa, thank you for always believing in me and supporting me. To Marshall and Teeffany, thank you for always encouraging me and helping me. To Patrick, thank you for always being patient with me and making me laugh. I am truly blessed to have you all in my life.

**ANALYSIS OF THE ABC TRANSPORTER CG31731**

**IN ENGULFMENT DURING PROGRAMMED CELL DEATH**

**IN THE *DROSOPHILA MELANOGASTER* OVARY**

**CLARISSA S. SANTOSO**

Boston University Graduate School of Arts and Sciences, 2017

Major Professor: Kim McCall, Professor of Biology

ABSTRACT

Programmed cell death (PCD) is an essential biological process in animal development and tissue homeostasis that is necessary to ensure the physiological well-being of the organism. During PCD, phagocytes facilitate the selective removal of excess, damaged, and potentially deleterious cells, in a multi-step engulfment process. Genetic studies in *Drosophila melanogaster*, *Caenorhabditis elegans*, and mammals have identified two evolutionarily conserved signal transduction pathways that act redundantly to regulate engulfment: the CED-1/-6/-7 and CED-2/-5/-12 pathways. Of these cell death (CED) proteins, the ABC transporter CED-7 is the only protein reported to be required in both the engulfing cell and the dying cell. However, its function in the cell death process remains the most enigmatic and the *ced-7* ortholog previously has not been identified in *Drosophila*. Homology searches revealed a family of putative *ced-7* orthologs that encode transporters of the ABCA family in *Drosophila*. To determine which of these genes functions similarly to *ced-7/ABCA1* in PCD, we analyzed their engulfment function

in oogenesis, during which 15 germ cells in each egg chamber undergo programmed cell death and are removed by neighboring phagocytic follicle cells. It has been shown that genetically knocking down individual engulfment genes results in inefficient clearance of the germ cells, which then persist in late-stage egg chambers. Only two of the putative *ced-7/ABCA1* genes are expressed significantly in the ovary, *CG31731* and *CG1718*, and we have characterized these genes using transposon insertions, deficiencies, and RNAi knockdowns. Our genetic analysis reveals that *CG31731* is necessary for germ cell clearance in the *Drosophila* ovary. Immunostaining shows that genetically knocking down *CG31731* results in uncleared germ cells which persist in late-stage egg chambers. Altogether, our findings suggest that CED-7/ABCA1/CG31731 play evolutionarily conserved roles during engulfment.

## TABLE OF CONTENTS

## LIST OF TABLES

## LIST OF FIGURES

## LIST OF ABBREVIATIONS

| | |
|---|---|
| ATP | Adenosine triphosphate |
| BSA | Bovine serum albumin |
| C | Celsius |
| *C. elegans* | *Caenorhabditis elegans* |
| $Ca^{2+}$ | Calcium |
| CED | Cell death abnormal |
| $CO_2$ | Carbon dioxide |
| DAPI | 4',6-diamidino-2-phenylindole dichloride |
| Dcp-1 | Death caspase-1 |
| Diap1 | *Drosophila* inhibitor of apoptosis-1 |
| Dlg | Discs large |
| DNA | Deoxyribonucleic acid |
| DOCK | Dedicator of cytokinesis |
| *Drosophila* | *Drosophila melanogaster* |
| DRSC | *Drosophila* Resource Stock Center |
| DYN-1 | Dynamin-1 |
| GEF | Guanine nucleotide exchange factor |
| GFP | Green fluorescent protein |
| *GR1* | *GR1-GAL4,G00089* |
| GTPase | Guanosine triphosphatase |

| | |
|---|---|
| Hid | Head involution defective |
| IAP | Inhibitor of apoptosis |
| mCD8 | Murine CD8 |
| Mi{MIC} | Minos-mediated integration cassette |
| miR | MicroRNA |
| mL | Milliliter |
| mRNA | Messenger RNA |
| *nanos* | *nanos-GAL4* |
| NGS | Normal goat serum |
| PBac | *PiggyBac* element |
| PBNG | Phosphate buffered saline with Triton X-100, BSA and NGS |
| PBT | Phosphate buffered saline with Triton X-100 |
| PCD | Programmed cell death |
| P{EPgy2} | P-element-based EY transposon |
| *PG150* | *PG150-GAL4* |
| PN | Persisting nurse cell nuclei |
| PtdSer | Phosphatidylserine |
| RHG | *reaper, hid, grim* |
| RNA | Ribonucleic acid |
| RNAi | RNA interference |
| SEM | Standard error of the mean |
| SH | Src Homology |

| | |
|---|---|
| Su(Hw) | Suppressor of *Hairy-wing* |
| TRiP | Transgenic RNAi Progect |
| TUNEL | Terminal deoxynucleotidyl transferase dUTP nick-end labeling |
| UAS | Upstream activation sequence |
| μL | Microliter |
| VDRC | Vienna *Drosophila* Resource Center |

# CHAPTER 1: INTRODUCTION

## 1.1 Programmed cell death

Programmed cell death (PCD) is an essential biological process that serves several physiological functions during development and homeostasis including the sculpting of tissues and organs, the regulation of cell turnover to balance cell proliferation, and the removal of damaged or deleterious cells (Jacobson et al., 1997; Elliott and Ravichandran, 2010; Fuchs and Steller, 2011). PCD is important in a variety of cells and tissues and abnormal regulation of PCD has been implicated in a wide range of disease pathogenesis including developmental malformations, physiological disorders, autoimmunity, neurodegeneration, and cancer (Elliott and Ravichandran, 2010; Fuchs and Steller, 2011).

The term "programmed cell death" was initially used to describe cell deaths that occur in predictable places and at predictable times during development (Jacobson et al., 1997). The current use of the term has expanded to refer to intentional cell deaths that occur in a controlled and regulated manner via the activation of an inherent death program (Jacobson et al., 1997; Fuchs and Steller, 2011). Cells undergoing PCD have been shown to proceed through four highly regulated steps: (1) specification of the dying fate, (2) execution of cell death, (3) recognition and engulfment by phagocytes, and (4) degradation inside the engulfing cells (Mangahas and Zhou, 2005). Although diverse signals can induce PCD, genetic and molecular studies in nematodes, arthropods, and mammals have identified a set of evolutionarily conserved cell death pathways and genes

that regulate each step (Jacobson et al., 1997; Elliott and Ravichandran, 2010; Fuchs and Steller, 2011).

The significance and mechanisms of PCD continue to be the subject of intense investigation and review. To date, over a dozen cell death modalities have been described, including apoptosis, necrosis, autophagic cell death, and phagoptosis, each distinguished on the basis of distinct morphological, molecular, and genetic features (Kroemer et al., 2009).

### 1.1.1 Apoptosis

Apoptosis represents the best-studied form of PCD. In apoptosis, a cell deliberately commits suicide in response to developmental death signals or physiological stress, such as oxidative stress and nutrient deprivation (Steller, 2008). When a cell commits to apoptosis, the apoptotic cell death pathway activates pro-apoptotic proteins such as cysteine aspartyl proteases (caspases), and inhibits anti-apoptotic proteins such as inhibitor of apoptosis (IAP) proteins. In healthy cells, IAPs prevent the activation of caspases. In apoptotic cells, the expression of IAP antagonists relieves caspases from suppression by IAPs and thereby allows their activation. Caspases serve as key executioners of apoptosis that specifically cleave proteins to dismantle the cell (Fuchs and Steller, 2011; Fuchs and Steller, 2015). As a result, apoptotic cells display characteristic morphological changes, such as nuclear chromatin condensation, DNA fragmentation, cell volume shrinkage, and plasma membrane blebbing (Kroemer et al., 2009). During the final steps of apoptosis, the cell corpse is swiftly engulfed and degraded by phagocytic cells before any leakage of the cell contents occurs (Jacobson et

al., 1997; Steller, 2008). Over time, apoptotic cells that are not promptly cleared can lose their membrane integrity and become secondarily necrotic (Elliot and Ravichandran, 2010).

### 1.1.2 Necrosis/necroptosis

Historically, necrosis has been described as a form of accidental cell death which results in the uncontrolled and unregulated lysis of the cell (Kroemer et al., 2009). However, accumulating evidence suggests that necrosis may be finely regulated by a set of signal transduction pathways and catabolic mechanisms. Recent research has identified several regulatory genes and small molecules, such as receptor interacting protein kinases (RIPK1 and RIPK3) and necrostatins, and demonstrated that necrosis can proceed through a series of defined molecular and morphological events (Kroemer et al., 2009; Fuchs and Steller, 2011; Fuchs and Steller, 2015). It is speculated that the necrotic cell death pathway is linked to the apoptotic cell death pathway, as it becomes activated when the lack of caspase activity fails to activate the apoptotic signaling pathways (Fuchs and Steller, 2015). "Necroptosis" is now recognized as a controlled and regulated form of necrotic PCD characterized by chromatin clumping and organelle swelling, followed by cell volume swelling leading to rupturing of the plasma membrane (Kroemer et al., 2009; Fuchs and Steller, 2015). The subsequent release of intracellular contents, including toxic levels of reactive oxygen species and inflammatory cytokines, into the extracellular space can provoke a strong inflammatory response (Jacobson et al., 1997; Elliot and Ravichandran, 2010; Fuchs and Steller, 2015). Pertinently, chronic inflammation has

been implicated as the impetus for a variety of autoimmune disorders and tumorigenesis (Elliot and Ravichandran, 2010).

### 1.1.3 Autophagic cell death

The word "autophagy" derives from Ancient Greek, meaning "self-devouring". Befittingly, autophagy is the cell's intracellular degradation system, regulated by a series of autophagy (ATG) genes. In autophagy, double-membraned isolation vesicles surround and sequester targeted cytoplasmic components in the cell, forming an autophagosome which fuses with lysosomes to become an autolysosome, to degrade the sequestered cellular contents. (Kroemer et al., 2009; Mizushima and Komatsu, 2011; Nelson and Baehrecke, 2014; Fuchs and Steller, 2015). The role of this catabolic process is highly context-dependent and has been shown to serve as both a pro-survival and pro-death mechanism. Induction of autophagy has been mainly observed as an adaptive response to stress, such as nutrient deprivation, allowing cells to consume their digested components for energy, and recycle amino acids to promote cell survival (Mizushima and Komatsu, 2011; Fuchs and Steller, 2015). Conversely, recent studies have also demonstrated that ATG genes are required to promote certain cell deaths, for example in the *Drosophila* midgut and salivary gland. Interestingly, during PCD of the salivary gland cells, the autophagic cell death pathway was observed to function in parallel with the apoptotic cell death pathway (Kroemer et al., 2009; Nelson and Baehrecke, 2014; Fuchs and Steller, 2015). However, in contrast to apoptosis, autophagic cells self-degraded and cleared with no association with phagocytic cells (Kroemer et al., 2009; Nelson and Baehrecke, 2014).

### 1.1.4 Phagoptosis

Traditionally, PCD has been regarded as a cell-autonomous suicide program in which a cell controls its own demise. Recently, several non-autonomous forms of PCD have been described in which the death of a cell is extrinsically regulated by another cell. An intriguing example of non-autonomous PCD is phagoptosis, in which a phagocytic cell devours and directly causes the death of a cell. The cell death process requires the phagocytic machinery and inhibition of phagocytosis prevents the cell death. Phagoptosis is a relatively new concept and thus the mechanism by which phagocytic cells can "kill" other cells has not been fully elucidated. It has been speculated that as in engulfment, phagosomes in the phagocytic cell containing the viable cell may fuse with lysosomes to degrade the phagocytosed cell (Brown and Neher, 2012).

## 1.2 Engulfment

Engulfment represents an important step in PCD that is necessary for the selective removal of cells fated to die. The process prevents the accumulation of cell corpses and ensures that dying or dead cells are removed before they release their harmful cellular contents (Mangahas and Zhou, 2005; Fullard et al., 2009; Elliot and Ravichandran, 2010). Defective engulfment and clearance mechanisms have been implicated as important contributing factors to the pathogenesis of inflammatory diseases such as chronic obstructive pulmonary disease, autoimmune diseases such as lupus, and neurodegenerative diseases such as Alzheimer's disease (Elliot and Ravichandran, 2010).

The engulfment step is generally performed by "professional" phagocytes, such as mammalian macrophages, whose primary function is the phagocytosis of dying cells and

cell corpses. In areas where professional phagocytes have little to no access, neighboring cells can function as "non-professional" phagocytes to remove these unnecessary cells (Mangahas and Zhou, 2005; Fullard et al., 2009; Elliott and Ravichandran, 2010). For example, *C. elegans* do not have professional phagocytes and engulfment is accomplished by neighboring cells including epidermal and muscle cells (Mangahas and Zhou, 2005; Fullard et al., 2009). Current evidence suggests that both professional and non-professional phagocytes carry out the same steps in the engulfment process (Elliott and Ravichandran, 2010).

The engulfment process can be described as a succession of 3 steps: (1) recruitment of phagocytes to the dying cells, (2) recognition of the dying cells by the phagocytes, and (3) internalization of the cell corpse by the phagocytes (Figure 1.1). In the early stages of PCD, dying cells secrete "find-me" signals, soluble chemoattractants that are sensed by and promote chemotaxis of motile phagocytes to the dying cells. Once in proximity of the dying cells, phagocytes can recognize and bind "eat-me" signals, such as phosphatidylserine (PtdSer), on the surface of dying cells. The physical engagement initiates a signal transduction cascade within the phagocytes that stimulates cytoskeletal rearrangements and extensions of a phagocytic cup around the cell corpse for its internalization and engulfment (Fullard et al., 2009; Elliott and Ravichandran, 2010). The entire process is tightly regulated by a common engulfment mechanism that has been evolutionarily conserved from nematodes to humans.

### 1.2.1 Identification of engulfment genes

Initial studies in *C. elegans* identified seven *ced* (cell death abnormal) genes: *ced-1, ced-2, ced-5, ced-6, ced-7, ced-10, ced-12,* that are involved in the engulfment process. Mutations in any of these genes in the phagocytic cell negatively affect engulfment and result in the accumulation of persisting cell corpses (Kinchen et al. 2005; Mangahas and Zhou, 2005; Fullard et al., 2009). Subsequent studies in *Drosophila,* mice, and humans indicated that these seven genes and their roles in engulfment are evolutionarily conserved (Mangahas and Zhou, 2005; Fullard et al., 2009).

Extensive genetic and molecular analyses in *C. elegans* suggest that these genes act in two parallel and partially redundant signaling pathways: *ced-1/-6/-7* and *ced-2/-5/-12,* that converge on CED-10 (Figure 1.2) (Kinchen et al., 2005; Mangahas and Zhou, 2005; Fullard et al., 2009). Single or double mutants within the same pathway display weaker phenotypes than double mutants between the two pathways. Whereas double mutants within the same pathway show engulfment defects no more severe than that of the stronger single mutant, double mutants between the two pathways show engulfment defects much more severe than that of either of the single mutants (Mangahas and Zhou, 2005). Moreover, double mutants between the two pathways show similar engulfment defects to that of *ced-10* mutants, and can be genetically rescued, with a reduction in the number of persisting cell corpses, following *ced-10* induction (Kinchen et al., 2005). Triple mutants do not display a stronger phenotype than any of the double mutants, suggesting that none of the seven genes act in a third pathway (Ellis et al., 1991). The

results of these studies are consistent with the model that the engulfment genes act in two parallel and partially redundant engulfment pathways that converge on CED-10.

### 1.2.2 *ced-10 (Rac1)*

*ced-10* encodes a homolog of the human Rac1, a small GTPase responsible for the cytoskeletal rearrangements that allow for the internalization of the cell corpse (Reddien and Horvitz, 2000). Consistent with the notion that CED-10 is required for cytoskeleton reorganization, *ced-10* mutants suffer from cell migration defects (Reddien and Horvitz, 2000; Kinchen et al., 2005). The Rac family of small GTPases has been demonstrated to act as molecular switches on the plasma membrane to regulate actin cytoskeleton rearrangements. In its inactive state, Rac-GDP is sequestered in the cytoplasm with minimal GTPase activity. Upon guanine exchange factor (GEF)-mediated GDP-to-GTP exchange, Rac-GTP exposes a prenyl group that anchors the enzyme to the plasma membrane. Active Rac-GTP catalyzes the local reorganization of the actin cytoskeleton to facilitate extensions of the plasma membrane (Chimini and Chavrier, 2000).

### 1.2.3 *ced-2/-5/-12* (*CrkII/DOCK180/ELMO*) pathway

The *ced-2/-5/-12* pathway has been relatively well-characterized since the pathway is also essential for multiple cell migration events (Reddien and Horvitz, 2000; Gumienny et al., 2001). Respectively, *ced-2, ced-5, ced-12* represent the *C. elgeans* homologs of the mammalian CrkII*, DOCK180, ELMO* genes. Sequence analyses indicates that *ced-2/CrkII* encodes an adaptor protein possessing several Src homology (SH) domains, SH2 and SH3; *ced-5/DOCK180* encodes a Rac-GEF possessing a DOCK homology region (DHR); and *ced-12/ELMO* encodes another adaptor protein, possessing

a proline-rich SH3-binding domain and a Pleckstrin homology (PH) domain (Mangahas and Zhou, 2005) .

Biochemical studies show that the SH3 domains of CED-2/CrkII can physically interact with CED-5/DOCK180. Furthermore, CED-5/DOCK180 and CED-12/ELMO can form a complex independent of CED-2/CrkII activity, and function together as a bipartite GEF to activate downstream CED-10/Rac1. While CED-12/ELMO alone does not possess any obvious catalytic domain, its PH domain was observed to possess Rac-GEF activity *in vitro* when cotransfected with CED-5/DOCK180 (Gumienny et al., 2001; Zhou et al., 2001; Brugnera et al., 2002; Lu et al., 2004). Additionally, assays performed using cultured mammalian cells revealed the formation of a CrkII-DOCK180-ELMO trimeric complex, most likely through DOCK180 bridging CrkII and ELMO (Gumienny et al., 2001). However, it is not clear whether the trimeric complex cooperatively functions to activate Rac1 or whether CrkII only transiently interacts with the DOCK180-ELMO complex. By analogy, these assays suggest that in *C. elegans*, CED-2 similarly associates with CED-5–CED-12 to form a trimeric complex upstream of CED-10 activation.

It has been proposed that CED-2 recruits the CED-5–CED-12 GEF complex to the plasma membrane where it can facilitate GTP-loading onto CED-10 to promote cytoskeletal rearrangements (Mangahas and Zhou, 2005). Consistent with this hypothesis, the mammalian DOCK180 DHR domain can bind phosphatidylinositols (PtdIns), specifically PtdIns(3,5)P2 and PtdIns(3,4,5)$P_3$, on the inner leaflet of the plasma membrane (Côté et al., 2005). While the *C. elegans* CED-5 DHR domain does not

detectably bind to any phospholipids, the CED-12 PH domain, which is required for GEF function with CED-5 (Gumienny et al., 2001), is observed to bind PtdIns(3,5)P2 and PtdIns(3,4,5)$P_3$ (Neukomm et al., 2011). Both the DOCK180 DHR domain and CED-12 PH domain is necessary for cytoskeletal rearrangements at the plasma membrane, suggesting that they mediate a PtdIns-dependent translocation of the GEF complexes to the plasma membrane for activation of CED-10/Rac1 and subsequent reorganization of the actin cytoskeleton (Côté et al., 2005; Neukomm et al., 2011).

Several upstream activators of the CED-2/-5/-12 pathway have been identified, including integrin α (INA-1). INA-1 is an engulfment receptor that recognizes dying cells and indirectly transduces the engulfment signal to the CED-2/-5/-12 pathway. SRC-1, a non-receptor tyrosine kinase, likely serves as the bridging molecule linking INA-1 to CED-2, as observed by SRC-1 binding to both the INA-1 cytoplasmic domain and CED-2. Moreover, INA-1 and SRC-1 colocalize at the phagocytic cup, suggesting that upon recognizing dying cells, INA-1 with SRC-1 recruits the CED-2–CED-5–CED-12 signaling module to promote activation of CED-10, which leads to the cytoskeletal rearrangements necessary for formation of a phagocytic cup (Hsu and Wu, 2010).

In mammalian cell culture, integrin $\alpha_v\beta_5$ was similarly implicated as an upstream receptor that indirectly transduces extracellular signals to the CrkII-DOCK180-ELMO Rac-activating complex through $p130^{cas}$, which interacts with CrkII (Albert et. al., 2000). These similarities between the *C. elegans* and mammalian engulfment pathways confirm an evolutionarily conserved mechanism that regulates cytoskeletal reorganization in phagocytic cells.

### 1.2.4 *ced-1/-6/-7* (*MEGF10/GULP/ABCA1*) pathway

The *ced-1/-6/-7* pathway is more complex and less understood. To begin with, several mammalian homologs have been proposed for some genes: *MEGF10, JEDI,* and *LRP1* for *ced-1*; *GULP* for *ced-6*; *ABCA1* and *ABCA7* for *ced-7* (Mangahas and Zhou, 2005; Kinchen and Ravichandran, 2007). These genes have been shown to differentially mediate multiple downstream activities, including CED-10/Rac1 activation, PtdSer exposure, and intracellular vesicle delivery (Hamon et al., 2000; Kinchen et al., 2005; Yu et al., 2006), although some of these activities are controversial (Mangahas and Zhou, 2005; Mapes et al., 2012). Until very recently, no upstream activating signals had been described. The lack of collective data has made it difficult to define the precise role and mechanism of this evolutionarily conserved engulfment pathway.

The best characterized gene in the pathway, *ced-1*, encodes a single-pass transmembrane receptor with a large extracellular region boasting 16 tandem copies of EGF-like repeats, and an intracellular region containing a functionally necessary SH2-binding and PTB-binding domain (Zhou et al., 2001). Its mammalian orthologs, MEGF10 and JEDI, display extensive structural and sequence similarities to CED-1 throughout their entirety, while LRP1 presents an extracellular architecture that is different from that of CED-1 (Mangahas and Zhou, 2005; Scheib et al., 2012). Nonetheless, MEGF10, JEDI, and LRP1 serve as transmembrane scavenger receptors in phagocytic cells, suggesting that CED-1 may similarly function to recognize signals on the surface of dying cells to facilitate engulfment (Zhou et al., 2001; Scheib et al., 2012). Indeed, CED-1/MEGF10/JEDI have been observed to localize to the surface membrane

of phagocytic cells and accumulate at the phagocytic cup surrounding the dying cells (Zhou et al., 2001; Hamon et al., 2006; Scheib et al., 2012).

The mechanism of CED-1/MEGF10 clustering around the cell corpse requires CED-7/ABCA1 (Zhou et al., 2001; Hamon et al., 2006), ATP-binding cassette (ABC) transporter proteins. In *C. elegans*, CED-7 activity is required in both the phagocytic cell and the dying cell for engulfment (Wu and Horvitz, 1998), which has made it complicated to determine exactly where in the signaling pathway CED-7 acts to promote CED-1 clustering. Moreover, the signaling mechanisms and functional interactions of CED-7 remain elusive. It is not yet known whether ABCA1 is also expressed in dying cells, but in mammalian cell culture, induction of ABCA1 in non-phagocytic cells is sufficient to confer engulfment ability *in vitro* (Hamon et al., 2000). Section 1.3 will discuss CED-7/ABCA1 in further detail.

Recently, TTR-52, a secreted transthyretin-like protein, was also observed to cluster around dying cells and also promote CED-1 clustering at the phagocytic cup. Secreted TTR-52 was further demonstrated to facilitate CED-1 recognition of PtdSer on the surface of dying cells by specifically binding to PtdSer and the extracellular domain of CED-1 (Wang et al., 2010), suggesting TTR-52 serves as a bridging molecule for CED-1-mediated engulfment of dying cells. Consistent with this model, normal cells ectopically exposing PtdSer were phagocytosed in a *ttr-52*- and *ced-1*-dependent manner (Darland-Ransom et al., 2008; Wang et al., 2010). However, *ttr-52* mutants only partially block the clustering of CED-1 around dying cells and show a weaker engulfment defect compared to *ced-1* mutants (Wang et al., 2010), suggesting that there are likely additional

bridging molecules and/or “eat-me” signals that could mediate the recognition of apoptotic cells by CED-1.

CED-1 has also been observed to interact with CED-6, a PTB-domain containing adaptor protein. Specifically, the cytoplasmic region of CED-1/LRP1 was demonstrated to physically associate with the PTB domain of CED-6/GULP (Su et al., 2002). CED-6 likely acts as a signaling adaptor downstream of CED-1 and CED-7, since over-expression of *ced-6* in a *ced-1* or *ced-7* mutant background rescues the associated engulfment defects (Liu and Hengartner, 1998). Additionally, mutations in *ced-6* do not disrupt CED-1 clustering or recognition of dying cells, which requires *ced-1* and *ced-7* (Zhou et al., 2001), but do prevent downstream activities including pseudopod extensions and phagocytic cup formation (Yu et al., 2006). While the immediate downstream molecular activities of CED-6 have not been elucidated, these observations lead us to speculate that CED-6 functions to transduce signals from CED-1 to CED-10 to promote cytoskeletal rearrangements.

Multiple cellular processes must occur in phagocytic cells for the successful engulfment of cell corpses including cytoskeletal rearrangements, membrane extensions, and membrane closure. The *ced-1/-6/-7* pathway has also been implicated in promoting membrane extensions at the growing phagocytic cup via another GTPase, Dynamin (DYN-1). DYN-1 was observed to localize to the growing phagocytic cup in a *ced-1-, ced-6-, ced-7*-dependent manner (Yu et al., 2006) to facilitate intracellular recruitment and fusion of endosomes to the plasma membrane (Yu et al., 2008), likely to provide lipid and protein materials for pseudopod extensions. Live imaging studies in *C. elegans*

have also observed a role for CED-1, CED-6, and DYN-1 signaling in promoting cell corpse degradation via RAB-7, a small GTPase that is involved in endocytic vesicle trafficking. RAB-7 localizes to phagosome membranes and is required for the recruitment and fusion of lysosomes to phagosomes for cell corpse degradation (Yu et al., 2008). In support of a role for the *ced-1/-6/-7* pathway in degradation, other studies have shown that defects in corpse degradation pathways also inhibit engulfment (Kinchen and Ravichandran, 2007).

Altogether, these observations suggest that the *ced-1/-6/-7* pathway may be involved in multiple steps during PCD including engulfment and degradation of the cell corpse. Nevertheless, questions remain including what are the upstream and downstream signaling activities of CED-6 and CED-7. Much more research is needed to clarify the roles and molecular mechanisms of this important signaling pathway in engulfment.

### 1.2.5 Engulfment in *Drosophila melanogaster*

In *Drosophila*, the role of the *ced-1/-6/-7* and *ced-2/-5/-12* engulfment pathways appear to be conserved in *draper/Ced-6* and *Crk/mbc/Ced-12*. With the exception of the *ced-7* homolog, which has not been identified, these *Drosophila* genes have been shown to act in phagocytic cells to promote engulfment in several *in vivo* systems including phagocytic follicle cells, engulfing glia, and hemocytes (Manaka et al., 2004; Awasaki et al., 2006; MacDonald et al., 2006; Timmons et al., 2016). Several other components of the engulfment machinery have also been identified in *Drosophila*.

Draper is observed to localize to the surface membrane of phagocytic cells, facing the dying cells. Whether Draper recognizes PtdSer exposed on the surface of dying cells

is under debate (Manaka et al., 2004; Tung et al., 2013). Pretaporter, an endoplasmic reticulum protein also exposed on the surface of dying cells, has been proposed as another "eat-me" signal recognized by Draper (Kuraishi et al., 2009). Six Microns Under (SIMU), another transmembrane receptor, was similarly demonstrated to bind dying cells upstream of Draper (Kurant et al., 2008).

The intracellular adapter protein Ced-6 has been show to co-localize and genetically interact with the PTB-binding domain of Draper (Awasaki et al., 2006; Kuraishi et al., 2009). However, *Ced-6* is not required in several engulfment processes including Wallerian degeneration (Lu et al., 2017) and developmental germ cell death (Timmons, 2015). Instead, Draper-mediated signaling events during engulfment in some systems seem to be dependent on Shark, a cytosolic tyrosine kinase observed to also interact with the cytosolic region of Draper (Ziegenfuss et al., 2008). Draper has also been implicated to regulate downstream Dynamin and Rab GTPases, namely Shibire, Rab5 and Rab7, for phagosome maturation and cell corpse degradation (Kurant et al., 2008; Etchegaray et al., 2016; Meehan et al., 2016; Timmons et al., 2016).

A GEF complex formed by DRK–DOS–SOS has been shown to act downstream of Draper to activate the small GTPase Rac1 (Lu et al., 2014). Similarly, in a parallel pathway to Draper, the GEF complex formed by Crk–MBC–Ced-12 also activates Rac1 (Geisbrecht et al., 2008; Ziegenfuss et al., 2012; Lu et al., 2014). Currently, the Crk/MBC/Ced-12 engulfment pathway remains relatively poorly characterized, though integrins have recently been proposed as an upstream engulfment receptor of the pathway (Meehan et al., 2016). Additionally, Ced-12 was found to be required for border cell

migration during oogenesis, and therefore *Ced-12* deficiency mutants are sterile (Geisbrecht et al., 2008, Timmons et al., 2016).

### 1.3 CED-7/ABCA1

The *C. elegans* CED-7 engulfment protein has become something of an enigma. Studies with CED-7 have not been able to address its molecular function during engulfment. The mammalian functional equivalent remains controversial as ABCA1 (Luciani and Chimini, 1996) and recently ABCA7 (Jehle et al., 2006) have been proposed as putative CED-7 mammalian homologs. Both ABCA proteins have been shown to be required in the engulfment of cell corpses, though the potential function of ABCA1 in engulfment has been better characterized. The *Drosophila* homolog of CED-7/ABCA1 has not been identified.

#### 1.3.1 Functional Characterization of CED-7/ABCA1

The *ced-7/ABCA1/ABCA7* genes encode members of the ABCA subfamily of ABC transporters proteins (Wu and Horvitz, 1998; Luciani and Chimini, 1996; Jehle et al., 2006). ABC transporters are known to localize to membranes and utilize the energy from ATP hydrolysis to drive the translocation of various substrates. Mutations that abolish the catalytic function of CED-7 or ABCA1/7 in phagocytic cells cause engulfment defects that lead to the accumulation of cell corpses *in vivo* (Luciania and Chimini, 1996; Wu and Horvitz, 1998; Hamon et al., 2000; Jehle et al., 2006), identifying a role for these transporters in engulfment. Moreover, the induced expression of full-length ABCA1 in non-phagocytic cell cultures confers engulfment ability (Hamon et al., 2000). Consistent with a role for ABCA1 during PCD, the protein is highly expressed on

the surface of active macrophages in the hindlimb interdigital PCD zones of developing mice (Luciania and Chimini, 1996; Hamon et al., 2000).

Deficiencies or loss-of-function mutations in *ced-7/ABCA1* exhibit only transient accumulation of cell corpses in development without any embryonic lethal consequences, but impair reproductive capability and lifespan in adults (Wu and Horvitz, 1998; Mangahas and Zhou, 2005; Hamon et al., 2000). In *ced-7* deficient mutants, cell corpses persist in developing embryos only until hatching, and then the cell corpses are rapidly cleared (Wu and Horvitz, 1998). This delay in cell corpse clearance is similarly observed in the limb bud of ABCA1-deficient developing mice, without any significant physiological consequences. However, homozygous ABCA1-deficient adult females suffered from abnormal placental development and did not produce litters. ABCA1 was found to be normally expressed at high levels in the placenta, where it appears to be important for fertility. Additionally, 4-weeks post-natal ABCA1-deficient mice exhibited a <25% survival rate, due to deep perivisceral hemorrhages (Hamon et al., 2000). Thus, functional CED-7/ABCA1 is necessary to ensure normal physiology and survival in adulthood.

CED-7/ABCA7 localizes to the surface membrane and is required for efficient cell clearance (Wu and Horvitz, 1998; Hamon et al., 2000). Intriguingly, whereas ABCA1 is clearly required in phagocytic cells (Hamon et al., 2000), genetic studies in *C. elegans* indicate CED-7 is required in both the phagocytic and the dying cells for efficient engulfment (Wu and Horvitz, 1998). Whether ABCA1 is expressed *in vivo* in dying cells has not been determined, although ABCA1 has been shown to be able to promote several

events in both the engulfing and dying cells *in vitro* (Hamon et al., 2000). Currently, CED-7 is the only protein reported to be required in both cells, and may provide a link between the cell death execution pathway and the engulfment pathway (Mangahas and Zhou, 2005).

Several separate studies support the idea that CED-7/ABCA1 function in both phagocytic cells and dying cells is important for cell corpse recognition by phagocytes (Hamon et al., 2000; Zhou et al., 2001; Yu et al., 2006). *In vitro* studies in red blood cells and thymocytes have demonstrated a requirement for ABCA1 in PtdSer exposure following an apoptotic stimulus. Prior to an apoptotic stimulus, wild-type and *ABCA1*-deficient cells display a similar asymmetrical distribution of PtdSer across the membrane bilayer. Following an apoptotic stimulus such as $Ca^{2+}$ stress or γ-irradiation, a two- to three-fold reduction in PtdSer exposure was observed in *ABCA1*-deficient cells compared to wild-type ABCA1-expressing cells. Phosphatidylcholine distribution was not affected in these experiments (Hamon et al., 2000). These observations suggest that ABCA1 can specifically promote the exposure of PtdSer in dying cells, which is necessary for cell corpse recognition by phagocytic cells.

The sequence similarity between CED-7 and ABCA1 suggests that CED-7 may also act to promote PtdSer exposure on the surface of dying cells. This hypothesis is consistent with the ability of ABC transporters to serve as floppases, which can specifically direct the externalization of lipids, for example PtdSer (Daleke, 2003). However, in engulfment defective *ced-7* mutants, PtdSer was clearly detected on the

surface of persisting cell corpses (Mapes et al., 2012), indicating that CED-7 is not required for the exposure of PtdSer *in vivo* in *C. elegans*.

Alternatively, CED-7 has been proposed to mediate the exocytosis of vesicles containing engulfment recognition signals from dying cells to phagocytic cells. Immuno-electron micrograph images show the presence of extracellular vesicles in wild-type *C. elegans*, which are absent in *ced-7* mutants and dramatically reduced in *ttr-52*-mutants, lacking the TTR-52 bridging molecule which can facilitate CED-1 recognition of PtdSer (Mapes et al., 2012). Some of the extracellular vesicles were observed to contain PtdSer and the event is accompanied by a loss of PtdSer on the surface of dying cells and the acquisition of PtdSer on the phagocyte membrane. These observations suggest that the vesicles are exocytosed from dying cells and acquired by phagocytic cells. The presence of PtdSer on the surface of phagocytic cells also requires the transmembrane and extracellular domains of CED-1 (Mapes et al., 2012). Thus we speculate a model wherein CED-7 in dying cells may function to exocytose vesicles, some containing TTR-52 targeted for exocytosis, and CED-1 at the phagocytic membrane may provide the docking site for vesicle fusion. The dramatic reduction, but not absence of, vesicles in *ttr-52* mutants suggests that CED-7 likely mediates the exocytosis of other molecules targeted for exocytosis.

This potential role for CED-7/ABCA1 in vesicle exocytosis is consistent with the ability of ABCA transporters to mediate the efflux of lipids and other materials from the plasma membrane (Vasiliou et al., 2009). In fact, the forced expression of ABCA1 has been shown to promote the shuttling of certain phospholipids and cholesterol to apo-AI to

form high density lipoproteins (HDL) (Hamon et al., 2000). In humans, *ABCA1*-deficiency is implicated in Tangier disease, a recessive disorder characterized by the lack of HDLs due to a defect in cellular release of lipids and cholesterol (Vasiliou et al., 2009). The over-expression of ABCA7 in cell culture has also been shown to mediate phospholipid efflux, but not cholesterol, to apo-AI (Wang et al., 2003). Interestingly, LRP1 and GULP are also implicated in cholesterol metabolism, suggesting a potentially conserved role for LRP1/GULP/ABCA1 (Hengartner, 2001).

The proposed function of CED-7 in shuttling vesicles from dying cells to phagocytes may explain the requirement for CED-7 in CED-1 clustering at the phagocytic cup (Zhou et al., 2001), where CED-1 may facilitate fusion of the shuttled vesicles to the phagocytic cell membrane. However, in mammalian cell cultures, where the expression of ABCA1 in dying cells has not been determined *in vivo*, the redistribution of MEGF10 at the phagocytic cup is sensitive to the presence of ABCA1 in phagocytic cells (Hamon et al., 2006). It has been proposed that CED-7/ABCA1 in phagocytic cells may function to generate lipid domains, such as lipid rafts at the phagocytic cup, to which CED-1 is recruited. This notion remains highly speculative and more studies need to be undertaken to validate this hypothesis.

CED-7/ABCA1 have also been implicated in intracellular vesicle trafficking. Recall, studies in *C. elegans* have demonstrated a role for CED-7 in intracellular endosome trafficking with DYN-1 and RAB7, which respectively facilitate the delivery of vesicles to the growing membrane for pseudopod extensions and to phagosomes for phagolysosomal maturation (Yu et al., 2006; Yu et al., 2008). Consistent with these

events, ABCA1 is known to mediate the transport of lipids from the Golgi to the plasma membrane, and was observed to localize to the plasma membrane, the Golgi stacks, and endolysosomal vesicles (Hamon et al 2000), cellular compartments which are involved in pseudopod extensions and phagolysosomal maturation. These observations support a role for CED-7 in intracellular vesicle trafficking for engulfment and possibly degradation of the cell corpse.

In summary, CED-7/ABCA1 may be involved in multiple activities to promote cell corpse engulfment, and may be performing different functions in dying cells verses phagocytic cells. In dying cells, CED-7 may act to present "eat-me" signals, such as PtdSer (Hamon et al., 2000), and bridging molecules, such as TTR-52 (Wang et al., 2010; Mapes et al., 2012), to engulfment receptors on phagocytic cells. In phagocytic cells, CED-7/ABCA1 may act to promote the formation of lipid rafts to assist CED-1/MEGF10 clustering at the phagocytic cup (Zhou et al., 2001; Hamon et al., 2006). CED-7 in phagocytic cells may also act upstream of CED-10 to promote actin cytoskeletal reorganization (Kinchen et al., 2005), upstream of DYN-1 to promote vesicle delivery for membrane extensions (Yu et al., 2006; Yu et al., 2008) and/or upstream of RAB-7 to promote cell corpse degradation (Yu et al., 2008). Most of the proposed activities of CED-7/ABCA1 involve some form of lipid transport, thus it is tempting to speculate that the transporter may function to transport lipids. Moreover, CED-7 is broadly expressed in *C. elegans* embryos, (Wu and Horvitz, 1998), suggesting it may be involved in processes other than PCD, as supported by the role of ABCA1 in cholesterol efflux (Hamon et al.,

2000). In summary, it is evident that additional studies are necessary to elucidate the precise role and mechanisms of this unique transporter.

### 1.3.2 Structure of CED-7/ABCA1 ABC transporters

ABC transporters represent one of the largest families of transmembrane proteins found in all species from bacteria to humans. In humans there are 49 *ABC* genes arranged in seven subfamilies, named ABCA through ABCG (Vasiliou et al., 2009). In mice and *Drosophila* there are 52 and 56 *ABC* genes, respectively, arranged in eight subfamilies, named ABCA through ABCH (Vasiliou et al., 2009; Flybase). These different classes of ABC transporters are important in a wide range of physiological processes including nutrient uptake, toxin secretion, and drug resistance, and can translocate a diverse variety of specific substrates, including sugars, ions, lipids, peptides, proteins, and lipoproteins (Rees et al., 2009; Beek et. al. 2014; Wilkens, 2015).

Crystal structures show that the structural organization of ABC transporters consists of four conserved core domains: two cytoplasmic nucleotide-binding domains (NBDs) and two transmembrane domains (TMDs) (Figure 1.3). The cytoplasmic NBDs contain several highly conserved sequences and motifs involved in the binding and hydrolysis of ATP, and serve as the catalytic motor domains utilizing the energy from ATP to drive the translocation of substrates. The membrane-spanning TMDs contain substrate-specific-binding sites and provide the translocation pathway for substrates across the membrane as they undergo conformational changes. These four conserved core domains, more importantly the conserved amino acid sequences and structural motifs in

the NBDs, are characteristic of all ABC transporters across all prokaryotic and eukaryotic organisms (Rees et al., 2009; Vasiliou et al., 2009; ter Beek et. al., 2014; Wilkens, 2015).

The catalytic NBDs of ABC transporters possess several loops and motifs that are highly conserved in primary sequence, order, and spatial distribution, across all ABC transporters. Most of these loops and motifs are similar to those found in other ATP-binding proteins, with the exception of the 'ABC signature motif', which is unique to ABC transporters. In sequential order, these loops and motifs include an 'A-loop' containing an aromatic residue, a 'Walker A motif' (GxxGxGKS/T where x is any amino acid), a 'Q-loop' containing a glutamine (Q) residue, an 'ABC signature motif' (L/YSGGQ/M), a 'Walker B motif' (φφφφDE where φ is a hydrophobic residue), a 'D-loop' containing an aspartate (D) residue, and an 'H-loop' containing a histidine (H) residue (Figure 1.3). These highly conserved loops and motifs are essential for ATP binding and hydrolysis. Mutations in any of these conserved regions result in proteins defective in ATP binding and hydrolysis, and substrate transport. These regions are presumed to also be involved in coupling ATP hydrolysis to conformational changes in the TMDs during substrate translocation (Rees et al., 2009; ter Beek et. al., 2014; Wilkens, 2015).

Contrastingly, the TMDs of ABC transporters lack homology in primary sequence and vary in structure and organization. Each TMD can have 6 to 10 α-helical structures, though most exporters have 6, for a total of 12 to 20 transmembrane segments in a complete ABC transporter. The TMDs of each transporter contain their respective substrate-binding sites, thus they can vary based on the chemical nature of their substrate,

for example a polar amino acid versus an uncharged sugar. In most cases, the two TMDs are identical or very similar in structure, however in some cases, the two TMDs can differ structurally and also functionally (Rees et al., 2009; ter Beek et. al., 2014; Wilkens, 2015).

Although structural and biochemical data have suggested common mechanistic features, such as ATP binding and hydrolysis, the transport mechanisms of ABC transporters have not been fully elucidated. The mechanism by which ATP binding and hydrolysis occurs and the conformational changes that are induced remains poorly understood. This is complicated by the variety of data between ABC transporters (Rees et al., 2009; ter Beek et. al., 2014; Wilkens, 2015). This variety is reflected in differences observed between the NBDs of ABCA1 and CED-7. In mammals, a K→M substitution preventing ATP binding and hydrolysis at either or both NBDs, leads to a complete loss-of-function in ABCA1 (Hamon et al., 2000). Interestingly, in *C. elegans*, the two NBDs seem to have different hierarchal roles. While a K→R substitution in the first NBD results in engulfment defects, the same mutation in the second NBD produced a limited effect (Wu and Horvitz, 1998). Such hierarchal orders of NBDs are not uncommon in ABC transporters and suggest that the two NBDs may have distinct roles in controlling the transport activity (ter Beek et. al., 2014; Wilkens, 2015). In these cases, the first NBD seems to control channel opening, whereas the second NBD seems to control channel closing (Wu and Horvitz, 1998).

### 1.3.3 Putative *Drosophila melanogaster* homologs of *ced-7/ABCA1*

The *Drosophila* genome carries 56 *ABC* genes, of which 10 encode members of the ABCA family (Table 1.2) (Flybase). In the *Drosophila* ovary, a well-established *in vivo* model for the study of PCD (Jenkins et al., 2013), only 2 of the ABCA encoding genes are expressed at appreciable levels, namely *CG31731* and *CG1718*.

*CG1718* has been proposed as the *Drosophila* homolog of ABCA1 for its role in lipid and cholesterol homeostasis. Specifically, the expression of *CG1718* was observed to be sensitive to dietary lipid and cholesterol concentrations, as larvae reared on a lipid-depleted medium compared to a standard medium exhibited lower levels of *CG1718* expression, and larvae reared on mediums containing increasingly higher cholesterol concentrations exhibited increasingly higher levels of *CG1718* expression (Bujold et al., 2010). These observations are consistent with the idea that under conditions of low lipid or cholesterol concentrations, genes that increase their efflux should be turned off. From these studies, CG1718 has been speculated to act as the functional homolog of ABCA1 in lipid and cholesterol efflux.

Recent studies in *Wolbachia*-infected *Drosophila* cell cultures have also supported a role for *CG1718* in lipid metabolism. The repression of *CG1718* in host cells was observed to have a negative effect on *Wolbachia* infection rates and reduce *Wolbachia* titer (White et al., 2017). The authors speculate that because *Wolbachia* lack essential fatty acid metabolic pathways and are enclosed in a host-derived outer membrane, they likely rely on their host's lipid metabolism for replication. This hypothesis is consistent with the requirement for host-derived lipids during replication in

other endosymbionts (Paredes et al., 2016). Therefore, *CG1718* may act to provide lipids to form the *Wolbachia* outer membrane.

Currently, there are no reports of a role for *CG1718* in PCD. Studies in the *Drosophila* brain did not find a role for *CG1718* during axon debris or neuronal-corpse clearance (Ziegenfuss, 2012). While it may be premature to rule out CG1718 as a putative homolog of CED-7, its non-requirement in this well-established model of PCD that is regulated by the conserved engulfment machinery suggests that other *Drosophila ABC* genes should also be examined.

Thus far, *CG31731*, has remained completely uncharacterized, except for a screen in which *CG31731* was found to be downregulated in the salivary glands of *E93* mutants. In *E93* mutants, the salivary glands fail to undergo developmental PCD (Dutta, 2008), suggesting that *CG31731* may be involved in promoting salivary gland PCD. Consistent with this hypothesis, *CG31731* is expressed at very high levels in the salivary gland (Flybase). To our knowledge, there have been no follow-up studies to investigate this putative role for *CG31731*.

Genome-wide analyses of *ABC* genes in other species, including *Daphnia pulex* (Sturm et al., 2009), *Tetranychus urticae* (Dermauw et al., 2013), and *Bombyx mori* (Li et al., 2015), have provided several phylogenetic analyses of *ABCA* encoding genes in *C. elegans, Drosophila,* and humans. Some of these phylogenetic trees present a closer evolutionary relationship between *CG31731,* compared to *CG1718*, and *ced-7/ABCA1* (Figure 1.4) (Sturm et al., 2009; Dermauw et al., 2013; Dermauw and Van Leeuwen, 2014; Li et al., 2015). Considering its putative role in PCD of the salivary gland (Dutta,

2008), *CG31731* may possess a more similar function to *ced-7/ABCA1* in engulfment. The lack of concrete evidence necessitates more research to determine whether *CG31731* may act as the functional equivalent of *ced-7/ABCA1* during PCD.

### 1.4 The *Drosophila melanogaster* ovary as a model system

For over a century, *Drosophila* have been extensively used as a model organism for genetic studies. *Drosophila* possess many characteristics that make them practical for laboratory research, including their short life cycle and a fast generation time, they are cheap and simple to maintain, and there is a wealth of information and genetic tools available for studies in *Drosophila*. A remarkable amount is known about their biology and their genome, which was completely sequenced in 2000. Moreover, the plethora of genetic tools has made it relatively straightforward to create transgenic mutants that harbor null mutations or tissue-specific gene knockouts, knockdowns, or over-expression, to study the function of a gene. While *Drosophila* only have four chromosome pairs that make up a relatively small genome, most of their genes are highly conserved with humans. In fact, many of the disease-causing genes in humans are also present in *Drosophila* (Elliott and Ravichandran, 2010; Fuchs and Steller, 2011). Thus, specific genes can be easily mutated for biomedical studies of human diseases and without the ethical issues of research involving human subjects.

The *Drosophila* ovary provides an excellent *in vivo* model system to study engulfment. It is the largest organ in the adult *Drosophila* (Bastock and St Johnston, 2008), such that it can be easily dissected, processed, and visualized under the microscope for analysis. Importantly, the ovary presents several PCD events including

developmental PCD during late oogenesis and starvation-induced PCD during mid-oogenesis, which exhibit features of apoptosis, necrosis, autophagy, and phagoptosis (Jenkins et al., 2013; Timmons et al., 2016). During both PCD events, 15 easily visualized nurse cells are normally engulfed and cleared. Since the system is closed to circulating macrophages, engulfment is accomplished by neighboring epithelial cells, which sufficiently act as non-professional phagocytes (Jenkins et al., 2013). Therefore, the ovary relatively easily allows for the *in vivo* study of engulfment by non-professional phagocytes in several different PCD modalities. Additionally, the ovary is not essential for survival and thus can be extensively manipulated for genetic studies.

### 1.4.1 Oogenesis in the *Drosophila melanogaster* ovary

The female *Drosophila* carries two ovaries that continuously produce eggs. Each ovary is comprised of a bundle of 15-20 ovarioles, which are sheaths containing progressively developing egg chambers (Figure 1.5). At the anterior tip of each ovariole, a germarium contains germline and somatic stem cells from which egg chambers are continuously produced. Egg chambers develop from the germarium towards the posterior end through 14 stages in oogenesis (Bastock and St Johnston, 2008; Wu et al., 2008; Jenkins et al., 2013). The entire process of oogenesis takes approximately one week from the budding of the egg chamber in stage 1 to the maturation into an egg in stage 14 (Bastock and St Johnston, 2008). At the end of oogenesis, the mature egg passes through the oviducts into the uterus, where they can be fertilized (Jenkins et al., 2013).

Each egg chamber contains 16 interconnected germline-derived cells surrounded by a layer of several hundred somatically-derived follicle cells. In the germarium,

germline stem cells produce cystoblasts, each of which undergo four incomplete mitotic divisions to form a syncytium of 16 cells interconnected by cytoplasmic ring canals. At around stage 2, one of the germline-derived cells differentiates into the oocyte, while the remaining 15 become polyploid nurse cells (NCs) (Bastock and St Johnston, 2008; Wu et al., 2008; Jenkins et al., 2013). From stage 2 to 10, the nurse cells provide nutrients, proteins, mRNAs, and organelles through the ring canals to the developing oocyte. Then at stages 10 and 11, the nurse cells dump their remaining cytoplasmic contents into the oocyte in a process known as "dumping", allowing the oocyte to grow and fill the entire egg chamber (Bastock and St Johnston, 2008; Jenkins et al., 2013). Finally, in stages 12 through 14, the follicle cells facilitate the removal of the remaining nurse cell debris, leaving only the mature oocyte by stage 14 (Figure 1.6) (Jenkins et al., 2013).

Throughout oogenesis, the somatically-derived follicle cells contribute several important functions to form the mature egg. Polar cells, one type of specialized follicle cells, provide the necessary differentiation signals to establish the fates of other specialized follicle cells including the border cells, the columnar follicle cells, and the stretched follicle cells. Then after stage 8, the border cells surround the polar cells and migrate to the oocyte where the polar cells form the micropyle. At the same time, the epithelial follicle cells migrate to the posterior end to deposit the vitelline membrane and eggshell over the oocyte, and provide yolk proteins to the maturing oocyte. The remaining ~50 follicle cells at the anterior end stretch over the nurse cells and facilitate the removal of the nurse cells. Finally in stage 13 and 14, a patch of follicle cells form the

dorsal appendages, which provide chorion proteins for the mature egg (Bastock and St Johnston, 2008).

### 1.4.2 Developmental PCD during late oogenesis

During late oogenesis in stages 12–14, the 15 germline-derived nurse cells undergo developmental PCD and are cleared by the neighboring somatically-derived stretched follicle cells, leaving only the mature oocyte by stage 14 (Figure 1.7). Beginning in stage 12 after "dumping", the remaining nurse cell nuclei are observed to become TUNEL- and LysoTracker- positive, indicating events of DNA degradation, and acidification, respectively. DNA degradation as observed by TUNEL staining is a hallmark of apoptosis. However, additional studies did not observe a role for caspases or the major *Drosophila* IAP genes, *reaper, hid,* and *grim* (RHG), and observed a requirement for the *Drosophila* inhibitor of apoptosis (Diap1) protein. Additionally, acidification during PCD could indicate a form of autophagic cell death, however ATG genes were also not required for these events. These genetic studies indicate that the nurse cells do not undergo apoptosis or autophagic cell death.

The presence of acidified vesicles was also observed surrounding the nurse cell nuclei (Jenkins et al., 2013). Genetic studies of lysosomal trafficking genes demonstrated their requirement in the stretched follicle cells for acidification of the nurse cell nuclei. Phagocytosis genes including *draper* and *Ced-12* in the stretched follicle cells and follicle cells were also required for the acidification and DNA degradation events in the nurse cell (Timmons et al., 2016). The genetic requirement for some genes in the follicle cells versus the stretched follicle cells suggest that they are synthesized earlier in oogenesis,

before stage 9 when the stretched follicle cell fate is established. Their proteins are likely present and also required in the stretched follicle cells for PCD of the nurse cells. Furthermore, genetic ablation of the stretched follicle cells prevents the death of the nurse cells. These observations indicate that the stretched follicle cells promote these nurse cell death events, and propose that they "kill" the nurse cells via phagoptosis (Timmons et al., 2016).

In stages 12–14, the phagocytic receptor Draper becomes enriched on the stretched follicle cell membrane, where it is required for clearance of the nurse cells (Timmons et al., 2016). The genetic knockout or knockdown of phagocytosis genes, including *draper, Ced-12,* and *integrins,* in the stretched follicle cells and follicle cells prevents removal of the nurse cell corpses, resulting in stage 14 egg chambers exhibiting persisting nurse cell nuclei (Timmons, 2015; Timmons et al., 2016).

### 1.4.3 Starvation-induced PCD during mid-oogenesis

Whereas PCD during late oogenesis occurs in the development of every egg, PCD during mid-oogenesis occurs in response to developmental abnormalities or physiological stress. PCD of the nurse cells in stages 7–9 can be reproducibly induced by protein starvation. The process requires active caspases, including death caspase 1 (Dcp-1), and ATG genes, suggesting apoptosis and autophagy both contribute to promote PCD during mid-oogenesis (Jenkins et al., 2013). Interestingly, enhanced expression of the phagocytic receptor, Draper, can induce PCD in mid-oogenesis egg chambers without starvation, suggesting a role for induced phagoptosis (Timmons, 2015).

In starvation-induced PCD, egg chambers proceed through 5 morphologically distinct phases primarily defined by changes in the nurse cell chromatin (Figure 1.8). Phase 0 healthy egg chambers contain 15 nurse cells with dispersed chromatin. In phase 1 dying egg chambers, the nurse cell chromatin becomes disordered. In phase 2, the chromatin in each nurse cell condenses into several small balls and the follicle cells begin to enlarge. In phase 3, the chromatin in each nurse cell becomes highly condensed in a single large ball as the follicle cells continue to enlarge. In phase 4, the condensed nurse cell chromatin becomes fragmented and some of the germline material is engulfed by the follicle cells. By phase 5, only a few if any nurse cell nuclear fragments remain as the follicle cells have engulfed the germline material, and enlarged inwards to constitute the entire egg chamber (Etchegaray et al., 2012).

Draper is required in the follicle cells for engulfment of the dying germline-derived cells. Starting around phase 3, Draper becomes expressed at the follicle cell apical membrane, where the phagocytic cup likely forms facing the germline material. Draper staining increasingly accumulates at the phagocytic cup and finally peaks at phase 5. By phase 5, Draper is also detected inside the follicle cells, suggesting that Draper becomes internalized during phagosome formation. In *draper* null mutants, dying egg chambers exhibit significant engulfment defects as follicle cells fail to enlarge and then die without clearing the nurse cell remnants and other germline debris (Etchegaray et al., 2012). Other engulfment receptors also required in the follicle cells for engulfment during mid-oogenesis PCD include integrins (Meehan et al., 2016).

**1.5 Thesis rationale**

Programmed cell death (PCD) is a critical biological process in animal development and tissue homeostasis to prevent disease pathogenesis (Jacobson et al., 1997; Elliott and Ravichandran, 2010; Fuchs and Steller, 2011). Engulfment represents the necessary step in PCD for the selective removal of excess, damaged, and potentially deleterious cells programmed to die. The process prevents the accumulation of cell corpses and secondarily necrotic cells, which have been implicated as important contributing factors to disease pathogenesis (Elliot and Ravichandran, 2010; Fuchs and Steller, 2011).

Genetic studies in *C. elegans, Drosophila,* and mammals have identified two evolutionarily conserved signal transduction pathways: *ced-1/-6/-7* and *ced-2/-5/-12,* that act in parallel to promote multiple events for engulfment (Kinchen et al. 2005; Mangahas and Zhou, 2005; Fullard et al., 2009). Of these engulfment machinery components, the ABC transporter CED-7 is the only protein reported to be required in both the phagocytic cell and the dying cell (Wu and Horvitz, 1998). Whether the mammalian ortholog ABCA1 is also expressed in dying cells has yet to be determined. The *Drosophila* ortholog of CED-7/ABCA1 has not been identified.

The *Drosophila* ovary provides an excellent *in vivo* model system to study engulfment. Egg chambers in the ovary undergo developmental and inducible PCD events, which exhibit features of apoptosis, necroptosis, autophagy, and phagoptosis (Jenkins et al., 2013; Timmons et al., 2016). Additionally, the ovary is not essential for survival and thus can be extensively manipulated for genetic studies (Bastock and St

Johnston, 2008). The plethora of genetic tools and wealth of information about *Drosophila* has made it relatively straightforward to create transgenic mutants that harbor null mutations or tissue-specific gene knockouts, knockdowns, or over-expression. (Elliott and Ravichandran, 2010; Fuchs and Steller, 2011).

The goal of our research is to elucidate the genetic pathways and molecular mechanisms which regulate PCD in the *Drosophila* ovary, by identifying and characterizing the missing components. Since components of the engulfment machinery are evolutionarily conserved, *in vivo* studies in *Drosophila* can provide invaluable information for understanding the mammalian equivalents. The research presented in this thesis characterizes the role of the ABC transporter gene, *CG31731*, in the engulfment of nurse cells during PCD events in the *Drosophila* ovary, and proposes that *CG31731* is the *Drosophila* homolog of *ced-7/ABCA1*.

**Table 1.1 The conserved engulfment proteins in *C. elegans, Drosophila,* and mammals.**

| ***C. elegans*** | ***Drosophila*** | **Mammals** |
|---|---|---|
| CED-1 | Draper | MEGF10, JEDI, LRP1 |
| CED-2 | Crk | CrkII |
| CED-5 | Myoblast City | DOCK180 |
| CED-6 | Ced-6 | GULP |
| CED-7 | **Unknown** | ABCA1, ABCA7 |
| CED-10 | Rac1 | Rac1 |
| CED-12 | Ced-12 | ELMO |
| DYN-1 | Shibire | Dynamin |
| INA-1 | Integrin αPS3/βPS | Integrin $\alpha_v\beta_5$ |

**Table 1.2. The ABC transporter encoding genes in *Drosophila melanogaster***

| Gene Name or CG# | Genome Location^ | Transporter Class | Ovary Expression (Microarray)* | Ovary Expression (RNA-Seq)** |
|---|---|---|---|---|
| CG33173 | 13E16-13E17 (X:15,773,171..15,778,703) | ABCA | (no data) | low |
| CG1819 | 19F1-19F1 (X:21,123,634..21,140,951) | ABCA | none | low |
| CG1494 | 19F3-19F3 (X:21,285,301..21,292,458) | ABCA | none | none |
| **CG1718** | **19F3-19F3 (X:21,292,308..21,306,665)** | **ABCA** | **moderate** | **moderate** |
| CG1801 | 19F3-19F4 (X:21,307,586..21,317,522) | ABCA | none | none |
| **CG31731** | **34D1-34D1 (2L:13,784,084..13,790,562)** | **ABCA** | **moderate** | **moderate** |
| CG8908 | 56F11-56F11 (2R:20,264,920..20,270,994) | ABCA | none | none |
| CG6052 | 74F3-74F3 (3L:17,723,718..17,729,244) | ABCA | none | none |
| CG32186 | 75A2-75A2 (3L:17,792,088..17,797,594) | ABCA | (no data) | none |
| CG31213 | 92C1-92C1 (3R:19,972,898..19,979,569) | ABCA | none | none |
| CG3156 | 1B5-1B5 (X:487,878..490,725) | ABCB | moderate | moderate |
| CG1824 | 11B2-11B2 (X:12,592,555..12,595,624) | ABCB | moderate | low |
| Mdr49 | 49E1-49E4 (2R:12,940,323..12,946,347) | ABCB | none | none |
| Mdr50 | 50E6-50E6 (2R:14,246,966..14,252,597) | ABCB | none | none |
| ABCB7 | 62A8-62A9 (3L:1,618,414..1,623,413) | ABCB | moderate | moderate |
| CG10226 | 65A10-65A10 (3L:6,234,323..6,240,068) | ABCB | none | none |
| Mdr65 | 65A10-65A10 (3L:6,240,500..6,245,746) | ABCB | none | none |
| Hmt-1 | 89A6-89A6 (3R:15,853,868..15,857,470) | ABCB | moderate | high |
| CG7806 | 29A3-29A4 (2L:8,311,399..8,317,011) | ABCC | moderate | moderate |
| CG7627 | 29B1-29B1 (2L:8,355,678..8,362,469) | ABCC | high | high |
| Sur | 31B1-31B1 (2L:10,182,557..10,199,117) | ABCC | low | none |
| MRP1 | 33F3-33F5 (2L:12,719,045..12,766,546) | ABCC | high | moderate |

| | | | | |
|---|---|---|---|---|
| CG31792 | 37B9-37B9 (2L:18,997,448..19,002,713) | ABCC | none | none |
| CG31793 | 37B9-37B9 (2L:19,003,367..19,008,234) | ABCC | low | low |
| CG9270 | 38F6-38F6 (2L:20,929,456..20,934,113) | ABCC | none | none |
| L(2)03659 | 45D1-45D1 (2R:9,390,165..9,395,281) | ABCC | low | none |
| CG10505 | 57D7-57D8 (2R:21,285,248..21,290,343) | ABCC | none | none |
| Mrp4 | 86E11-86E11 (3R:11,569,250..11,575,937) | ABCC | (no data) | low |
| CG4562 | 92B4-92B4 (3R:19,865,417..19,875,678) | ABCC | low | low |
| CG5789 | 96A6-96A7 (3R:24,536,204..24,543,914) | ABCC | moderate | moderate |
| CG11897 | 98F13-98F13 (3R:29,158,122..29,164,966) | ABCC | very high | very high |
| CG11898 | 98F13-98F13 (3R:29,165,643..29,171,508) | ABCC | none | none |
| Pmp70 | 18F1-18F1 (X:19,750,770..19,759,280) | ABCD | moderate | moderate |
| CG2316 | 102A6-102A6 (4:184,076..193,829) | ABCD | high | moderate |
| pix (pixie) | 66E6-66E6 (3L:8,972,056..8,974,765) | ABCE | high | high |
| CG1703 | 10D1-10D1 (X:11,611,927..11,615,128) | ABCF | high | high |
| CG9281 | 13E8-13E8 (X:15,705,806..15,710,539) | ABCF | moderate | very high |
| CG9330 | 76B8-76B8 (3L:19,586,253..19,589,111) | ABCF | moderate | high |
| w (white) | 3B6-3B6 (X:2,790,599..2,796,466) | ABCG | none | low |
| CG4822 | 21B2-21B2 (2L:116,970..121,754) | ABCG | low | none |
| CG3164 | 21B2-21B2 (2L:122,624..130,791) | ABCG | moderate | moderate |
| CG17646 | 22B1-22B2 (2L:1,732,524..1,750,612) | ABCG | (no data) | low |
| CG31689 | 23A3-23A3 (2L:2,725,674..2,739,830) | ABCG | moderate | moderate |
| CG9664 | 23E1-23E1 (2L:3,291,245..3,294,706) | ABCG | none | none |
| CG9663 | 23E1-23E3 (2L:3,294,926..3,303,130) | ABCG | low | low |
| E23 | 23E4-23E5 (2L:3,334,875..3,354,829) | ABCG | high | high |

| | | | | |
|---|---|---|---|---|
| Atet | 24E1-24E1 (2L:4,333,913..4,345,776) | ABCG | low | low |
| CG5853 | 30F1-30F1 (2L:9,940,773..9,947,648) | ABCG | low | low |
| bw (brown) | 59E2-59E3 (2R:23,527,805..23,538,499) | ABCG | low | none |
| CG32091 | 68D1-68D1 (3L:11,631,392..11,642,902) | ABCG | low | low |
| st (scarlet) | 73A3-73A3 (3L:16,497,651..16,500,460) | ABCG | none | none |
| CG31121 | 96B2-96B4 (3R:24,881,466..24,894,605) | ABCG | (no data) | none |
| CG11069 | 96B4-96B4 (3R:24,894,742..24,897,613) | ABCG | (no data) | none |
| CG11147 | 25F4-25F4 (2L:5,733,675..5,741,244) | ABCH | low | low |
| CG33970 | 97A8-97A10 (3R:26,318,355..26,362,588) | ABCH | low | low |
| CG9990 | 98E1-98E2 (3R:28,675,041..28,695,939) | ABCH | low | low |

^Top indicates band position and bottom indicates chromosome and sequence location.
*Expression levels: none (0-9.999), low (10-99.999), moderate (100-499.999), high (500-999.999), very high (>999.999). (Data from FlyAtlas Anatomy Microarray, Flybase).
**Expression levels: none (0-0), low (1-10), moderate (11-50), high (51-100), very high (101-1000) (Data from modENCODE Anatomy RNA-Seq, Flybase).

**Figure 1.1 The general process of engulfment**

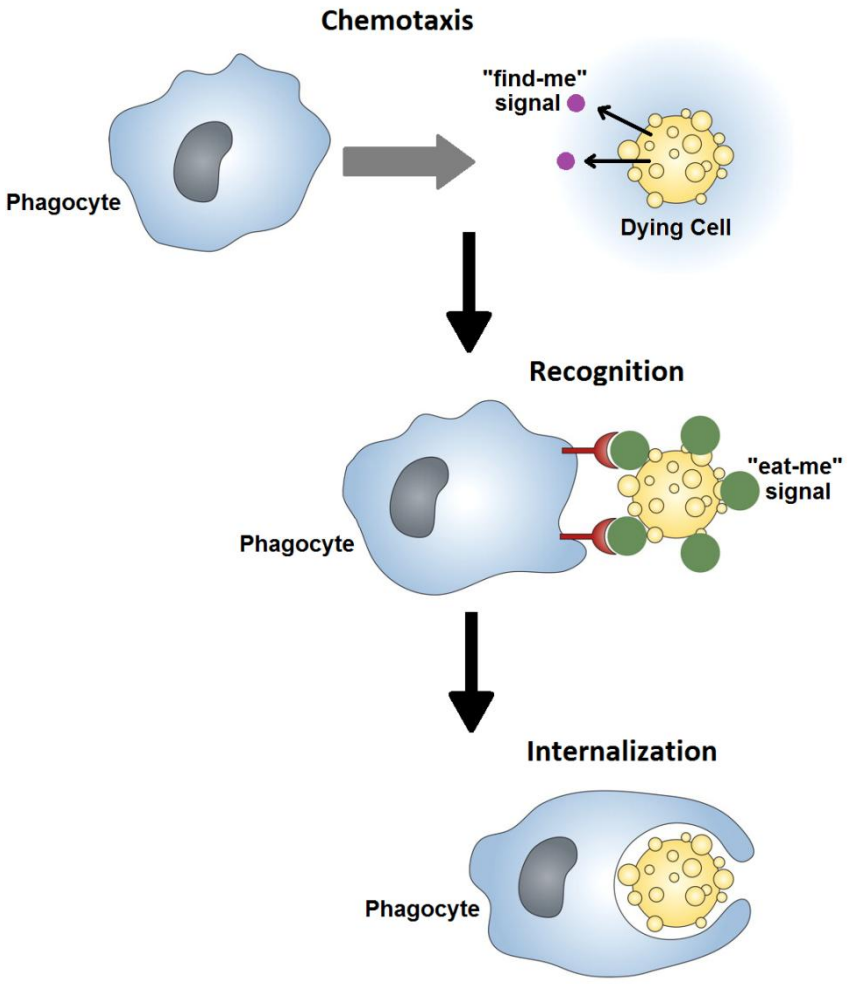


The engulfment process can be described as a succession of 3 steps: (1) “find-me” signals secreted by the dying cell recruit the phagocyte to the dying cell, where (2) the phagocyte recognizes “eat-me” signals presented by the dying cell, and through a cascade of signaling events (3) the phagocyte internalizes the cell corpse. (Figure modified from Ravichandran, 2010)

**Figure 1.2 The engulfment signaling pathway identified in *C. elegans***

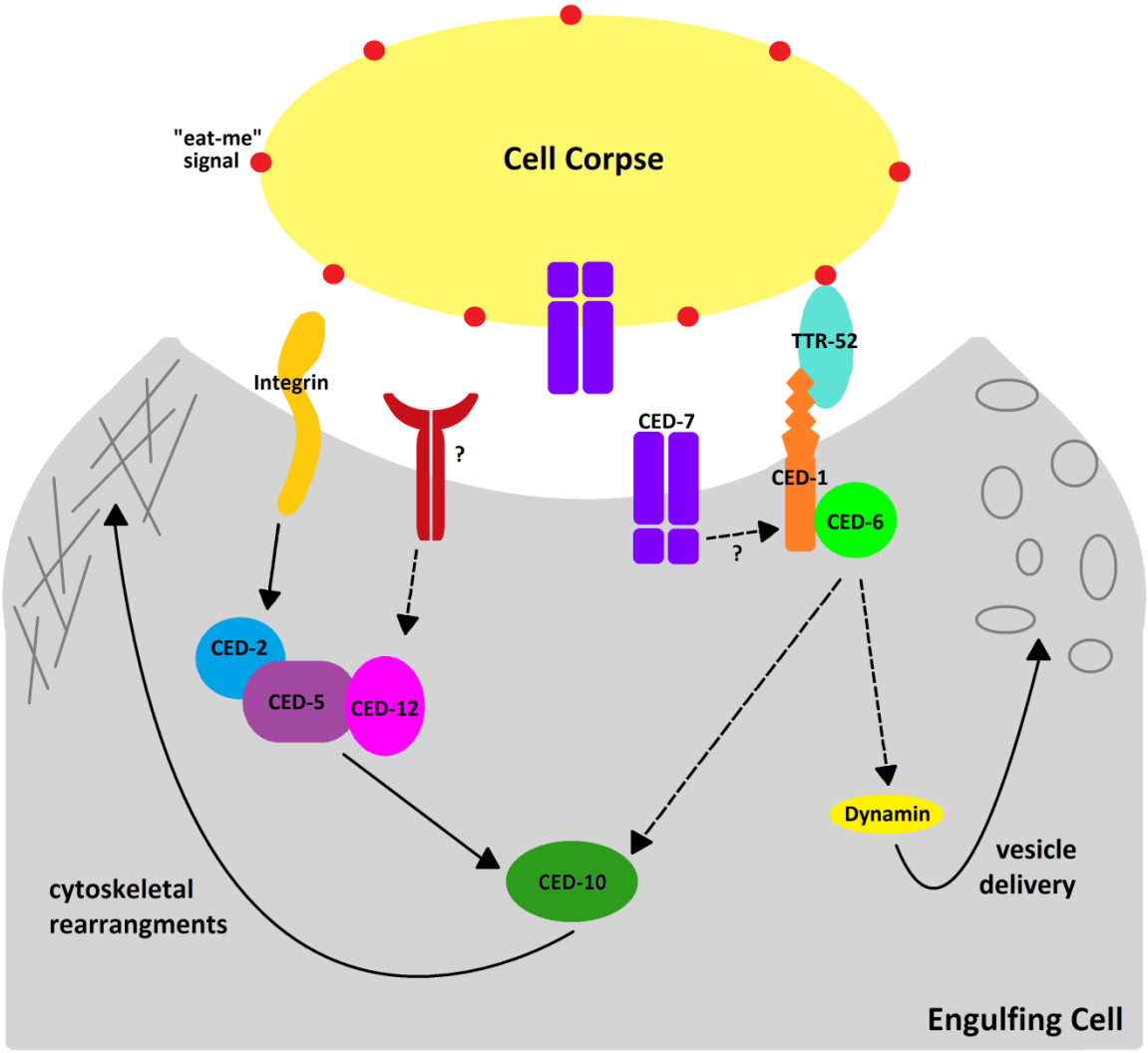


In *C. elegans*, two distinct parallel but partially redundant signal transduction pathways facilitate pseudopod extensions during engulfment. The CED-1/-6/-7 and CED-2/-5/-12 pathways converge on CED-10 to promote cytoskeletal rearrangements. The CED-1/-6/-7 pathway also acts on Dynamin to promote vesicle delivery to the membrane. CED-1 recognizes “eat-me” signals via the bridging molecule TTR-52, and integrins and other ligand receptors have been identified upstream of the CED-2/-5/-12 pathway.

**Figure 1.3 The general structure of ABC transporters**

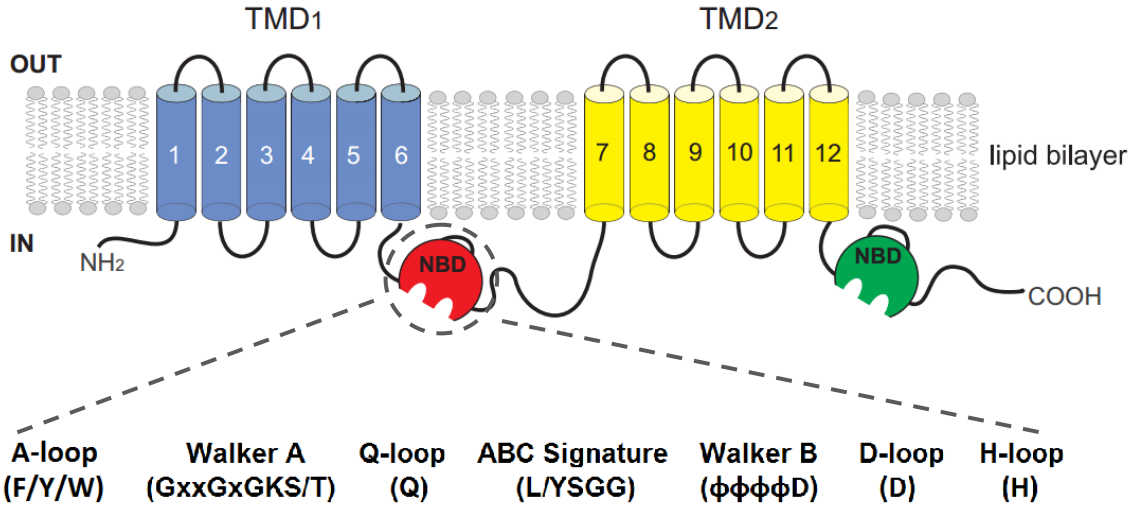


ABC transporters comprise of two transmembrane domains (TMD1 and TMD2) and two cytoplasmic nucleotide-binding domains (NBD1 and NBD2). In most ABC transporters, each TMD consists of 6 transmembrane α-helices (cylinders) for a total of 12 transmembrane segments in a complete transporter. In all ABC transporters, the NBDs contain several highly conserved amino acid sequences involved in the binding and hydrolysis of ATP. (Figure modified from Dermauw and Van Leeuwen, 2014)

**Figure 1.4 Phylogeny tree of ABCA proteins in *C. elegans, Drosophila,* and humans**

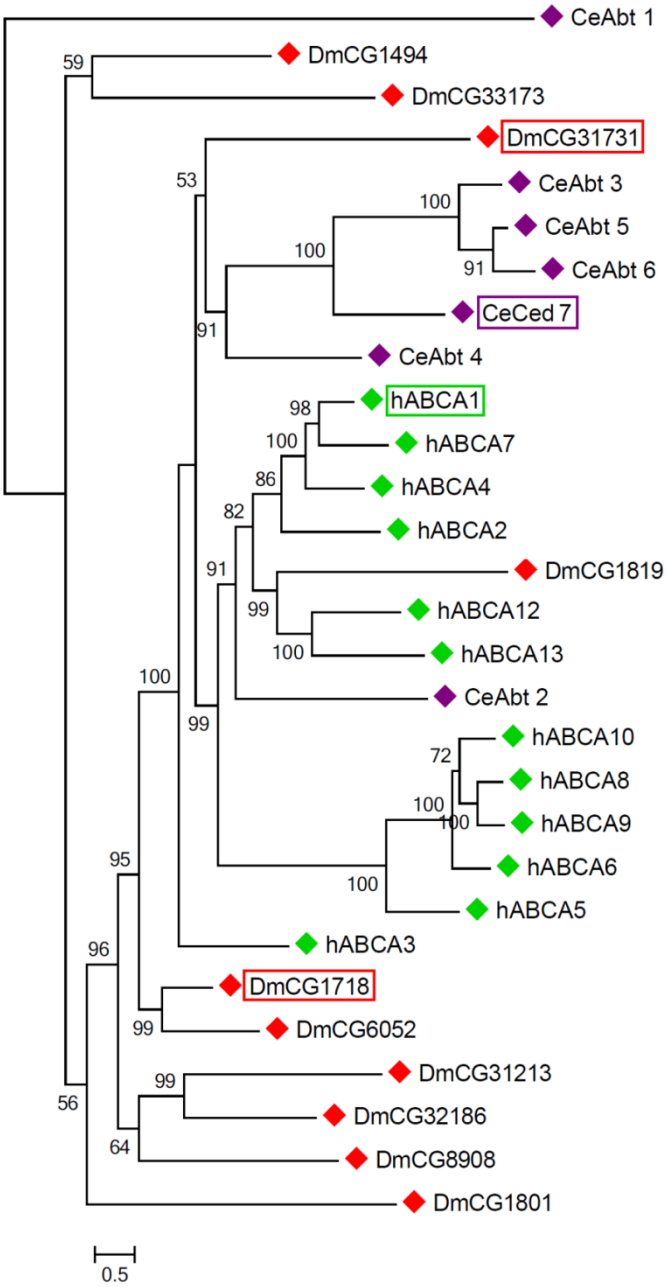


The predicted full-length amino acid sequences of ABCA proteins in *C. elegans* (Ce, purple), *D. melanogaster* (Dm, red), and humans (h, green) were aligned using MUSCLE and subjected to a maximum likelihood analysis using Treefinder. Numbers at each branch point represent the bootstrap values from 1000 replicates. Scale bar represents a 0.5 amino acid substitution per site. (Modified from Dermauw et al., 2013)

**Figure 1.5 The *Drosophila* ovary and female reproductive structures**

**A** **B**

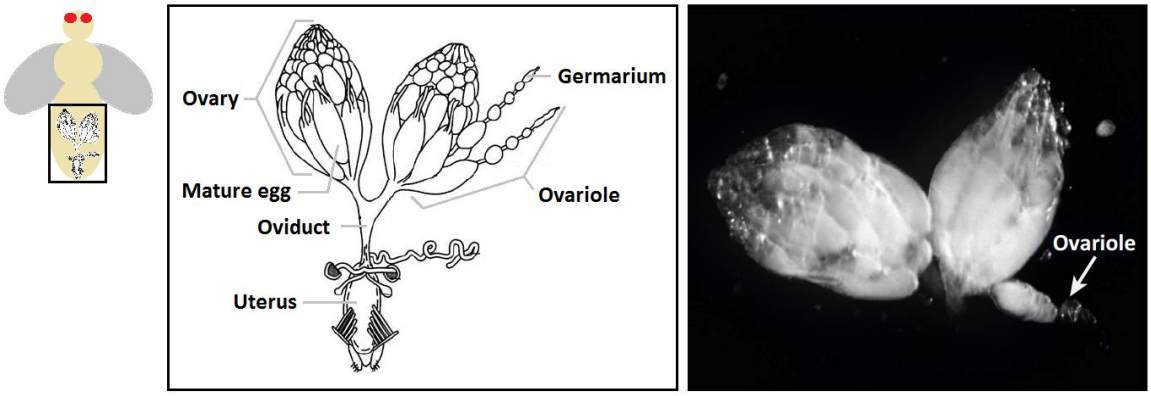


**(A)** An illustration of the *Drosophila* female reproductive system. Each female carries two ovaries comprised of a bundle of ovarioles, sheaths containing a germarium and progressively developing egg chambers. Egg chambers are produced from the germarium at the anterior tip and develop towards the posterior tip until they mature into an egg. Mature eggs pass through the oviduct into the uterus where they can be fertilized. (Figure modified from Flybase)

**(B)** Two dissected ovaries from the female *Drosophila*. An ovariole (arrow) is separated from the bundle. (Figure from Jenkins et al., 2013)

**Figure 1.6 The progression of oogenesis**

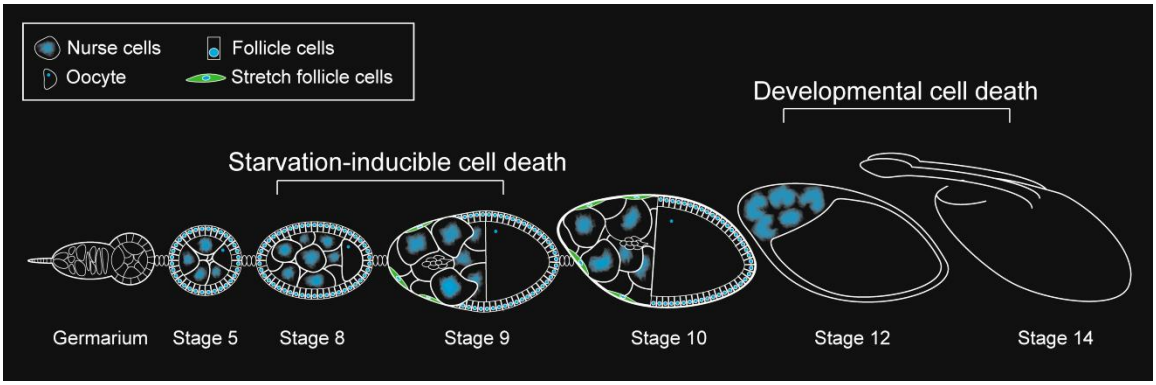


A schematic of progressively developing egg chambers in an ovariole. Egg chambers are produced from the germarium and contain a single oocyte and 15 nurse cells surrounded by a layer of follicle cells. After stage 8, a series of migration and differentiation events occur to establish the stretched follicle cells, which stretch to surround the nurse cells. Between stages 10 and 12, "dumping" of the nurse cell cytoplasmic contents occur. Then from stage 12 to 14, the nurse cells undergo developmental PCD and are removed. By stage 14, only the mature oocyte which has filled the entire egg chamber remains, and the dorsal appendages have fully formed. Protein-starvation in the *Drosophila* diet can induce PCD in stage 7 to 9 mid-oogenesis egg chambers. (Figure kindly provided by Alla Yalonetskaya)

**Figure 1.7 Developmental PCD during late oogenesis**

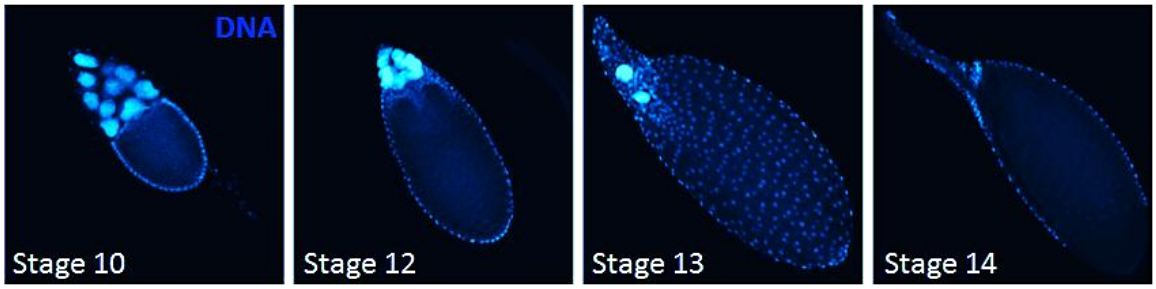


Egg chambers in the late-stages of oogenesis stained with DAPI (blue) to label DNA. In the stage 10 egg chamber, the nurse cells are surrounded by stretched follicle cells and still contain their cytoplasm, and the nurse cell nuclei appear dispersed. In the stage 12 egg chamber, the nurse cells have dumped their cytoplasmic contents into the oocyte and the nurse cell nuclei appear condensed. In the stage 13 egg chamber, most of the nurse cells have been cleared and only 2 highly condensed nurse cell nuclei remain. Additionally, the dorsal appendages begin to form. In the stage 14 egg chamber, all of the nurse cells have been cleared, leaving only the mature oocyte. (Images acquired by Alla Yalonetskaya)

**Figure 1.8 Starvation-induced PCD during mid-oogenesis**

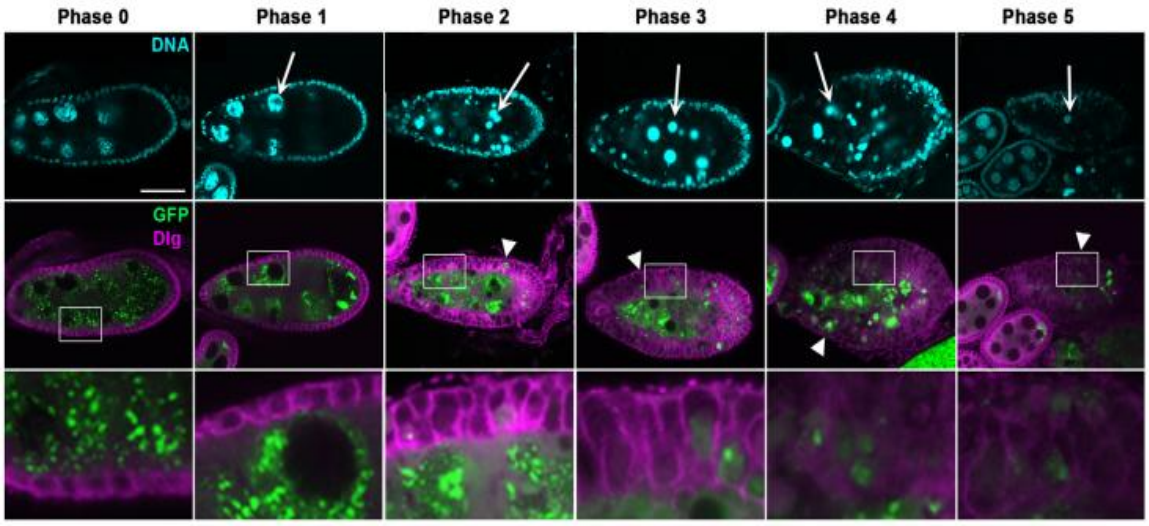


Healthy and dying egg chambers in mid-oogenesis stained with DAPI (blue) to label DNA, and Dlg (magenta) to label follicle cell membrane. Egg chambers express a germline-specific GFP gene trap, G89 (green). In the phase 0 healthy egg chamber, the nurse cell chromatin is dispersed. In the phase 1 dying egg chamber, the nurse cell chromatin becomes disordered (arrow). In the phase 2 dying egg chamber, the chromatin in each nurse cell condenses into several small balls (arrow) and the follicle cells begin to enlarge (arrowhead). In the phase 3 dying egg chamber, the chromatin in each nurse cell becomes highly condensed in a single large ball (arrow) as the follicle cells continue to enlarge (arrowhead). In the phase 4 dying egg chamber, the condensed nurse cell chromatin becomes fragmented (arrow) and germline material becomes present inside the follicle cells (arrowhead). In the phase 5 dying egg chamber, only a few nurse cell fragments remain as the follicle cells have enlarged inwards to constitute the entire egg chamber (arrowhead). (Figure from Etchegaray et al., 2012)

# CHAPTER 2: MATERIALS AND METHODS

## 2.1 *Drosophila* stocks and husbandry

All stocks (Table 2.1) were obtained from Harvard Transgenic RNAi Project (TRiP), Bloomington *Drosophila* Stock Center (BDSC), or Vienna *Drosophila* Resource Center (VDRC), with the exception of $draper^{A5}$ strains (Freeman et al., 2003) provided by Estee Kurant, and *draper dsRNA* ($draper^{RNAi}$) strains (MacDonald et al., 2006) provided by Marc Freeman. For all experiments, stocks and crosses were reared on standard cornmeal molasses yeast medium at 25ºC.

## 2.2 Tissue-specific drivers, knockdowns and over-expression

All tissue-specific RNAi knockdown and over-expression lines were generated using the GAL4/UAS binary system (Figure 2.1). In this binary system, the *GAL4* yeast transcription factor recognizes and binds to upstream activation sequences/UAS sites. For all our experiments, expression of *GAL4* was placed under control of an endogenous tissue-specific enhancer, specifically *GR1* in the all follicle cells after stage 3 including the stretched follicle cells (Figure 2.2), *PG150* only in the specialized stretched follicle cells after stage 10, and *nanos* in the nurse cells. The regulated expression of *GAL4* under these tissue-specific drivers allowed for the spatiotemporal expression of a target transgene inserted downstream of a UAS site. For most of our experiments, *GR1-GAL4* was used to drive the expression of RNAi constructs specifically in the follicle cells.

**2.3 Preparation of ovaries**

Adult males and females were transferred to a vial containing fresh medium and a teaspoon of yeast paste, and conditioned for approximately 2 days. To induce death in mid-stage egg chambers, adults were also transferred to apple juice agar vials and starved of nutrients for the last 16-20 hour period prior to dissections.

**2.4 Ovary dissection and fixation**

Adults were anesthetized on a $CO_2$ pad and females were sorted from males. Subsequently, using forceps each female was submerged in a glass well containing Grace's Insect Media (Fisher) and their reproductive structures were gently pulled out from the posterior tip. Whole ovaries were separated from the other organs and transferred to a clean well containing Grace's media and then to a 0.5 mL Eppendorf tube containing fix solution. In order to minimize tissue degradation, dissections were performed in <20 minutes and then immediately fixed in a Grace's Fix containing 300µL Grace's media + 200µL heptane + 100µL <1 week old 16% paraformaldehyde (Electron Microscopy Sciences) for 20 minutes while rotating at room temperature.

**2.5 DAPI staining**

DAPI (4',6-diamidino-2-phenylindole) is a DNA-specific stain that emits blue fluorescence. Post-fixation, ovaries were quickly rinsed 2 times, and then washed 3 times for 20 minutes each with 1X Phosphate Buffered Saline + 0.1% Triton-X (PBT) while rotating at room temperature. If desired, ovaries were quickly rinsed in 1X PBS prior to adding 1-2 drops of Vectashield Mounting Media with DAPI (Vector Laboratories). Ovaries were stored in DAPI at least overnight at 4ºC, until mounted.

**2.6 Antibody staining**

Standard antibody staining methods were used. Post-fixation, ovaries were quickly rinsed 2 times, washed 3 times for 20 minutes each with PBT, and then blocked for 1 hour in PBT + 0.5% BSA +5% NGS (PBNG), all while rotating at room temperature. Ovaries were then incubated in primary antibodies (Table 2.2) diluted in PBNG while rotating overnight at 4ºC. The next day, ovaries were similarly rinsed 2 times and then washed 4 times for 30 minutes each with PBT, before incubated in secondary antibodies (Table 2.2) diluted in PBNG for 1 hour in the dark, all while rotating at room temperature. For all subsequent steps, ovaries were protected from light using aluminum foil. Following secondary antibody, ovaries were again washed 4 times for 30 minutes each with PBT, then quickly rinsed with 1X PBS and stored in 1-2 drops of DAPI at least overnight at 4ºC, until mounted.

**2.7 LysoTracker staining**

Immediately following dissection, ovaries were incubated in LysoTracker Red DND-99 (Invitrogen) diluted 1:50 in 1X PBS for 3 minutes on the shaker at room temperature. Ovaries were then quickly rinsed, washed 3 times for 5 minutes each with 1X PBS, fixed in Grace's Fix for 20 minutes, washed 3 times for 20 minutes each with PBT, all while rotating at room temperature, prior to being stored in 1-2 drops of DAPI at least overnight at 4ºC, until mounted.

**2.8 TUNEL staining**

TUNEL (terminal deoxynucleotidyl transferase (TdT)-mediated dUTP nick end labeling) is a technique used to detect the 3'-OH ends of DNA fragments. Post-fixation,

brains were washed 3 times for 10 minutes each with PBT, then once for 15 minutes with 1X PBS + 0.2% Triton X-100, while rotating at room temperature. Brains were then washed for 10 minutes in equilibration buffer prior to incubated in 45µL equilibration buffer + 5µL nucleotide mix + 1µL TdT enzyme for 3 hours at 37ºC in the dark. To stop the reaction, 300µL 2X SSC was added to the sample for 1 minute, the brains were washed for 15 minutes in 300µL 2X SSC while rotating at room temperature. Finally, brains were washed 3 times for 10 minutes each with PBT and then stored in 1-2 drops of DAPI at least overnight at 4ºC, until mounted.

**2.9 Mounting**

Using a glass Pasteur pipette, ovaries in DAPI were transferred onto a glass slide and teased apart using Tungsten needles (Carolina Biologicals). A cover slip was then placed over the slide and sealed with nail polish. Slides were stored at 4ºC and taken out only for imaging.

**2.10 Microscopy and imaging**

Egg chambers were viewed using the Olympus BX60 fluorescence microscope, and images were captured using the Olympus Cell Sense Entry software. For confocal imaging, egg chambers were viewed using the Olympus FluoView FV10i microscope, and images captured using the associated program. Confocal images were processed in ImageJ and all figures were put together in Microsoft PowerPoint.

**2.11 Quantifications**

The number of persisting nurse cell nuclei (PN) in each stage 14 egg chamber was quantified. Each stage 14 egg chamber was then grouped into bins of 0 PN, 1-3 PN, 4-6

PN, 7-9 PN, 10-12 PN, 13-15 PN, and each bin was presented as a percentage of all stage 14 egg chambers quantified per genotype. Alternatively, the average number of PN in a stage 14 egg chamber from each genotype was presented. “n” represents the total number of stage 14 egg chambers quantified.

The number of late-stage egg chambers exhibiting LysoTracker positive nurse cells versus no LysoTracker staining was quantified. Egg chambers were staged as stage 11 if they were still completing dumping, stage 12 if they had completed dumping, stage 13 if the dorsal appendage had started to form, and stage 14 if the dorsal appendage had fully extended and thickened. The data was presented in a graph showing the percentage of egg chambers exhibiting LysoTracker positive nurse cells from each stage 11, 12, 13, and 14.

**Table 2.1 Stocks**

| Stock # | Associated Alleles | Stock Description | Source |
|---|---|---|---|
| | $w^{1118}$ | *w[1118]* | |
| | *GAL4, G00089* | *GR1-GAL4,-G00089/TM6B* | |
| | *GAL4* | *PG150-GAL4* | Ellen LeMosy |
| | *GAL4* | *nanos-GAL4* | |
| | *GFP* | *UAS-GFP* | |
| 27383 | $CG31731^{\Delta}$ | *w[1118]; Df(2L)BSC812, P+PBac{w[+mC]=XP3.WH3}BSC812/SM6a* | BDSC |
| 18531 | $CG31731^{PBac}$ | *w[1118]; PBac{w[+mC]=WH}CG31731[f02254]* | BDSC |
| 59537 | $CG31731^{Mi\{MIC\}}$ | *y[1] w[*]; Mi{y[+mDint2]=MIC}CG31731[MI14571]/SM6a* | BDSC |
| 22597 | $CG31731^{P\{EPgy2\}}$ | *y[1] w[67c23];P{w[+mC] y[+mDint2]=EPgy2}CG31731[EY22955]* | BDSC |
| v11082 | $CG31731^{RNAi\text{-}GD1133}$ | *w[1118] P{GD1133}v11082* | VDRC |
| v107135 | $CG31731^{RNAi\text{-}KK104197}$ | *P{KK104197}VIE-260B* | VDRC |
| 65080 | $CG31731^{RNAi\text{-}HMC06027}$ | *y[1] sc[*] v[1]; P{y[+t7.7] v[+t1.8]=TRiP.HMC06027}attP40* | TRiP |
| 38353 | $CG1718^{RNAi\text{-}HMS01821}$ | *y[1] v[1]; P{y[+t7.7] v[+t1.8]=TRiP.HMS01821}attP40* | TRiP |
| 38329 | $CG1718^{RNAi\text{-}HMS01796}$ | *y[1] sc[*] v[1]; P{y[+t7.7] v[+t1.8]=TRiP.HMS01796}attP2* | TRiP |
| v44449 | $CG1718^{RNAi\text{-}GD3708(49)}$ | *w[1118]; P{GD3708}v44449* | VDRC |
| v44451 | $CG1718^{RNAi\text{-}GD3708(51)}$ | *w[1118]; P{GD3708}v44451* | VDRC |
| v105608 | $CG1718^{RNAi\text{-}KK100452}$ | *P{KK100452}VIE-260B* | VDRC |
| 58885 | $CG1718^{miR\text{-}1007\text{-}KO}$ | *w[*] TI{TI}mir-1007[KO] CG1718[mir-1007-KO]* | BDSC |
| | $draper^{-/-}$ | *draperΔ5* | Estee Kurant |
| 67034 | $draper^{RNAi}$ | *y[1] w[*]; P{w[+mC]=UAS-drpr.dsRNA}2/CyO* | Marc Freeman |
| 28556 | $Ced\text{-}12^{RNAi}$ | *y[1] v[1]; P{y[+t7.7] v[+t1.8]=TRiP.HM05042}attP2* | TRiP |

**Table 2.2 Antibodies**

| Antibody | Host | Dilution | Source |
|---|---|---|---|
| anti-Draper | Rabbit | 1:200 | Marc Freeman |
| anti-Discs Large (Dlg) | Mouse | 1:100 | Developmental Studies Hybridoma Bank |
| anti-cleaved Dcp-1 | Rabbit | 1:100 | Cell Signaling Technology |
| anti-mouse Cy3 | Goat | 1:100 | Jackson ImmunoResearch |
| anti-rabbit Cy3 | Goat | 1:100 | Jackson ImmunoResearch |
| anti-rabbit AlexaFluor 647 | Goat | 1:100 | Jackson ImmunoResearch |

**Figure 2.1 The GAL4/UAS binary system**

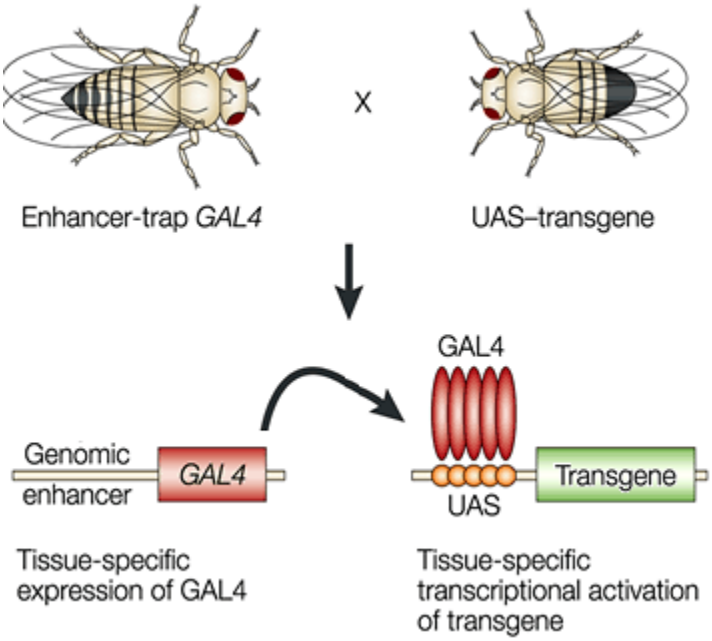


In the GAL4-UAS binary system, one parent carries the *GAL4* yeast transcription factor downstream of an endogenous tissue-specific enhancer, while the other parent caries the target transgene downstream of a UAS site. In their resulting offspring, GAL4 can recognize and bind the UAS site to induce tissue-specific expression of the target transgene. (Figure modified from Muqit and Feany, 2002)

**Figure 2.2 GR1-GAL4 expression in egg chambers**

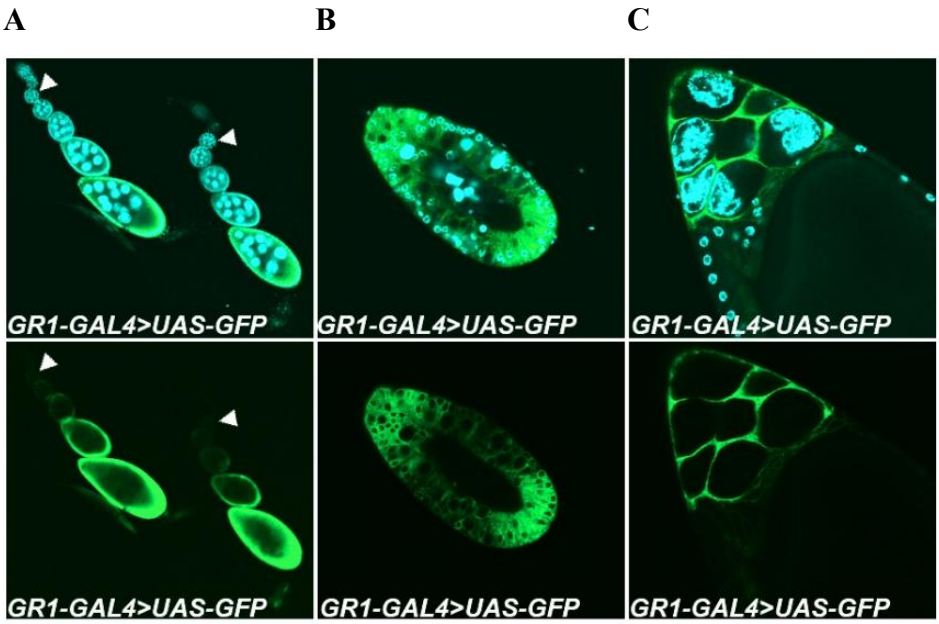


Images show egg chambers expressing endogenous GFP specifically in the follicle cells (*GR1-GAL4/UAS-GFP*). *GR1*-mediated *GFP* expression is observed beginning in stage 3 egg chambers (arrowheads), specifically in the **(A)** epithelial follicle cells including those in **(B)** mid-stage dying egg chambers and in the **(C)** specialized stretched follicle cells. (Figure from Timmons, 2015)

# CHAPTER 3: RESULTS AND DISCUSSION

## 3.1 Background

Programmed cell death (PCD) is a necessary biological process in animal development and tissue homeostasis that facilitates the selective removal of excess, damaged, and potentially deleterious cells. (Jacobson et al., 1997; Elliott and Ravichandran, 2010; Fuchs and Steller, 2011). Cells undergoing PCD are rapidly cleared by phagocytes in a multi-step engulfment process involving recognition followed by internalization of the dying cell (Figure 1.1) (Fullard et al., 2009; Elliot and Ravichandran, 2010). Genetic studies in *C. elegans* have identified two parallel but partially redundant signaling pathways, CED-1/-6-/7 and CED-2/-5/-12, that regulate the engulfment process (Figure 1.2) (Kinchen et al., 2005; Mangahas and Zhou, 2005). These pathways appear to be conserved in mammals in MEGF10/GULP/ABCA1 and Crk/DOCK180/ELMO, and in *Drosophila* in Draper/Ced-6 and Crk/MBC/Ced-12, respectively (Table 1.1) (Mangahas and Zhou, 2005; Fullard et al., 2009). The *Drosophila* homolog for CED-7/ABCA1 has not been identified. To elucidate the precise roles and molecular mechanisms of these evolutionarily conserved signaling pathways during engulfment, it would be beneficial to identify and characterize all the components of the engulfment machinery, especially the *Drosophila* homolog for CED-7/ABCA1.

The *ced-7/ABCA1* genes encode ABCA transporters (Wu and Horvitz, 1998; Luciani and Chimini, 1996). To search for putative *ced-7/ABCA1* orthologs, we identified 56 *ABC* genes in the *Drosophila* genome, 10 of which encoded members of the ABCA

family, and only 2 are expressed at appreciable levels in the ovary, *CG31731* and *CG1718* (Table 1.2). *CG1718* was previously implicated in lipid and cholesterol homeostasis (Bujold et al., 2010; White et al., 2017), suggesting that the protein may act as the functional equivalent of *ABCA1*. However, separate studies did not observe a role for *CG1718* in axon degeneration (Ziegenfuss, 2012). *CG31731* has remained largely uncharacterized, although several genome wide phylogenetic analyses of ABCA proteins in *Drosophila, C. elegans,* and humans, have identified a closer evolutionary relationship between *ced-7/ABCA1* and *CG31731* versus *CG1718* (Figure 1.4) (Dermauw et al., 2013; Dermauw and Van Leeuwen, 2014). The lack of data for either gene implies much more research is needed to determine whether they are involved in PCD.

To identify a potential role for *CG31731* or *CG1718* in PCD, we analyzed their function during developmental and starvation-induced PCD in the *Drosophila* ovary. During the late-stages of oogenesis, 15 germline-derived nurse cells undergo developmental PCD and are cleared by neighboring phagocytic follicle cells (Figure 1.7). It has been shown that phagocytosis genes including *draper* and *Ced-12*, are required in the follicle cells for the death and removal of the nurse cells, suggesting that the follicle cells directly promote the death of the nurse cell by phagoptosis. Genetically knocking down these and other engulfment genes in the follicle cells disrupts clearance of the nurse cell remnants, resulting in stage 14 egg chambers that exhibit persisting nurse cells (Timmons et al., 2016).

During mid-oogenesis, the nurse cells can undergo PCD in response to physiological stress. Mid-stage egg chambers from adult females starved of protein can

exhibit apoptotically and autophagically dying nurse cells (Jenkins et al., 2013). As the nurse cells degenerate, the surrounding phagocytic follicle cells synchronously enlarge to engulf the germline debris (Figure 1.8). Functional mutations in engulfment genes including *draper*, *Ced-12*, and *αPS3/βPS integrin* do not appear to affect the death of the nurse cells, however cause defects in their engulfment as follicle cells fail to enlarge normally and only minimally uptake the germline debris. Strikingly, these engulfment defects are accompanied by premature death and disappearance of the follicle cells by phase 5 dying egg chambers, leaving behind unengulfed germline material (Etchegaray et al., 2012; Timmons, 2015; Meehan et al., 2015).

Our observations strongly suggest that *CG31731* is required in the follicle cells for nurse cell clearance during PCD in both late and mid-oogenesis. We show that genetically knocking down *CG31731* in the follicle cells results in persisting nurse cells in late-stage egg chambers, and engulfment defective follicle cells in mid-stage dying egg chambers. We did not find an independent role for *CG1718* in these PCD events, although we have some evidence to speculate that *CG1718* may provide a compensatory mechanism for *CG31731*. Altogether, our findings suggest that CED-7/ABCA1 plays an evolutionarily conserved role during engulfment in *Drosophila* through *CG31731*.

### 3.2 *CG31731* and *CG1718* encode ABC transporters similar to *ced-7/ABCA1*

A search of protein databases revealed that the predicted amino acid sequences of *CG31731* and *CG1718* encode ABC transporters. Like other ABC transporters, *CG31731* and *CG1718* each encode two membrane-spanning TMDs and two cytosolic NBDs with predicted ATP-binding and catalytic capability. Each NBD in CG31731 and CG1718 was

found to contain an ‘A-loop’ (aromatic), ‘Walker A motif’ (GxxGxGKS/T), ‘Q-loop’ (glutamine, Q), ‘ABC signature motif’ (L/YSGGQ/M), ‘Walker B motif’ (φφφφDE), ‘D-loop’ (aspartate, D), and ‘H-loop’ (histidine, H), in highly conserved sequential and spatial organization (Figure 3.2 and Figure 3.3), classifying these proteins as ABC transporters. Additional structural analyses of the predicted amino acid sequences indicate that each CG31731 TMD contains 6 hydrophobic α-helical segments making a 12-pass transporter (Figure 3.1A), while each CG1718 TMD contain 7 hydrophobic α-helical segments making a larger 14-pass transporter (Figure 3.1B). In comparison, both CED-7 and ABCA1each contain 15 transmembrane segments (Figure 3.1C-D) (UniProt.org).

Using Basic Local Alignment Search Tool (BLAST) algorithms to compare the predicted amino acid sequences of CG31731 and CG1718 with CED-7 and ABCA1, a substantial amout of similarity and identity was found throughout their entire length, and most notably in the regions of the catalytic NBDs (Figure 3.2 and Figure 3.3). CG31731 was found to be 20% identical to CED-7 with 577 similar amino acid positions, and 18% identitical to ABCA1 with 584 similar amino acid positions. Even more immpresive, CG1718 was found to be 25% identical to both CED-7 and ABCA1 with 642 and 562 similar amino acid positions, respectively. The greater sequence similarity to CED-7 and ABCA1 suggests *CG1718* is evolutionarily closer to *ced-7* and *ABCA1* compared to *CG31731*. However, CED-7 and ABCA1 only share 18.5% identity and 635 similar amino acid positions, indicating that a higher identity does not necessarily correlate to functional homology.

Additional homology searches using the *Drosophila* RNAi Screening Center (DRSC) Interative Ortholog Prediction Tool (DIOPT) revealed that *CG31731* is the best predicted ortholog of *ced-7* in *Drosophila*. *CG1718* was also listed as a putative *ced-7* ortholog, although the gene ranked much lower than *CG31731* and several other predicted *Drosophila* genes. Unexpectedly, both the human and mouse *ABCA1* was not predicted as an ortholog of *ced*-7, though it was for *CG31731* and *CG1718*, albeit very low on the list. Nonetheless, *ABCA1* has been experimentally shown to be required for engulfment in multiple systems, serving as the functional equivalent of *ced-7*. *ABCA7*, which does not appear on the list, has also been shown to have a role in engulfing glia (Jehle et al., 2006). These discrepancies highlight the inadequacy of identifying orthologs merely via sequence analyses. To unambiguously determine the *ced-7* ortholog in *Drosophila*, it was necessary to study the functional role of putative genes including *CG31731* and *CG1718* in PCD.

### 3.3 *CG31731* and *CG1718* genes and insertions

The *CG31731* gene is located on chromosome 2L, 34D1 on the cytogenetic map, and extends from 13,784,084–13,790,562. There are 2 mRNA transcripts associated with the gene, *CG31731-RC* and *CG31731-RB* (Figure 3.5A). Structural analyses of the predicted amino acid sequence translated from each transcript indicate that *CG31731-RC* merely encodes a truncated protein containing 6 transmembrane segments, while *CG31731-RB* encodes the full 12-pass ABC transporter (Uniprot.org). The *CG1718* gene is located on chromosome X, 19F3 on the cytogenetic map, and extends from 21,292,308–21,306,665. There are 3 mRNA transcripts associated with the gene,

*CG1718-RB, CG1718-RC,* and *CG1718-RD* (Figure 3.6). Sequence alignment indicated that all 3 transcripts encode almost identical polypeptides that form 14-pass ABC transporters (UniProt.org).

A number of genetic tools are readily available to study the *in vivo* function of both genes. There are three alleles of *CG31731*, each carrying a different transgenic transposon: *P{EPgy2}*, *PBac{WH}*, or *Mi{MIC}* (Figure 3.5A-B). The *P{EPgy2}* construct is inserted after the first 2 nucleotides in the first coding exon, and contains GAGA and UAS-binding sites upstream of the promoter (Bellen et al., 2004; Bellen et al., 2011). These elements and the inserted orientation of the *P{EPgy2}* construct allows for GAL4-transcriptional regulation of the gene to over-express the gene. The *PBac{WH}* construct is inserted towards the end of the first coding exon, and contains Su(Hw)-binding sequences, an FRT site, and a UAS-binding site (Bellen et al., 2011). The Su(Hw) sequences allow for the binding of Su(Hw) proteins, which serve as molecular insulators that alter the local chromatin organization to inactivate the gene. Lastly, the *Mi{MIC}* construct is inserted in the intronic region between the second and third exon, and contains a splice acceptor site followed by stop codons in all three reading frames, and a downstream EGFP coding sequence followed by a polyadenylation signal (Venken et al., 2011). The insertion of the *Mi{MIC}* construct in an intron allows it to function as both a gene trap and a protein trap to prematurely terminate transcription and translation of the gene. The resulting protein should in theory only contain a single transmembrane segment without any ABC transporter activity. Collectively, these transgenic alleles provide the tools to over-express or disrupt *CG31731* to study its function.

Additionally, there are 3 RNAi lines available from the GD, KK, and HMC RNAi libraries, that specifically target the *CG31731* mRNA transcripts. Respectively, the $GD^{1133}$ and $KK^{104197}$ RNAi constructs target exons 13 and 14, and therefore only knock down the *CG31731-RB* transcript encoding the full ABC transporter. The $HMC^{06027}$ RNAi construct targets exon 6 and therefore could knock down both the *CG31731-RB* and *–RC* transcripts (Figure 3.5A). At the time this project began, only the GD and KK RNAi lines, which both encode long hairpin RNAs, were available. To optimize our study of *CG31731* in the germline-derived nurse cells, we requested DRSC/TRiP to generate the HMC RNAi line, which expresses short hairpin RNA sequences for effective knockdown in the germline. In *C. elegans*, CED-7 was reported to be required in both the phagocytic cells and the dying cells for efficient engulfmen (Wu and Horvitz, 1998). Using these RNAi lines and various GAL4 tissue-specific drivers, we can suppress *CG31731* gene expression only in specific cell types, including in the somatically-derived phagocytic follicle cells or the germline-derived dying nurse cells, to identify in which cell type it may be functioning.

Similarly, a number of RNAi constructs are readily available for the study of *CG1718* (Figure 3.6). There are 2 HMS RNAi lines which express short hairpin RNA sequences, and 2 GD and 1 KK RNAi line which express long hairpin RNA sequences, for RNAi-mediated *CG1718* gene silencing in the germ cells or somatic cells. All the RNAi constructs target regions in all 3 mRNA transcripts associated with the *CG1718* gene. Furthermore, there is an additional *miR-1007* knockout mutant strain, in which the expression of *CG1718* was reported to be affected (Chen et al., 2014). The *miR-1007*

gene is nestled in one of the intronic regions of *CG1718*. A systematic study of *Drosophila* microRNA (miR) functions conveniently generated the $CG1718^{miR\text{-}1007\text{-}KO/\ miR\text{-}1007\text{-}KO}$ strain, confirmed via PCR. Quantitative RT-PCR of the *CG1718* host gene in $CG1718^{miR\text{-}1007\text{-}KO/\ miR\text{-}1007\text{-}KO}$ mutants showed a reduced expression of *CG1718* (Chen et al., 2014), suggesting that the $miR\text{-}1007^{KO}$ mutation generates a hypomorphic allele of *CG1718*.

### 3.4 *CG31731* mutants have persisting nurse cell corpses in the ovary

To determine whether *CG31731* or *CG1718* can act as a functional equivalent for *ced-7/ABCA1* during PCD, we analyzed their engulfment function in oogenesis, during which 15 germline-derived nurse cells undergo PCD and are cleared. In wild-type developing egg chambers, clearance of the 15 nurse cells begin after they complete "dumping" of their cytoplasmic contents into the oocyte in stage 12. By stage 14, all the nurse cells are cleared leaving only the mature oocyte. To observe any engulfment defects, we stained fixed ovaries with DAPI to label DNA from *CG31731* mutants and looked for the presence of uncleared persisting nurse cell nuclei.

In several different *CG31731* mutant strains, we observed significant engulfment defects characterized by the presence of ≥4 persisting nurse cell nuclei in stage 14 egg chambers. In ovaries from homozygous $CG31731^{PBac/\ PBac}$ or $CG31731^{Mi\{MIC\}/Mi\{MIC\}}$ mutants, and hemizygotes in trans to a deficiency, $CG31731^{PBac/-}$ or $CG31731^{Mi\{MIC\}/-}$, most developing egg chambers failed to clear all 15 nurse cells by stage 14 and exhibited persisting nurse cell nuclei (Figure 3.7A). Homozygous $CG31731^{PBac/\ PBac}$ mutants displayed the weakest engulfment defective phenotype with only approximately 34% of

the stage 14 egg chambers displaying ≥4 persisting nurse cell nuclei. Interestingly, the heterozygous *CG31731*$^{PBac/Mi\{MIC\}}$ and hemizygous *CG31731*$^{PBac/-}$ mutants displayed a similar phenotype to the *CG31731*$^{Mi\{MIC\}/Mi\{MIC\}}$ mutants, with approximately 74-80% of stage 14 egg chambers displaying ≥4 persisting nurse cell nuclei, and an average of 6 persisting nuclei per stage 14 egg chamber (Figure 3.7B-C). The weaker phenotype observed in the *CG31731*$^{PBac/\ PBac}$ egg chambers relative to the other mutants suggests the *CG31731*$^{PBac}$ allele is a weak hypomorph. The strongest phenotype was observed in hemizygous *CG31731*$^{Mi\{MIC\}/-}$ mutants, of which approximately 95% displayed ≥4 with an average of 8 persisting nurse cell nuclei per stage 14 egg chamber (Figure 3.7B-C). The *Mi{MIC}* insertion provides both a gene trap and a protein trap, which in theory should efficiently generate a null allele. However, the more severe persisting phenotype in *CG31731*$^{Mi\{MIC\}/-}$ mutants with a deficiency allele compared to homozygous *CG31731*$^{Mi\{MIC\}/Mi\{MIC\}}$ mutants suggest that the *CG31731*$^{Mi\{MIC\}}$ allele only causes a partial loss of expression in *CG31731*, unless other genes affected by the deficiency are contributing to the more severe phenotype. Based on only our genetic analyses, the *CG31731*$^{Mi\{MIC\}}$ allele is not a null but a strong hypomorph. While the expression of the *CG31731*$^{PBac}$ and *CG31731*$^{Mi\{MIC\}}$ alleles is not certain, it is evident that the manner by which both mutations disrupt the *CG31731* gene show that *CG31731* plays an important role in nurse cell clearance during late oogenesis.

The *P{EPgy2}* construct did not appear to disrupt the *CG31731* gene as egg chambers from heterozygous and hemizygous *CG3173*$^{P\{EPgy2\}}$ mutants did not display any significant defects in engulfment or persisting nuclei phenotype (Figure 3.8A-B).

This is not surprising since none of the elements in the *P{EPgy2}* construct provides the means to negatively regulate *CG31731* gene expression. In theory, the *P{EPgy2}* insert could disrupt the gene since the construct is inserted such that it interrupts the start codon (Figure 3.4). However, several other ATG start codons downstream of the insertion, one of which starts the second exon (Figure 3.4), would allow normal transcription of *CG31731*. In this case, starting transcription at the second exon is likely inconsequential, since the first exon encodes a likely non-essential non-membrane-spanning segment of TMD1. Thus, the $CG3173^{P\{EPgy2\}}$ allele likely encodes a functional CG31731 ABC transporter. Enhanced expression of *CG31731* with the *P{EPgy2}* construct specifically in the phagocytic stretched follicle cells, the follicle cells, or the dying nurse cells, also did not disrupt nurse cell clearance (Figure 3.9A-B).

We found that mutants carrying only one copy of a hypomorphic allele or a deficiency of *CG31731* in trans to a WT allele did not exhibit any notable defects in nurse cell clearance (Figure 3.10). Although a few stage 14 egg chambers had persisting nurse cell nuclei, in most developing egg chambers all 15 nurse cells were removed by stage 14. These findings suggest that *CG31731* is not haploinsufficient, and one copy of the *CG31731* allele is sufficient for its protein function during engulfment.

**3.5 *CG31731* is required in the follicle cells for nurse cell clearance during developmental PCD**

Our analyses of the $CG31731^{PBac}$, $CG31731^{Mi\{MIC\}}$, and $CG31731^{-}$ mutants show that *CG31731* is involved in nurse cell clearance during oogenesis. We next wanted to discern in which cell type *CG31731* function is required to facilitate removal of the nurse

cells. Studies in *C. elegans* showed that CED-7 is required in both the phagocytic cell and the dying cell for efficient engulfment of cell corpses (Wu and Horvitz, 1998), while studies in mammals showed that ABCA1 expression in phagocytic cells is sufficient for engulfment (Hamon et al., 2000). In the *Drosophila* ovary, the nurse cells become surrounded by the phagocytic stretched follicle cells, which facilitate the engulfment of the dying nurse cells. The loss of important engulfment proteins including Draper and Ced-12 in the stretched follicle cells and follicle cells have been shown to prevent engulfment of the nurse cell corpses (Timmons et al., 2016). To determine in which cell type *CG31731* acts during engulfment of the nurse cells, we used tissue specific drivers to express *CG31731* RNAi constructs specifically in the stretched follicle cells, follicle cells, or nurse cells.

Unexpectedly, the expression of *CG31731* RNAi specifically in the stretched follicle cells (*PG150>CG31731*$^{RNAi}$) did not disrupt clearance of the nurse cells (Figure 3.11A-B). Most of the stage 14 egg chambers successfully cleared all 15 nurse cells and did not have any persisting nurse cell nuclei. We speculated that perhaps *CG31731* is expressed much earlier in development before the stretched follicle cells specialize from the follicle cells. Consistent with this hypothesis, we observed a requirement for *CG31731* expression in the follicle cells, as *CG31731* knockdown specifically in the follicle cells (*GR1>CG31731*$^{RNAi}$) resulted in stage 14 egg chambers exhibiting persisting nurse cell nuclei (Figure 3.12A). Approximately 87% of the stage 14 egg chambers expressing the *GD*$^{1133}$ RNAi construct and 67% expressing either the *KK*$^{104197}$ or *HMC*$^{06027}$ RNAi construct displayed ≥4 persisting nurse cell nuclei, with an average of 7

and 4-5 persisting nuclei respectively (Figure 3.12B-C). In developing egg chambers, the stretched follicle cells differentiate from the follicle cells during a series of migration events after stage 8. These data indicated that *CG31731* is primarily expressed before stage 8 in the follicle cells, where it is required for nurse cell clearance. The stretched follicle cells likely retain some of its molecular components that were present in the cell prior to becoming specialized follicle cells, suggesting that while *CG31731* expression is not required in the stretched follicle cells, presence of the CG31731 protein is likely required in these specialized follicle cells for their phagocytic function.

To verify that the *CG31731* RNAi constructs specifically knock down *CG31731*, we expressed the *CG31731* RNAi constructs in a $CG31731^{P\{EPgy2\}}$ background, where *CG31731* expression should be enhanced. The rescue of engulfment defects observed in $GR1>CG31731^{RNAi}$ egg chambers with the $CG31731^{P\{EPgy2\}}$ allele would suggest that the RNAi constructs accurately target *CG31731*. However, we did not observe any reduction in persisting nurse cell nuclei, or rescue phenotype in these double mutants. Instead, our quantifications indicate a similar phenotype between these double mutants and $GR1>CG31731^{RNAi}$ only egg chambers (Figure 3.13). After these experiments, it was discovered that the $CG31731^{P\{EPgy2\}}$ parental stock used generate the F1 double mutants was contaminated. While we are not certain that the double mutants weren't also contaminated, at the time the double mutants were generated, they were visually checked to carry the correct markers and balancers. Assuming the double mutants were correct, we considered the possibility that the $GD^{1133}$ and $KK^{104197}$ RNAi constructs may be targeting other genes. This is unlikely since both sequences perfectly target several

hundred nucleotide sequences in *CG31731* transcripts. Moreover, a BLAST search of the sequences of both RNAi constructs identified *CG31731* as the single on-target hit, consistent with the information provided by VDRC. Another possibility is that there is not enough GAL4 synthesized to simultaneously drive the expression of both $CG31731^{RNAi}$ and $CG31731^{P\{EPgy2\}}$, and GAL4 may preferentially bind the UAS sequences upstream of the $CG31731^{RNAi}$ rather than $CG31731^{P\{EPgy2\}}$ transgene. Alternatively, the RNAi machinery may be superbly robust and efficiently knock down *CG31731* mRNA transcripts even when in abundance, effectively silencing *CG31731* gene expression. From our data, it is not clear exactly what is happening at the molecular level, but the simultaneous expression of $CG31731^{P\{EPgy2\}}$ does not appear to rescue the engulfment defects in follicle cell specific $CG31731^{RNAi}$ expressing egg chambers.

In *C. elegans*, CED-7 was found to be required in the phagocytic and the dying cells for efficient engulfment (Wu and Horvitz, 1998). To determine whether *CG31731* may also act in dying cells in *Drosophila*, we knocked down *CG31731* specifically in the nurse cells ($nanos>CG31731^{RNAi}$), which undergo PCD during oogenesis. Contrarily, we did not observe a requirement for *CG31731* in the dying nurse cells. Egg chambers expressing $CG31731^{RNAi}$ specifically in the nurse cells did not appear to have any engulfment defects and were able to clear the nurse cells normally (Figure 3.14A-B). While GD and KK RNAi libraries generate long hairpin RNA sequences, which are typically ineffective for RNAi-mediated knockdown in the germline, the $HMC^{06027}$ encoded short hairpin RNA sequence should competently knockdown *CG31731* expression in the germline-derived nurse cells. The lack of persisting nurse cell corpses in

any of these *CG31731* RNAi expressing stage 14 egg chambers suggest that unlike CED-7, CG31731 is not required in the dying cells for their engulfment.

**3.6 *CG1718* may act with *CG31731* in the follicle cells for nurse cell clearance during developmental PCD**

We also examined the engulfment function of *CG1718*, another putative CED-7 homolog, in nurse cell clearance during oogenesis. *CG1718* encodes another ABCA protein that is expressed in the ovary, and has been proposed as the *Drosophila* homolog of ABCA1 for its activity in lipid and cholesterol homeostasis (Bujold et al., 2010). However, studies in neuronal corpses and engulfing glia did not observe a role for *CG1718* (Ziegenfuss, 2012). To determine whether *CG1718* has a role in nurse cell clearance, we looked for persisting nurse cell nuclei in *CG1718* mutants.

Similar to our genetic studies of *CG31731*, we did not observe a requirement for *CG1718* in the nurse cells for their removal. Egg chambers expressing $CG1718^{RNAi}$ specifically in the nurse cells ($nanos>CG1718^{RNAi}$) normally cleared all 15 nurse cell remnants by stage 14 (Figure 3.15). Intriguingly, while egg chambers expressing one of four different $CG1718^{RNAi}$ transgenes specifically in the follicle cells ($GR1>CG1718^{RNAi}$) also appeared to normally clear the dying nurse cells, expression of the $HMS^{01821}$ RNAi construct specifically in the follicle cells resulted in moderate engulfment defects (Figure 3.16A-B). Quantification of the stage 14 egg chambers expressing $CG1718^{HMS01821}$ in the follicle cells indicated approximately 45% displayed ≥4 and an additional 30% displayed 1-3 persisting nurse cell nuclei (Figure 3.16B). Unique from the other *CG1718* RNAi constructs, the $HMS^{01821}$ RNAi sequence targets the 3 prime untranslated regions

(3'UTRs) of the *CG1718* transcripts (Figure 3.6). While studies have reported that compared to the coding region the 3'UTR is often less accessible, some studies have shown that the 3'UTR can provide more effective targets for RNAi-mediated knock down of certain genes (Lai et al., 2013). It is tempting to speculate that the other *CG1718* RNAi constructs, which target the coding regions of *CG1718*, ineffectively knock down *CG1718*, while the $HMS^{01821}$ RNAi construct effectually does. Another possibility is that the $HMS^{01821}$ RNAi encoded sequence may be targeting another gene. A BLAST search of the RNAi sequence on Flybase identified *CG1718* as the single on-target hit (E-value=0.00018). The search also revealed potential off-target hits including the intronic region of *pointed* (E-value=0.17348), the 3'UTR of *smooth* (E-value=0.17348), the coding exon of *CG44004* (E-value=0.68550), and the 3'UTR of *snx6*. Perhaps not by coincidence, *pointed* has been implicated in phagocytosis in S2 cells (Stroschein-Stevenson et al., 2006) and in follicle cell development (Dobens and Raftery, 2000). Therefore the phenotypes observed in egg chambers expressing $CG1718^{HMS01821}$ in the follicle cells may actually be associated with off-target knockdown of *pointed*. Nevertheless, there is still a possibility that the knockdown was on-target and that *CG1718* may act in the phagocytic follicle cells for removal of the nurse cells during oogenesis.

Since *CG1718* and *CG31731* both encode ABC transporters of the ABCA family, which share a common function in lipid transport, we wondered whether they could provide compensatory roles for each other. We used the *GR1-GAL4* driver to express both $CG1718^{HMS01821}$ and $CG31731^{P\{EPgy2\}}$ specifically in the follicle cells, to

simultaneously knock down *CG1718* and over-express *CG31731*. The rescue of engulfment defects observed in *GR1>CG1718*$^{HMS01821}$ egg chambers with an over-expression of *CG31731* would suggest that CG31731 can compensate for the lack CG1718. Our quantifications of these mutants showed that expression of *CG31731*$^{P\{EPgy2\}}$ did not significantly reduce or rescue the number of persisting nurse cell corpses in follicle cell-expressing *CG1718*$^{HMS01821}$ egg chambers (Figure 3.17B-C). These data do not definitively rule out the potential for compensatory functions between the *ABCA* genes, especially since the over-expression of *CG31731* with the *P{EPgy2}* construct is questionable. Additional studies are needed to determine whether CG1718 and CG31731 can actually compensate for each other during engulfment in the ovary.

In *CG1718*$^{miR\text{-}1007\text{-}KO/\ miR\text{-}1007\text{-}KO}$ mutants, the expression of *CG1718* was reported to be reduced (Chen et al., 2014). We also analyzed egg chambers from these mutants and did not observe any prominent engulfment defects as most developing egg chambers successfully cleared the nurse cells by stage 14 (Figure 3.18A-C). To further explore a potential relationship between CG1718 and CG31731, we generated *CG1718*$^{miR\text{-}1007\text{-}KO/\ miR\text{-}1007\text{-}KO}$+*CG31731*$^{PBac/\ PBac}$ double mutants carrying homozygous hypomorphic alleles of both genes. To our surprise, these double mutants exhibited a much more severe persisting nuclei phenotype than either single mutant alone (Figure 3.18A). Interestingly, the *CG1718*$^{miR\text{-}1007\text{-}KO/\ miR\text{-}1007\text{-}KO}$+*CG31731*$^{PBac/\ PBac}$ mutants displayed a similar engulfment defective phenotype to *CG31731*$^{PBac/-}$, *CG31731*$^{PBac/Mi\{MIC\}}$, and homozygous *CG31731*$^{Mi\{MIC\}/Mi\{MIC\}}$ mutants (Figure 3.7A-C), with approximately 83% of egg chambers displaying ≥4 persisting nurse cell nuclei, and an average of 6 persisting nuclei

per stage 14 egg chamber (3.18B-C). The much more severe phenotype observed in *CG1718*$^{miR\text{-}1007\text{-}KO/\ miR\text{-}1007\text{-}KO}$+*CG31731*$^{PBac/\ PBac}$ double mutants indicate a functional relationship between the two ABCA transporters, and suggest *CG1718* may provide a compensatory function for *CG31731* during nurse cell clearance in developing egg chambers.

**3.7 *CG31731* acts in parallel to *Ced-12* likely in the same pathway as *draper***

The engulfment mechanism is primarily regulated by two parallel signaling pathways, CED-1/-6/-7 and CED-2/-5/-12 (Mangahas and Zhou, 2005; Fullard et al., 2009). Previous work in our lab has shown that the Draper and Ced-12 pathways act in parallel to regulate engulfment of the nurse cells during oogenesis. Double mutants expressing *draper*$^{RNAi}$+*Ced-12*$^{RNAi}$ in the follicle cells exhibit a significantly more severe persisting nurse cell phenotype compared to either single mutant alone (Timmons et al., 2016). In *C. elegans* and mammals, CED-7/ABCA1 acts in the same pathway as CED-1/MEGF10 parallel to CED-12/ELMO. The similarities we have observed between CG31731 and CED-7 suggest CG31731 may act in the same pathway as Draper and parallel to Ced-12. To ascertain which pathway CG31731 is involved in during engulfment, we generated *CG31731*+*draper* and *CG31731*+*Ced-12* double mutants and analyzed the severity of their engulfment defects in nurse cell clearance.

We showed that homozygous *CG31731*$^{Mi\{MIC\}/Mi\{MIC\}}$ mutants exhibit a strong engulfment defect in developing egg chambers, of which approximately 74% display ≥4 persisting nurse cell nuclei and each stage 14 egg chamber display an average of 6 persisting nuclei (Figure 3.7B-C). Because *Ced-12* deficiency mutations are lethal due to

the requirement for Ced-12 during border cell migration (Geisbrech et al., 2012), we knocked down *Ced-12* expression only in the phagocytic follicle cells (*GR1>Ced-12$^{RNAi}$*). In these *Ced-12* mutants, approximately 94% of stage 14 egg chambers display ≥4 persisting nurse cell nuclei, with an average of 7 persisting nuclei (Figure 3.20B-C). Impressively, in the *CG31731$^{Mi\{MIC\}/Mi\{MIC\}}$+GR1>Ced-12$^{RNAi}$* double mutants, 99.9% of the stage 14 egg chambers displayed ≥4 persisting nurse cell, and a considerable percentage of them completely failed to clear any of the nurse cell corpses (Figure 3.20C). We were excited to find that the double mutants exhibited a much more severe engulfment defect than either single mutant alone. Similar to *draper$^{RNAi}$+Ced-12$^{RNAi}$* double knockdowns, *CG31731$^{Mi\{MIC\}/Mi\{MIC\}}$+GR1>Ced-12$^{RNAi}$* double mutants exhibit severely impaired engulfment mechanisms in a large majority of the egg chambers. These findings demonstrate that CG31731 acts in parallel to Ced-12, and its function is important for engulfment of the nurse cells.

To clarify whether CG31731 acts in the same pathway as Draper, we analyzed these double mutants. Our analyses of *CG31731$^{Mi\{MIC\}/Mi\{MIC\}}$+ draper$^{\Delta 5}$*double mutants compared to *draper$^{\Delta 5}$*single mutants showed a similar phenotype between the two *draper* mutants. Respectively, 99.5% and 100% of stage 14 egg chambers from *draper$^{\Delta 5}$*and *CG31731$^{Mi\{MIC\}/Mi\{MIC\}}$+draper$^{\Delta 5}$*mutants exhibited ≥4 persisting nurse cell nuclei (Figure 3.21C), and both mutants displayed an average of approximately 9-10 persisting nurse cell corpses (Figure B). The similar engulfment defects observed between *CG31731$^{Mi\{MIC\}/Mi\{MIC\}}$+draper$^{\Delta 5}$*double mutants and *draper$^{\Delta 5}$*mutants alone, indicate that CG31731 likely acts in the same pathway as Draper.

The evolutionarily conserved engulfment mechanism implicates a role for ABC transporters, specifically those of the ABCA family. Consistent with CED-7/ABCA1 acting in the same pathway as CED-1/MEGF10 and parallel to CED-12/ELMO (Mangahas and Zhou, 2005; Fullard et al., 2009), our double mutant analyses show that CG31731 acts in the same pathway as Draper and in parallel to Ced-12. Altogether, our findings thus far strongly suggests CG31731 may serve as the functional equivalent for CED-7/ABCA1 in *Drosophila*, and that the function of a CED-7-/ABCA1-like transporter is conserved in *Drosophila* through CG31731.

**3.8 *CG31731* promotes Draper enrichment surrounding the nurse cells**

During engulfment, CED-1/MEGF10 is observed to accumulate at the phagocytic cup and cluster around cell corpses (Zhou et al., 2001; Hamon et al., 2006). Presumably, in the presence of dying cells, CED-1/MEGF10 clusters at the phagocytic cup to recognize dying cells and facilitate their clearance. *In vivo* and *in vitro* studies in *C. elegans* and mouse cell culture respectively show that the uniform clustering of CED-1/MEGF10 around cell corpses require CED-7/ABCA1 activity (Zhou et al., 2001; Hamon et al., 2006). Our analyses of *CG31731* propose an orthologous function to *ced-7/ABCA1*, suggesting that the CG31731 protein may similarly be required for Draper enrichment during engulfment of the nurse cells in oogenesis.

To examine whether CG31731 may function to promote Draper clustering around the nurse cells, we analyzed late stage egg chambers stained with anti-Draper antibody to label Draper, and DAPI to label DNA, from WT and $CG31731^{Mi\{MIC\}/Mi\{MIC\}}$ mutants. In WT late stage egg chambers, Draper staining becomes enriched specifically in the

phagocytic stretched follicle cells, and clearly surrounds each dying nurse cell (Figure 3.22A) (Timmons et al., 2016). However, in *CG31731*$^{Mi\{MIC\}/Mi\{MIC\}}$ late stage egg chambers, Draper staining is disorganized, unevenly enriched in the stretched follicle cells, and scattered around the nurse cells (Figure 3.22B). Even more strikingly, in some areas Draper staining is completely absent around the nurse cells. These observations indicate that in *CG31731*$^{Mi\{MIC\}/Mi\{MIC\}}$ egg chambers, Draper fails to properly accumulate on the stretched follicle cell membranes and encircle the dying nurse cells, suggesting a role for CG31731 in Draper clustering at the phagocytic cup.

Draper functions as a recognition receptor of dying cells on the surface of phagocytic cells (Freeman et al., 2003). The lack of Draper staining in some areas of *CG31731*$^{Mi\{MIC\}/Mi\{MIC\}}$ egg chambers suggests that Draper is absent from the stretched follicle cells, and thus Draper-mediated recognition of the dying nurse cells is not achieved, resulting in their persistence. Consistent with Draper known to normally localize to the membrane of engulfing cells, we detected normal Draper staining along the follicle cell membranes of mid-stage egg chambers, suggesting Draper localization to the follicle cell membrane is not disrupted. In the mere failure of Draper accumulation around the nurse cells, Draper staining should still be detected in the stretched follicle cells. Therefore we speculate that perhaps in areas lacking Draper staining, the stretched follicle cells failed to extend and reach the nurse cells, and are themselves absent. Consistent with this hypothesis, when *draper* is knocked down specifically in the follicle cells, some nurse cells do not appear to be surrounded by the stretched follicle cells (Timmons et al, 2016). It is speculated that CED-7 with CED-1 and DYN-1 may function

to promote intracellular vesicle delivery to the membrane to provide lipid and protein sources to the growing phagocytic cup (Zhou et al., 2008). Perhaps in *CG31731*$^{Mi\{MIC\}/Mi\{MIC\}}$ mutants and in *draper*$^{RNAi}$ mutants, a lack of membrane material at the growing phagocytic cup prevents the stretched follicle cells from extending and reaching some nurse cells. This would explain the areas lacking Draper staining, which appear to be farthest from the stretched follicle cells spanning the outer limits of the egg chamber.

**3.9 *CG31731* has a role in acidification of the nurse cells**

Previous work in our lab has shown that in addition to recognition of the dying nurse cells, Draper activity in the follicle cells is also required for acidification and subsequent degradation of the nurse cells (Timmons et al., 2016). Since Draper enrichment and clustering around the nurse cells is disrupted in *CG31731*$^{Mi\{MIC\}/Mi\{MIC\}}$ mutants, we wondered whether acidification of the nurse cells was also disrupted in these mutants. We looked at egg chambers stained with LysoTracker to label acidified compartments, and DAPI to label DNA, from WT and *CG31731*$^{Mi\{MIC\}/Mi\{MIC\}}$ mutants. In WT developing egg chambers, LysoTracker-positive nurse cells can be detected in stage 12-14 egg chambers (Figure 3.23A/C). The majority of the nurse cells become acidified in stage 12 egg chambers, and by stage 13, almost all the nurse cells have been acidified and cleared with only a few remaining in the LysoTracker or DAPI channel. By stage 14, all the nurse cells appear to have been acidified and cleared, with occasionally a few detected in the LysoTracker channel but no nurse cell nuclei detected in the DAPI channel (Figure 3.23A). Noticeably, LysoTracker-positive staining visibly corresponds to

a reduction and sometimes absence in DAPI staining of the nurse cell nuclei, suggesting that the acidification of the nurse cell nuclei is directly associated with their degradation and subsequent clearance by our quantification methods.

In comparison, in *CG31731*$^{Mi\{MIC\}/Mi\{MIC\}}$ mutants LysoTracker staining is disrupted, although not completely blocked. Compared to WT where approximately 77% of stage 12 egg chambers exhibit a substantial amount of LysoTracker-positive nurse cells, in *CG31731*$^{Mi\{MIC\}/Mi\{MIC\}}$ mutants over 85% of stage 12 egg chambers do not exhibit any LysoTracker staining (Figure 3.23C). Intriguingly, a slightly higher percentage of stage 13 and stage 14 *CG31731*$^{Mi\{MIC\}/Mi\{MIC\}}$ egg chambers compared to WT exhibit LysoTracker-positive staining, suggesting in these mutants acidification of the nurse cells is delayed. In *CG31731*$^{Mi\{MIC\}/Mi\{MIC\}}$ late stage egg chambers that do exhibit LysoTracker staining, a markedly fewer number of nurse cells are LysoTracker-positive and most of the stage 14 persisting nuclei do not appear to become acidified, suggesting acidification may be blocked in these persisting nuclei. Since our observations in WT egg chambers illustrated a direct link between acidification, degradation, and clearance of the nurse cells, it makes sense that all these events are blocked in uncleared persisting nuclei. Altogether, these observations suggest CG31731 has a role in promoting acidification of the nurse cells for their effective removal.

We showed that in *CG31731*$^{Mi\{MIC\}/Mi\{MIC\}}$ mutants, Draper fails to properly accumulate around the dying nurse cells. Previous work from our lab has shown that LysoTracker staining of the nurse cells requires Draper activity (Timmons et al., 2016). We speculated that perhaps the delay in nurse cell acidification in *CG31731*$^{Mi\{MIC\}/Mi\{MIC\}}$

egg chambers results from abnormal Draper activity. However, the acidification defect in *draper*$^{RNAi}$ egg chambers was found to be much more pronounced with acidification blocked rather than delayed in over 70% of egg chambers (Timmons et al., 2016), suggesting that in *CG31731*$^{Mi\{MIC\}/Mi\{MIC\}}$ egg chambers the function of Draper is not completely disrupted since acidification proceeds relatively normally in stage 13-14 egg chambers. Therefore the lack of acidified nurse cells in most stage 12 egg chambers and in persisting nuclei in *CG31731*$^{Mi\{MIC\}/Mi\{MIC\}}$ mutants is unlikely a direct result of changes in Draper activity. Instead, the acidification of nurse cells appears to be coordinated by lysosomal machinery, including V-ATPases, on the stretched follicle cell membrane (personal communication, Albert Mondragon). If in *CG31731*$^{Mi\{MIC\}/Mi\{MIC\}}$ mutants the stretched follicle cells fail to surround some nurse cells, lysosomal machinery on the stretched follicle cell membrane would not surround these nurse cells. This would explain their lack of acidification and their subsequent persistence. Alternatively, if CG31731 is required for intracellular trafficking of vesicles to the membrane, perhaps CG31731 is also required for intracellular trafficking of lysosomal machinery, including V-ATPases, to the stretched follicle cell membrane. While more experiments need to be undertaken to elucidate the precise role of CG31731 in engulfment and processing of the nurse cells, we have shown that CG31731 is required for the acidification, subsequent degradation, and clearance of the nurse cells.

### 3.10 *CG31731* is required in the follicle cells for engulfment during induced PCD

The engulfment mechanism regulated by the *ced-1/-6/-7* and *ced-2/-5/-12* pathways is important in engulfing cells for efficient clearance of cell corpses in multiple

PCD systems in *C. elegans* (Mangahas and Zhou, 2005). Likewise, our lab has previously shown that the *draper* and *Ced-12* pathways in *Drosophila* are required in phagocytic cells in at least two distinct PCD events in the ovary, in developmental PCD during which the nurse cells undergo phagoptosis, and in starvation-induced PCD during which the nurse cells undergo apoptosis and autophagic cell death (Etchegaray et al., 2012; Jenkins et al, 2013; Timmons et al, 2016). We have shown that *CG31731* is required in the phagocytic follicle cells during developmental PCD for proper removal of the nurse cells. To determine whether *CG31731* is similarly conserved in another PCD system, we investigated its role during starvation-induced PCD in the ovary.

We selected $CG31731^{Mi\{MIC\}/-}$ and follicle cell specific $CG31731^{RNAi\text{-}GD1133}$ mutants, which show the strongest persisting nurse cell nuclei phenotype, and starved the adults for a 16-20 hour period to induce PCD in mid-stage egg chambers. Subsequently, we dissected and stained the ovaries with anti-Dlg to label follicle cell membranes, anti-cleaved Dcp-1 to label active caspases and apoptotic germline debris, and DAPI to label DNA, and observed egg chambers from each phase as sorted by the changes in nurse cell chromatin (Figure 3.22). Healthy phase 0 egg chambers resembled the control, suggesting that *CG31731* mutant egg chambers develop normally through mid-oogenesis. Phase 1-2 dying egg chambers also resembled the control, appearing to initiate PCD normally. While phase 3 dying egg chambers exhibited slightly enlarged follicle cells, they appeared to only minimally uptake the germline material with fewer engulfed Dcp-1 positive vesicles present inside the follicle cells. Nevertheless, the follicle cells were still able to engulf some nurse cell debris and nurse cell nuclei could be seen inside the

follicle cells. Some of these engulfed nurse cell nuclei only faintly stained with DAPI, suggesting they have been acidified for degradation. By phase 4-5, these *CG31731* mutant dying egg chambers exhibited severe engulfment defects and premature follicle cell death. The few intact healthy-looking follicle cells exhibiting dispersed chromatin were enlargement defective, and majority of the follicle cells exhibited pyknotic nuclei without any membrane markers. In these phase 5 dying egg chambers, follicle cell membranes and nuclei disappear, leaving behind egg chambers with completely unengulfed germline material. The majority of the dying egg chambers found in the ovaries of *CG31731* mutants were these phase 5 egg chambers, indicating a pronounced defect in corpse clearance. These observations signify severe impairments in the engulfment machinery, and illustrate an important role for *CG31731* in the follicle cells to ensure proper enlargement of the follicle cells in engulfment. We did not observe any obvious engulfment defects in dying egg chambers when $CG31731^{RNAi\text{-}GD1133}$ or $CG31731^{RNAi\text{-}HMS06027}$ was expressed only in the germline (data not shown), suggesting CG31731 function is primarily required in the phagocytic follicle cells during engulfment of the dying germline material.

**3.11 *CG31731* is unlikely to act in neuronal corpses or engulfing glia in the brain**

Our studies of *CG31731* thus far have focused on PCD events in the ovary, where we found it is required in the phagocytic follicle cells for clearance of the germline debris. We were curious to know whether *CG31731* may also be involved in other PCD systems in *Drosophila*. To explore a potential role for *CG31731* outside the ovary, we looked in the brain, where engulfing glia are responsible for the clearance of degenerating

axons. It has been demonstrated that ensheathing glia require components of the Draper pathway for engulfment of axonal debris (Freeman et al., 2003; MacDonald et al., 2006; Kurant, 2011; Etchegaray et al., 2016). Our experiments in the ovary strongly suggest that *CG31731* is a key component of the Draper pathway. Therefore, perhaps *CG31731* may also have a role with Draper in the brain.

Previous work in the lab has endeavored to characterize PCD in the brain. In WT brains stained with DAPI to label DNA, healthy neuronal nuclei show dispersed DNA with a single condensed spot corresponding to heterochromatin. In contrast, in brains which exhibit defective glial phagocytosis, for example in $draper^{\Delta 5}$mutants, a substantial number of neuronal nuclei appear highly condensed into single balls, indicating pyknosis. TUNEL labeling in $draper^{\Delta 5}$ brains shows that the presence of these pyknotic nuclei correspond to approximately 700 TUNEL-positive corpses. In comparison, WT brains only exhibit 1 or 2 TUNEL-positive corpses (Etchegaray et al., 2016). Using the same methods, we looked at $CG31731^{Mi\{MIC\}/Mi\{MIC\}}$ brains stained with DAPI to label DNA and TUNEL to label fragmented DNA, and did not observe any obvious signs of defective glial phagocytosis. In $CG31731^{Mi\{MIC\}/Mi\{MIC\}}$ brains, the chromatin morphology of neurons appeared similar to those in WT brains and there was no accumulation of pyknotic nuclei. TUNEL labeling only detected a single apoptotic corpse, which is normal (Figure 2.24). These results suggest that CG31731 does not have a role in PCD and engulfment in the *Drosophila* brain. This may not be unexpected given that *CG31731* is expressed at much lower levels in the brain compared to in the ovary (Flybase). In humans, there are multiple functional homologs for CED-7 including ABCA1 and

ABCA7. We speculate that perhaps another *ABCA* gene, not CG31731 or CG1718 (Ziegenfuss, 2012), provides an ABCA transporter role for glia-mediated neuronal corpse clearance in the *Drosophila* brain.

### 3.12 Summary of findings

Here, we report that *Drosophila CG31731* encodes an ABC transporter similar to *ced-7/ABCA1.* Like *ced-7/ABCA1*, the *CG31731* gene encodes an ABCA type transporter. Sequence alignment shows that the predicted polypeptide possesses substantial similarity and identity to that of CED-7/ABCA1. More importantly, our genetic analyses identify a role for *CG31731* in cell corpse clearance during PCD in the *Drosophila* ovary *in vivo*.

To observe a role for *CG31731* in engulfment, we looked at 2 distinct PCD modalities in the ovary, in late stage developing and in mid-stage dying egg chambers. During the development of every egg chamber, 15 nurse cells are selectively removed by the surrounding phagocytic stretched follicle cells between stages 12-14 (Jenkins et al., 2013). It has been shown that phagocytosis genes in the stretched follicle cells non-autonomously regulate the death of the nurse cells, likely via phagoptosis (Timmons et al., 2016). Additionally, during starved conditions, mid-stage egg chambers can be induced to activate apoptotic and autophagic cell death pathways (Jenkins et al., 2013). In these mid-stage dying egg chambers, the surrounding follicle cells synchronously enlarge through 5 phases of death to engulf the dead germline debris (Etchegaray et al., 2012).

Using the *Drosophila* ovary as an *in vivo* model system, we show that genetically knocking down *CG31731* specifically in the phagocytic follicle cells leads to engulfment

defects in both late stage developing and mid-stage dying egg chambers. In late oogenesis, engulfment defects are apparent in egg chambers that fail to clear all 15 dying nurse cells by stage 14. Similarly, in mid-oogenesis, engulfment defects are evident in dying mid-stage egg chambers that fail to engulf the dead germline debris by phase 5. In contrast, genetically repressing *CG31731* expression only in the dying nurse cells did not lead to any obvious engulfment defects in either system of PCD. Together, these observations in 2 distinct PCD modalities demonstrate a conserved role for *CG31731* specifically in the phagocytic cells for cell corpse clearance.

Other core components of the engulfment machinery, including *draper* and *Ced-12*, have previously been shown to also be required in the phagocytic follicle cells for removal of the dying nurse cells (Timmons et al., 2016). Our double mutant analyses of $CG31731^{Mi\{MIC\}/Mi\{MIC\}}$ with $draper^{\Delta 5}$ or $Ced\text{-}12^{RNAi}$ show that *CG31731* likely acts in the same pathway as *draper*, parallel to *Ced-12*. Correspondingly, *ced-7/ABCA1* acts in the same pathway as *ced-1/MEGF10*, parallel to *ced-12/ELMO* (Mangahas and Zhou, 2005), strongly suggesting *CG31731* provides a *ced-7/ABCA1*-like role in this conserved engulfment mechanism. Moreover, as *ced-7/ABCA1* was demonstrated to be required for CED-1/MEGF10 clustering at the phagocytic cup, we similarly observed a disruption in Draper enrichment around the nurse cells in *CG31731* mutants. Altogether, these findings identify a functional relation between *ced-7/ABCA1* and *CG31731* in signaling events during engulfment.

A prominent feature in the removal of nurse cells during developmental PCD is the acidification and subsequent clearance of the nurse cell nuclei. In WT developing egg

chambers, majority of the nurse cells are acidified in stage 12 and cleared even before stage 14. In contrast, in *draper*$^{\Delta 5}$mutants, acidification is completely blocked in approximately 70% of developing egg chambers (Timmons et al., 2016). Our observations suggest in *CG31731*$^{Mi\{MIC\}/Mi\{MIC\}}$ mutants, acidification only occurs in the few cleared nurse cells and is delayed to stage 13. Acidification appears to be blocked in persisting nurse cell nuclei. These observations are very similar to those in *ced-1* pathway mutants in *C. elegans*, wherein engulfment is delayed and blocked in some corpses, and degradation is delayed in engulfed corpses. Taken together, these similar defects in PCD observed between homologous genes in *Drosophila* and *C. elegans* demonstrate a conserved engulfment and possibly degradation mechanism of cell corpses involving *CG31731* in *Drosophila*.

We also observed a role for *CG1718*, another *ABCA* gene in *Drosophila*. Most noticeably, in the lack of a WT *CG31731* allele, our data suggests *CG1718* may provide a compensatory function for *CG31731*. This observation leads us to speculate that perhaps there are multiple *ced-7* homologs in *Drosophila*. Moreover, we did not observe a role for *CG31731* in neuronal corpse clearance, and a separate lab also did not observe a role for *CG1718* in engulfing glia (Ziegenfuss, 2012), suggesting there is perhaps yet another *ced-7/ABCA1* ortholog that is involved in PCD events in the *Drosophila* brain. In mammals ABCA1 and ABCA7 appear to provide redundant functions for lipid efflux in some tissues (Hamon et al., 2000; Wang et al., 2003), supporting the possibility for redundancy between ABCA type transporters.

In summary, we have shown that *CG31731*, an ABCA encoding gene, plays a similar role to *ced-7/ABCA1* during engulfment and PCD events in the *Drosophila* ovary. As the evolutionarily conserved engulfment mechanism implicates a role for ABC transporters, our findings strongly suggest CED-7/ABCA1 is conserved in *Drosophila* through at least *CG31731*, and perhaps other unidentified ABCA transporters as well.

**Table 3.1 Quantification of persisting nuclei**

| | |
|---|---|
| Very Strong | 75%-100% stage 14 egg chambers have >4 PN |
| Strong | 50%-75% stage 14 egg chambers have >4 PN |
| Moderate | 25%-50% stage 14 egg chambers have >4 PN |
| Weak | 10%-25% stage 14 egg chambers have >4 PN |
| None | 0%-10% stage 14 egg chambers have >4 PN |

| Genotype | 0 PN | 1-3 PN | 4-6 PN | 7-9 PN | 10-12 PN | 13-15 PN | n |
|---|---|---|---|---|---|---|---|
| $w^{1118}$ | 0.90 | 0.10 | 0.00 | 0.00 | 0.00 | 0.00 | 124 |
| $CG31731^{PBac/PBac}$ | 0.39 | 0.27 | 0.23 | 0.10 | 0.01 | 0.00 | 302 |
| $CG31731^{PBac/-}$ | 0.06 | 0.14 | 0.34 | 0.32 | 0.12 | 0.02 | 113 |
| $CG31731^{Mi\{MIC\}/Mi\{MIC\}}$ | 0.15 | 0.11 | 0.22 | 0.35 | 0.15 | 0.01 | 136 |
| $CG31731^{Mi\{MIC\}/-}$ | 0.01 | 0.03 | 0.21 | 0.44 | 0.27 | 0.04 | 567 |
| $CG31731^{PBac/Mi\{MIC\}}$ | 0.07 | 0.15 | 0.24 | 0.33 | 0.17 | 0.04 | 410 |
| $CG31731^{P\{EPgy2\}/PBac}$ | 0.90 | 0.10 | 0.00 | 0.00 | 0.00 | 0.00 | 702 |
| $CG31731^{P\{EPgy2\}/Mi\{MIC\}}$ | 0.96 | 0.04 | 0.00 | 0.00 | 0.00 | 0.00 | 243 |
| $CG31731^{P\{EPgy2\}/-}$ | 0.94 | 0.06 | 0.00 | 0.00 | 0.00 | 0.00 | 328 |
| $CG31731^{PBac/+}$ | 0.88 | 0.09 | 0.02 | 0.00 | 0.00 | 0.00 | 86 |
| $CG31731^{Mi\{MIC\}/+}$ | 0.77 | 0.17 | 0.05 | 0.01 | 0.00 | 0.00 | 144 |
| $CG31731^{P\{EPgy2\}/+}$ | 0.94 | 0.05 | 0.01 | 0.00 | 0.00 | 0.00 | 89 |
| $CG31731^{\Delta/+}$ | 0.80 | 0.20 | 0.00 | 0.00 | 0.00 | 0.00 | 102 |
| $PG150\text{-}GAL4/UAS\text{-}CG31731^{P\{EPgy2\}}$ | 0.96 | 0.04 | 0.00 | 0.00 | 0.00 | 0.00 | 212 |
| $GR1\text{-}GAL4/UAS\text{-}CG31731^{P\{EPgy2\}}$ | 0.97 | 0.03 | 0.00 | 0.00 | 0.00 | 0.00 | 520 |
| $nanos\text{-}GAL4/UAS\text{-}CG31731^{P\{EPgy2\}}$ | 1.00 | 0.00 | 0.00 | 0.00 | 0.00 | 0.00 | 1259 |
| $PG150\text{-}GAL4/UAS\text{-}CG31731^{RNAi\text{-}GD1133}$ | 0.82 | 0.16 | 0.01 | 0.00 | 0.00 | 0.00 | 422 |
| $PG150\text{-}GAL4/UAS\text{-}CG31731^{RNAi\text{-}KK104197}$ | 0.95 | 0.05 | 0.00 | 0.00 | 0.00 | 0.00 | 209 |

| | | | | | | | |
|---|---|---|---|---|---|---|---|
| *PG150-GAL4/UAS-CG31731$^{RNAi\text{-}HMC06027}$* | 0.96 | 0.01 | 0.03 | 0.00 | 0.00 | 0.00 | 81 |
| *GR1-GAL4 G89/UAS-CG31731$^{RNAi\text{-}GD1133}$* | 0.04 | 0.11 | 0.33 | 0.34 | 0.15 | 0.03 | 784 |
| *GR1-GAL4 G89/UAS-CG31731$^{RNAi\text{-}KK104197}$* | 0.05 | 0.28 | 0.40 | 0.22 | 0.04 | 0.00 | 459 |
| *GR1-GAL4 G89/UAS-CG31731$^{RNAi\text{-}HMC06027}$* | 0.04 | 0.30 | 0.44 | 0.22 | 0.00 | 0.00 | 27 |
| *nanos-GAL4/UAS-CG31731$^{RNAi\text{-}GD1133}$* | 0.89 | 0.11 | 0.00 | 0.00 | 0.00 | 0.00 | 122 |
| *nanos-GAL4/UAS-CG31731$^{RNAi\text{-}KK104197}$* | 0.94 | 0.06 | 0.00 | 0.00 | 0.00 | 0.00 | 105 |
| *nanos-GAL4/UAS-CG31731$^{RNAi\text{-}HMC06027}$* | 0.97 | 0.03 | 0.00 | 0.00 | 0.00 | 0.00 | 73 |
| *GR1-GAL4 G89/UAS-Ced-12$^{RNAi}$* | 0.01 | 0.05 | 0.27 | 0.49 | 0.17 | 0.01 | 288 |
| *CG31731$^{Mi\{MIC\}/Mi\{MIC\}}$ + GR1-GAL4 G89/UAS-dced-12$^{RNAi}$* | 0.00 | 0.00 | 0.01 | 0.20 | 0.56 | 0.23 | 697 |
| *draper$^{\Delta 5}$* | 0.00 | 0.01 | 0.08 | 0.40 | 0.41 | 0.10 | 192 |
| *CG31731$^{Mi\{MIC\}/Mi\{MIC\}}$ + draper$^{\Delta 5}$* | 0.00 | 0.00 | 0.09 | 0.55 | 0.34 | 0.02 | 491 |
| *nanos-GAL4/UAS-CG1718$^{RNAi\text{-}HMS01821}$* | 0.98 | 0.02 | 0.00 | 0.00 | 0.00 | 0.00 | 128 |
| *nanos-GAL4/UAS-CG1718$^{RNAi\text{-}HMS01796}$* | 0.98 | 0.02 | 0.00 | 0.00 | 0.00 | 0.00 | 185 |
| *nanos-GAL4/UAS-CG1718$^{RNAi\text{-}GD3708(49)}$* | 0.98 | 0.02 | 0.00 | 0.00 | 0.00 | 0.00 | 169 |
| *nanos-GAL4/UAS-CG1718$^{RNAi\text{-}GD3708(51)}$* | 0.99 | 0.01 | 0.00 | 0.00 | 0.00 | 0.00 | 302 |
| *nanos-GAL4/UAS-CG1718$^{RNAi\text{-}KK100452}$* | 0.97 | 0.03 | 0.00 | 0.00 | 0.00 | 0.00 | 186 |
| *GR1-GAL4 G89/UAS-CG1718$^{RNAi\text{-}HMS01821}$* | 0.23 | 0.32 | 0.33 | 0.11 | 0.01 | 0.00 | 230 |
| *GR1-GAL4 G89/UAS-CG1718$^{RNAi\text{-}HMS01796}$* | 0.94 | 0.06 | 0.00 | 0.00 | 0.00 | 0.00 | 254 |
| *GR1-GAL4 G89/UAS-CG1718$^{RNAi\text{-}GD3708(49)}$* | 0.99 | 0.01 | 0.00 | 0.00 | 0.00 | 0.00 | 1118 |
| *GR1-GAL4 G89/UAS-CG1718$^{RNAi\text{-}GD3708(51)}$* | 0.98 | 0.02 | 0.00 | 0.00 | 0.00 | 0.00 | 92 |
| *GR1-GAL4 G89/UAS-CG1718$^{RNAi\text{-}KK100452}$* | 0.97 | 0.03 | 0.00 | 0.00 | 0.00 | 0.00 | 1631 |
| *GR1-GAL4 G89/UAS-CG1718$^{RNAi\text{-}HMS01821}$, UAS-CG31731$^{P\{EPgy2\}}$* | 0.11 | 0.59 | 0.30 | 0.00 | 0.00 | 0.00 | 63 |
| *CG1718$^{miR\text{-}1007\text{-}KO/miR\text{-}1007\text{-}KO}$* | 0.84 | 0.13 | 0.02 | 0.01 | 0.01 | 0.00 | 171 |
| *CG1718$^{miR\text{-}1007\text{-}KO/miR\text{-}1007\text{-}K}$ + CG31731$^{PBac/\ PBac}$* | 0.01 | 0.16 | 0.38 | 0.34 | 0.11 | 0.00 | 238 |

**Figure 3.1 CG31731, CG1718, CED-7, and ABCA1 protein domains**

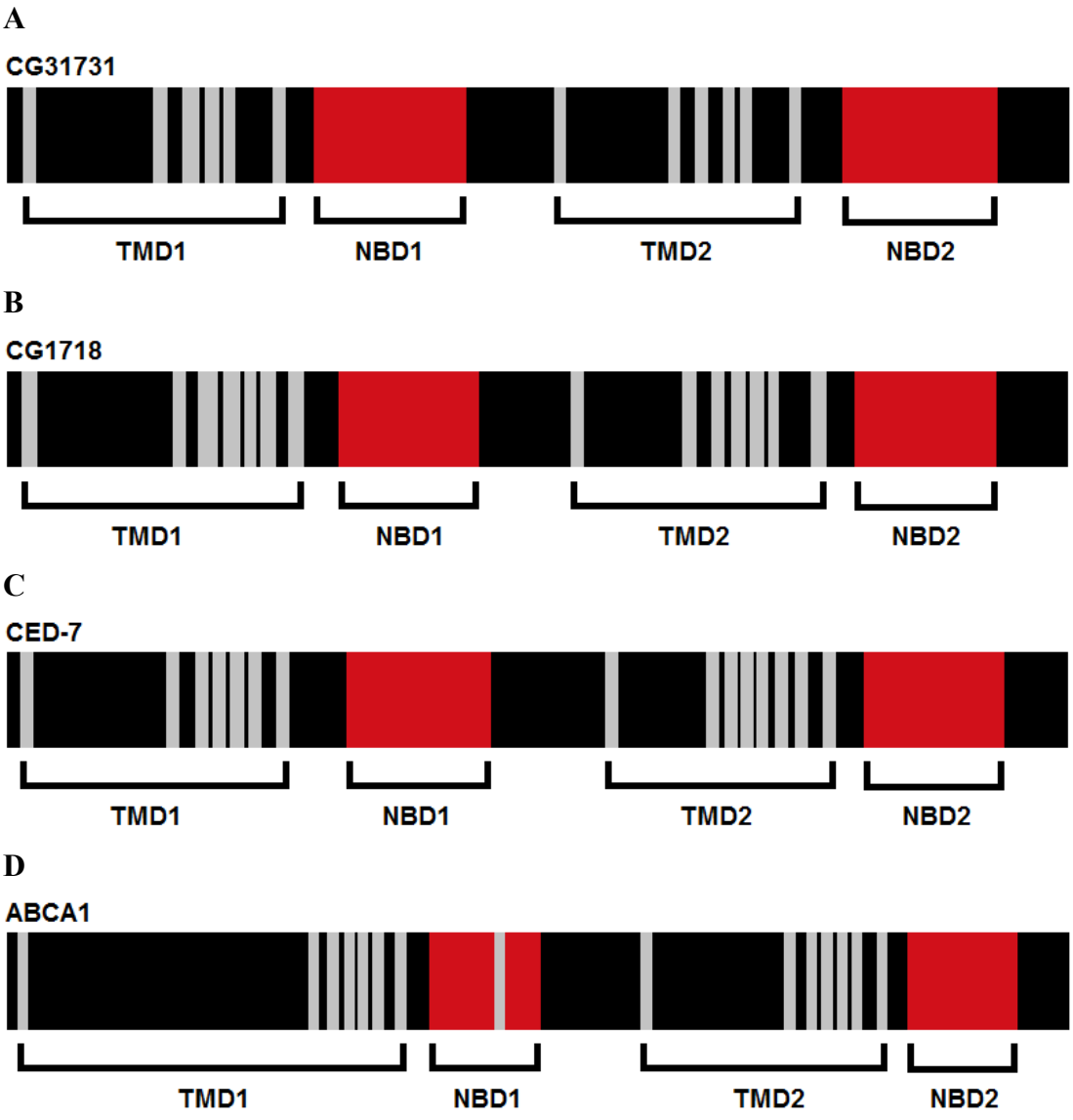


Schematic of the primary structures of **(A)** CG31731, **(B)** CG1718, **(C)** CED-7, and **(D)** ABCA1. The transmembrane segments (grey) and NBDs (red) are shown.

**Figure 3.2 *CG31731* predicted amino acid sequence aligned with *ced-7* and *ABCA1***

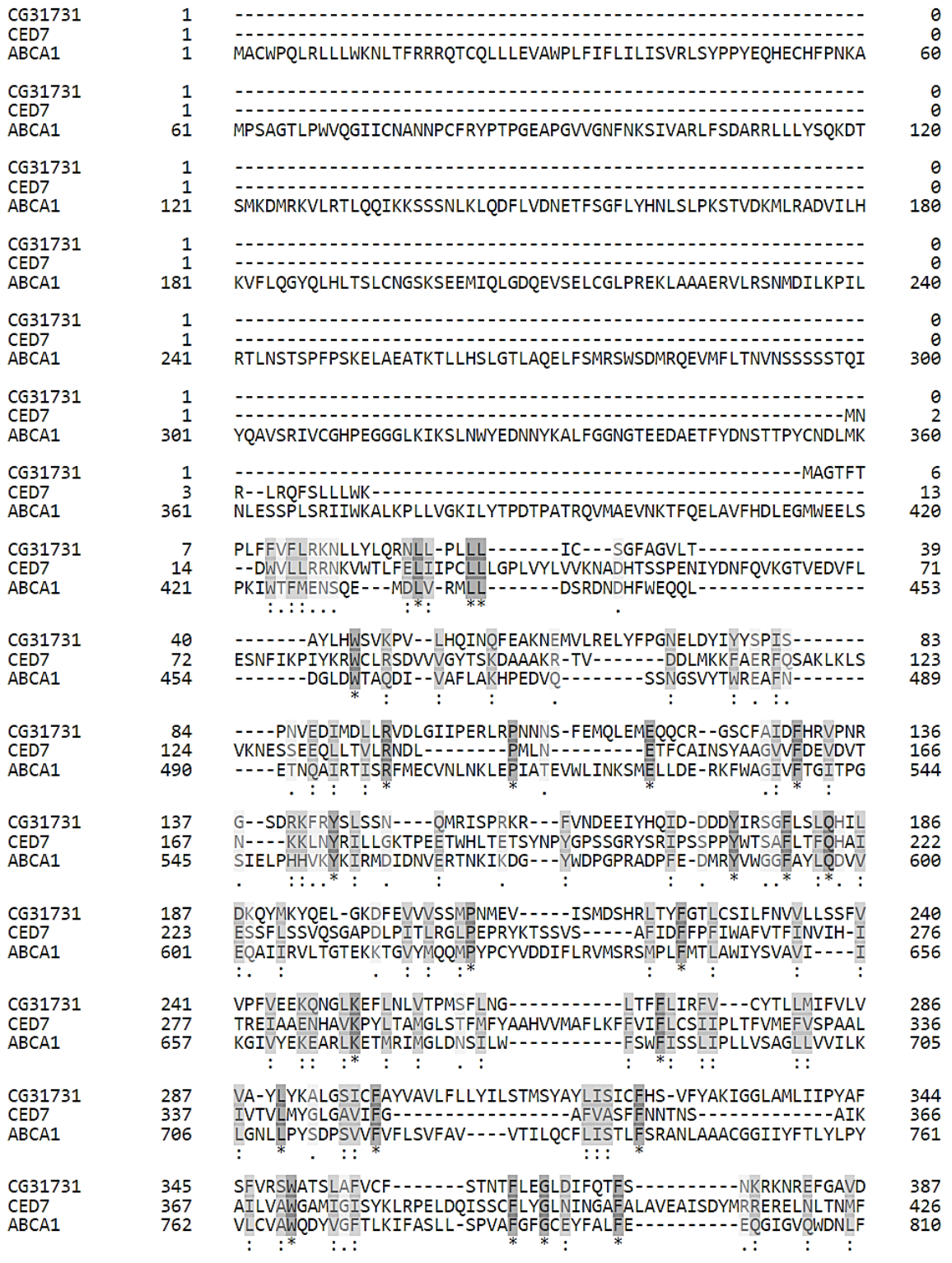

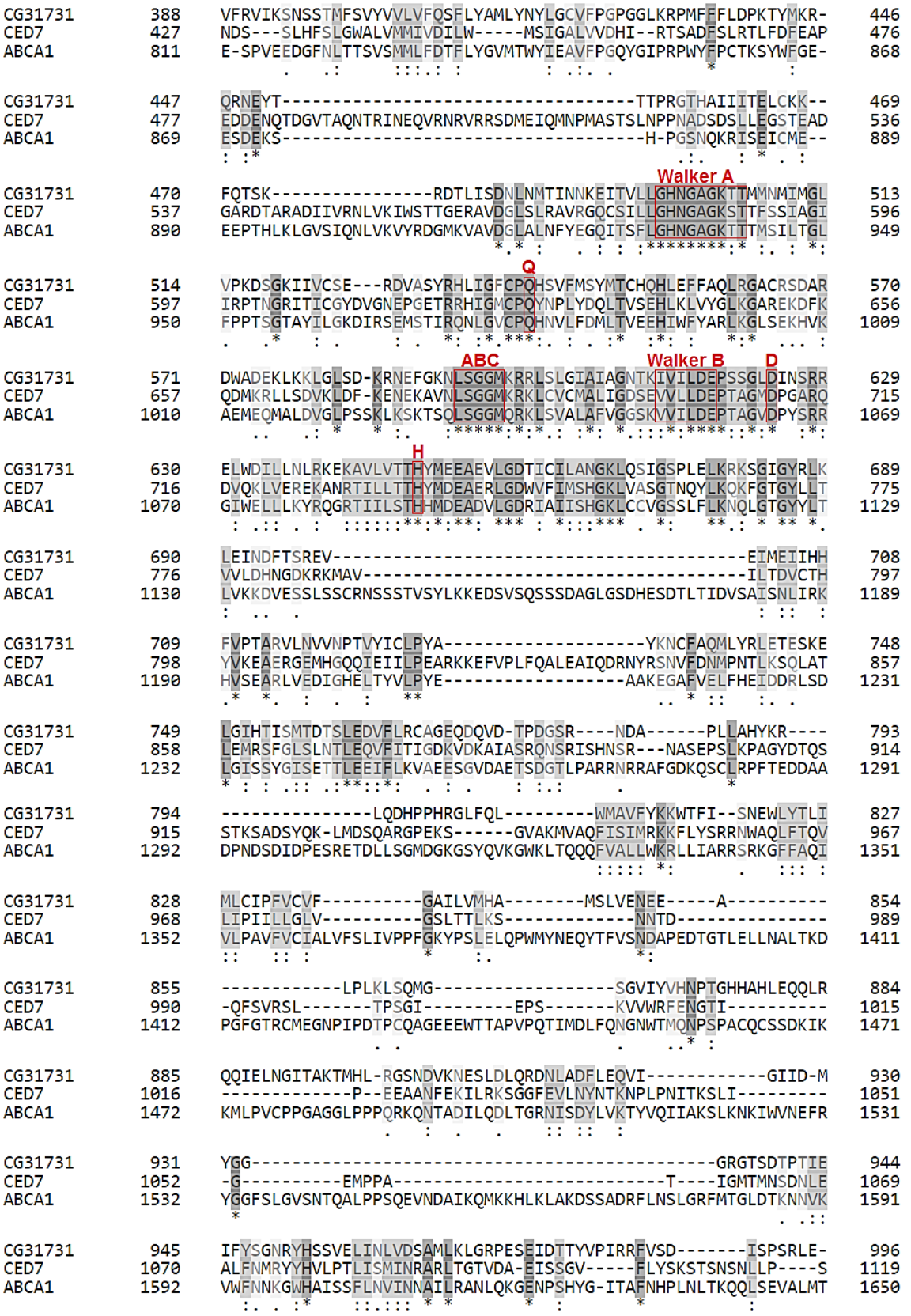
Walker A
Q
ABC
Walker B
D
H

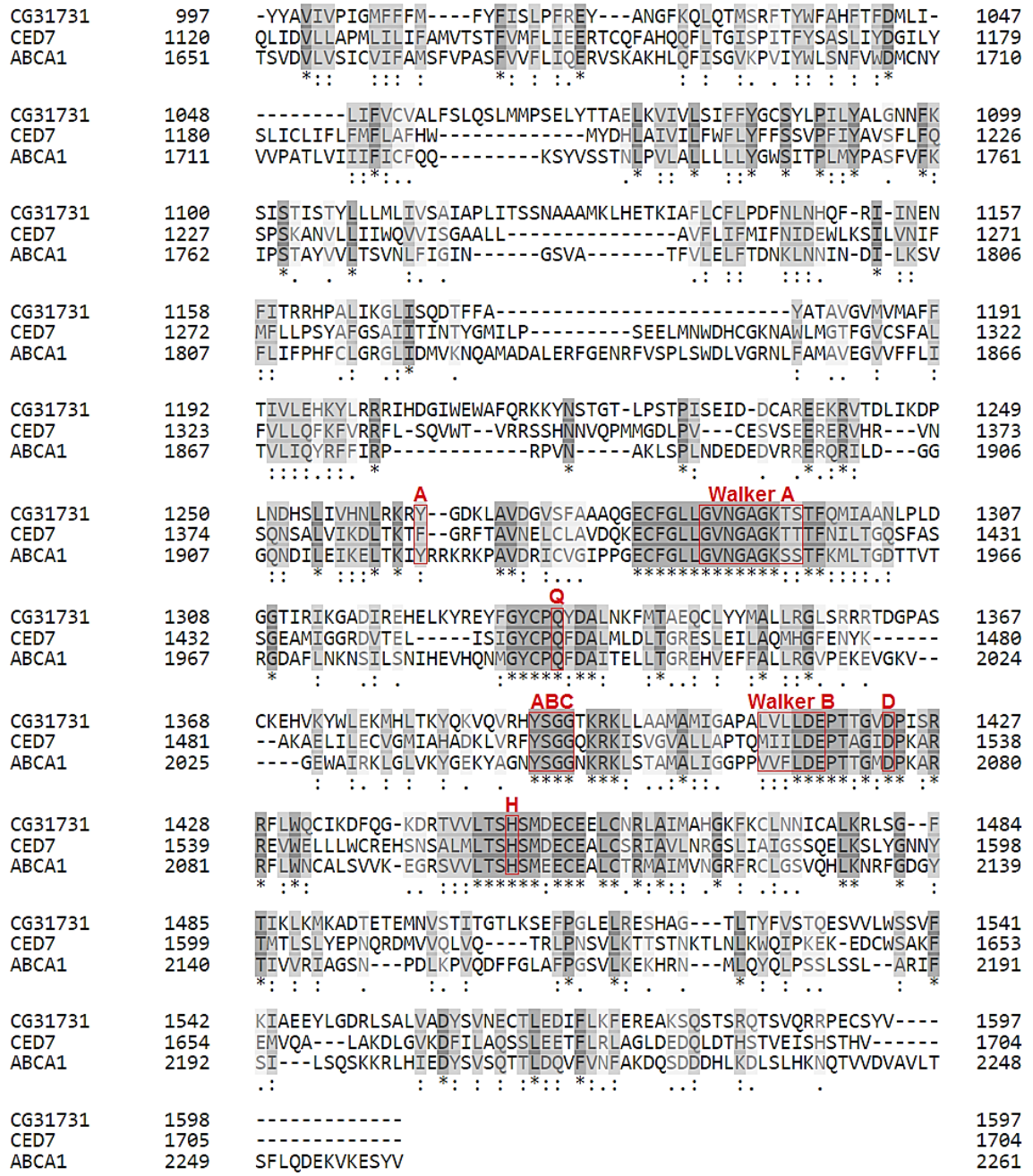


Alignment of the predicted amino acid sequences of *Drosophila* CG31731, *C. elegans* CED-7, and human ABCA1. The similarities (light grey) and identities (dark grey) between the three sequences are highlighted. The highly conserved A-loop, Walker A motif, Q- loop, ABC signature motif, Walker B motif, D-loop, and H-loop, are indicated (red). (Sequence alignment provided by UniProt.org)

**Figure 3.3 *CG1718* predicted amino acid sequence aligned with *ced-7* and *ABCA1***

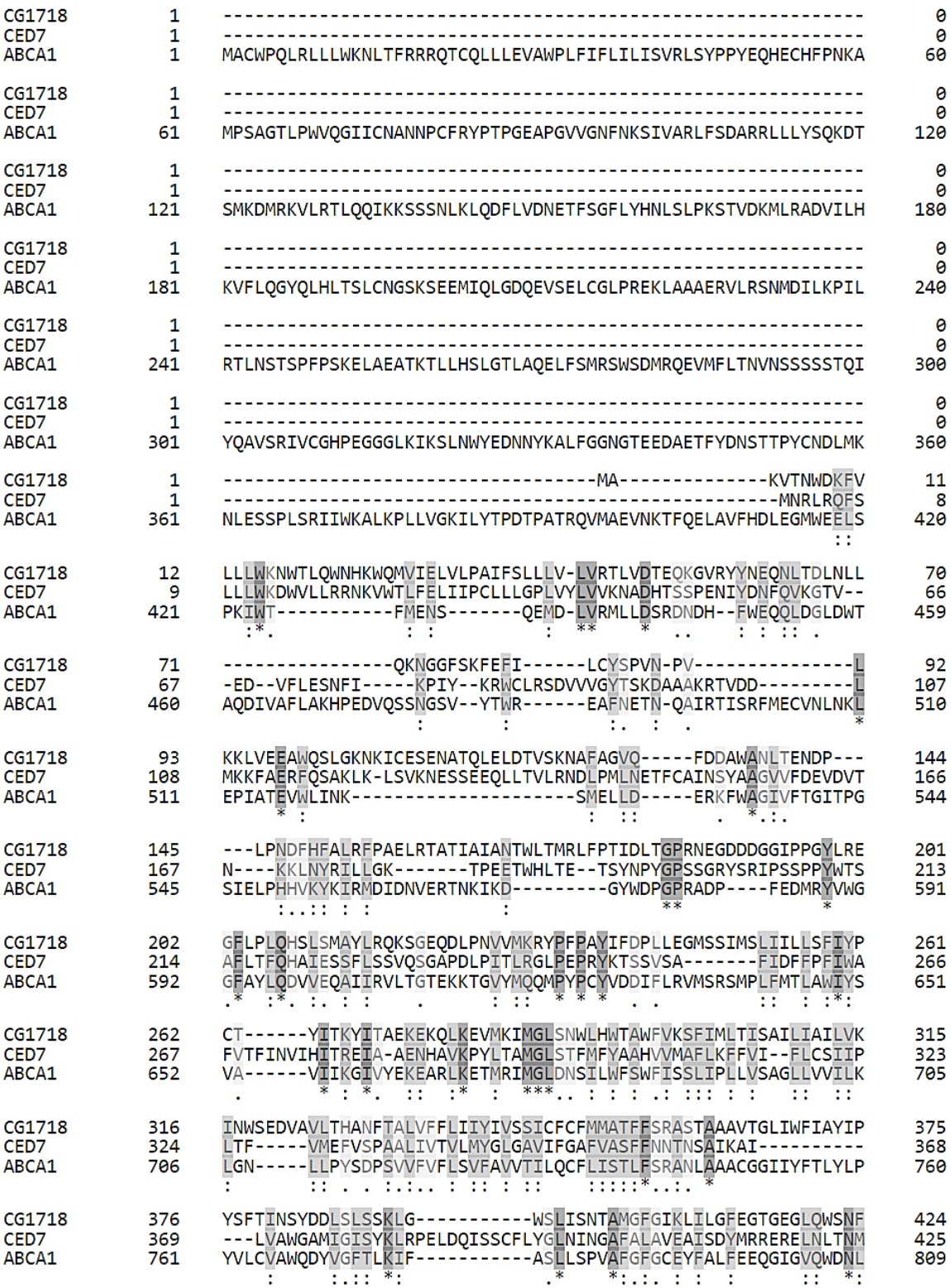

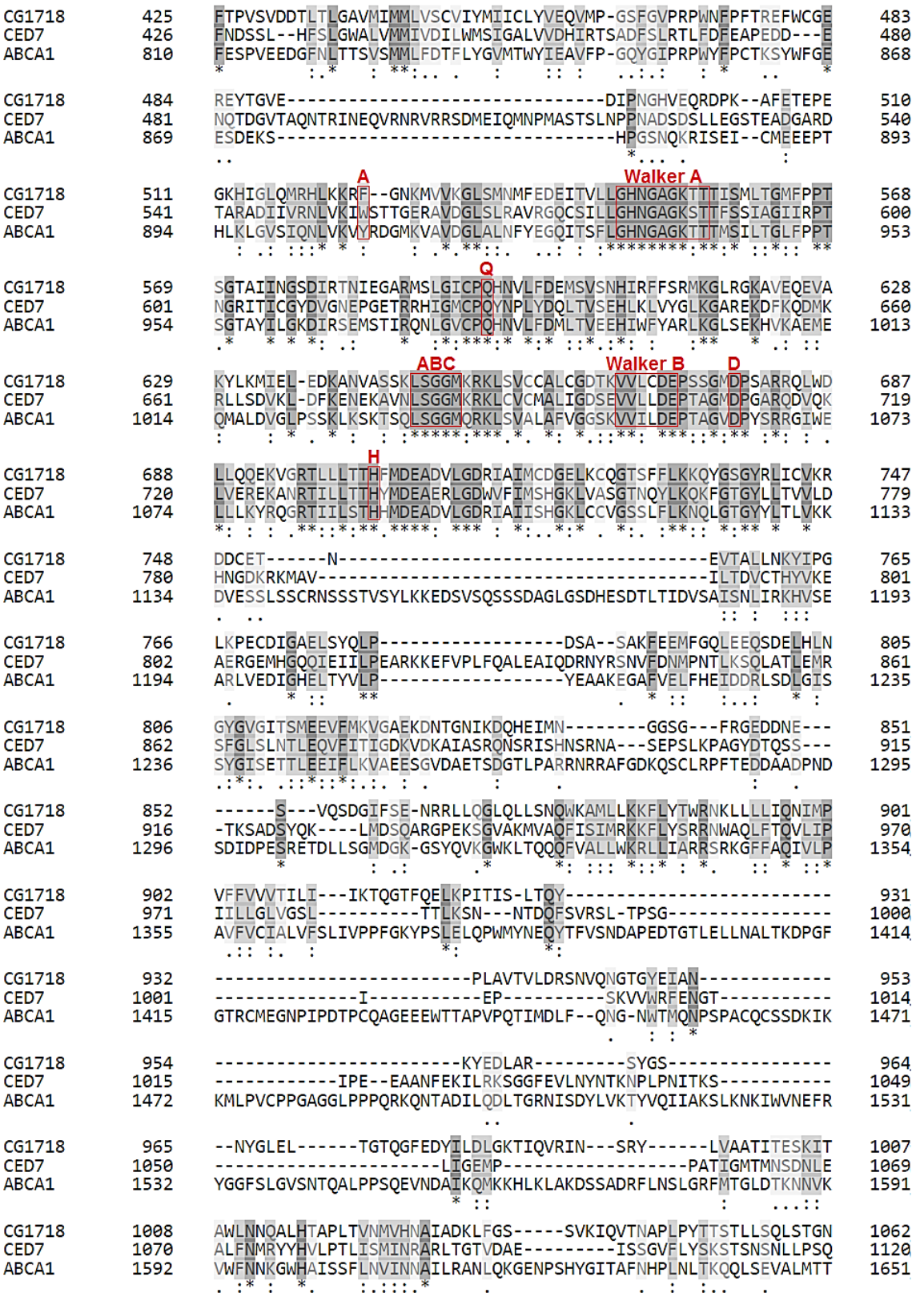
A
Walker A
Q
ABC
Walker B
D
H

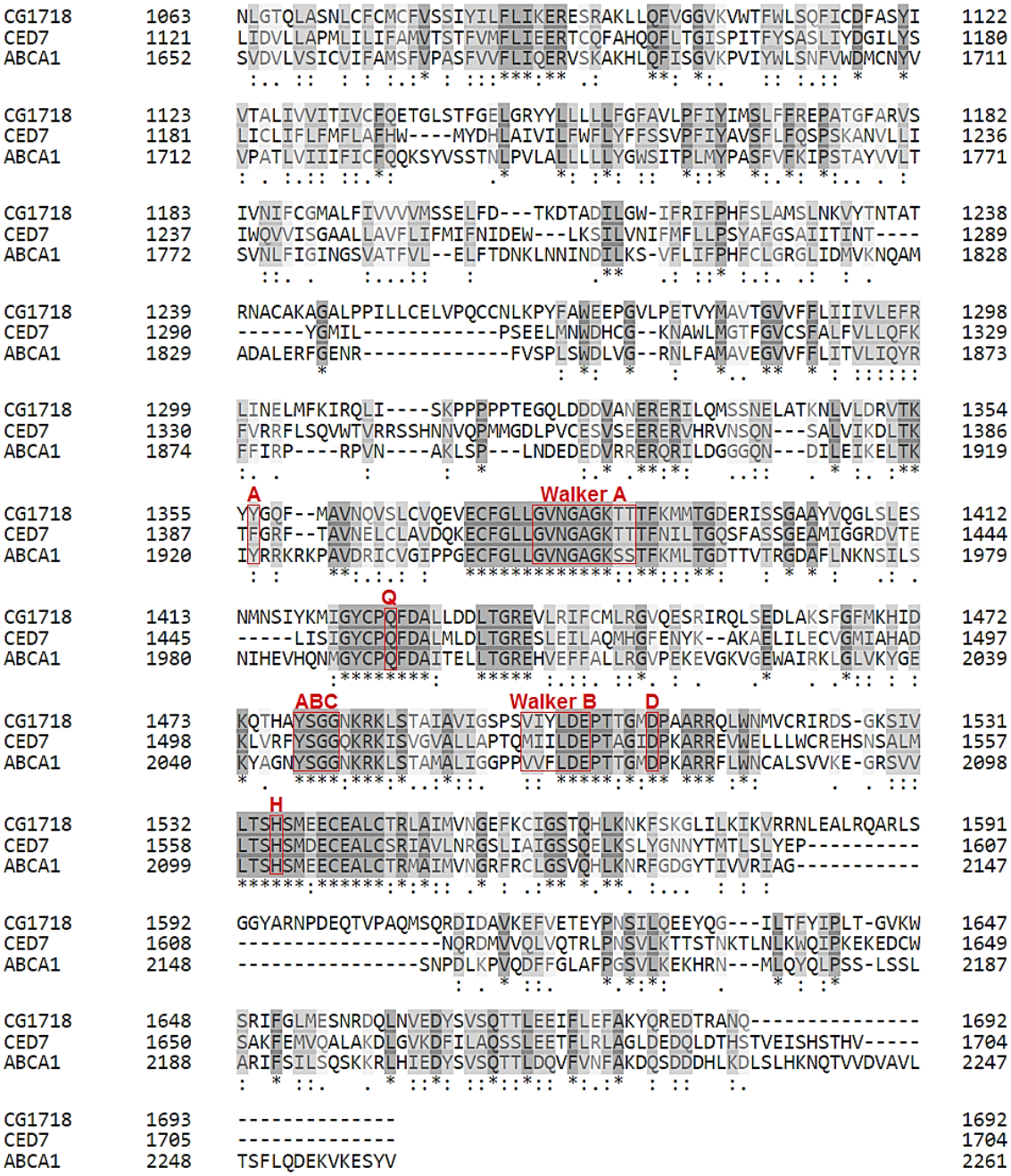


Alignment of the predicted amino acid sequences of *Drosophila* CG1718, *C. elegans* CED-7, and human ABCA1. The similarities (light grey) and identities (dark grey) between the three sequences are highlighted. The highly conserved A-loop, Walker A motif, Q- loop, ABC signature motif, Walker B motif, D-loop, and H-loop, are indicated (red). (Sequence alignment provided by UniProt.org)

**Figure 3.4 *CG31731* gene region**


TAAGTATTACTATCGACGTTGATAGAGAAAAAATGCCATTCAACAAAGCAAAGTAAAATT
AGGGAAAAGTTGATGTTAAACAGAAAATGGCTGGGACTTTTACCCCGCTGTTCTTCGTCT
TTCTGCGGAAGAATTTGCTCTACTTGCAACGCAACTTGCTGCCCCTGCTCCTTATCTGCT
CCGGATTTGCCGGAGTACTCACCGCGTACCTCCACTGGTCCGTCAAGCCCGTGCTTCACC
AAATTAACCAGTTTGAAGCAAAGAATGAAgtaagtttccctcgcactgctactttatctg
ctttttatatttgtacatacgtatgcatgtgataacaaacctgtgaccacactaatcctt
atcattggacttcaatttatttattagATGGTTCTTAGAGAATTGTACTTTCCCGGTAAT
GAGCTGGATTACATTTACTACTCACCCATCTCTCCCAATGTAGAGGACATTATGGATCTC
CTGCGTGTAGATCTGGGAATTATACCAGAGCgtaagtgcatttccaaattatctcataaa
ttagatatgtggaaaagtttgtatggtaaacgtaaacgtttccgaccatataaagcttat
atgtacttttgataacgatcatacaaaatAACATACAAAATTCACTGCATATATTTGCGA
TACTATCTTCTAGATTGTATTTAACAATATTTCATTGCGCAGGACTTCGGCCCAACAACA
ACAGCTTCGAGATGCAGCTGGAGATGGAGCAACAGTGCCGTGGAAGCTGCTTCGCAATTG
ACTTCCACCGGGTACCGAACCGTGGCTCTGACAGAAAGTTCCGATACAGCCTCAGCTCAA
ATCAGATGCGCATTTCGCCCAGAAAGCGATTTGTGAACGACGAGGAAATTTATCACCAGA
TAGGTGCGTGTTCAATTTTTCCATTGTTACCGTTTAACGAACCCGCATGTTGGTTTTTGT
TTATCAGATGATGATGATTATATTCGTTCCGGATTCCTGTCCTTGCAACACATATTGGAC
AAACAGTATATGAAATACCAGGAGCTCGGGAAAGACTTTGAGGTGGTGGTCAGCTCGATG
CCCAACATGGAGGTCATCAGCATGGATAGTCATCGATTGACATATTTCGGAACACTGTGC
AGCATTCTATTCAATGTGGTCCTACTAAGCAGCTTTGTGGTGCCCTTTGTGGAGGAGAAG
CAAAACGGACTGAAGGAGTTTCTCAACCTGGTCACGCCCATGAGTTTCCTCAACGGCCTC
ACTTTCTTTCTCATTCGGTTTGTGTGCTACACATTGCTTATGATCTTTGTCCTGGTCGTT
GCATATTTATACAAGGCCCTGGGCTCCATCTGCTTTGCTTACGTGGCAGTGTTGTTTCTG
CTTTACATTTTGTCAACCATGTCGTATGCTTATCTGATCTCTATTTGCTTCCACTCAGgt
aagtaattacattgatatattcagcaaagtttactaatcttctacataacttacagTTTT
CTATGCGAAAATCGGAGGGCTGGCAATGCTAATAATTCCCTATGCATTCTCATTTGTTCG
AAGCTGGGCCACATCGCTGGCATTTGTGTGTTTTAGCACGAATACCTTTCTGGAGGGATT
GGATATTTTTCAGACATTTTCAAATAAGCGTAAGAgtttaaattggttttagtagctta
acatttaaatttgaacactggctttttttgaagATCGCGAATTCGGTGCTGTGGATGTAT
TTCGCGTAATCAAAAGCAATTCCTCAACGATGTTTTCGGTCTACGTGGTTCTCGTCTTTC
AATCCTTTTTGTATGCCATGCTCTACAACTATTTGGGTTGTGTTTTTCCCGGTCCTGGTG
GACTAAAGCGACCGATGTTCTTTTTCCTAGATgtaagtactatttccgaagtccgaacca
atgatatttaatgtcggtatcagatcaaaattttcgctcgtgtgatatattttcttatct
cgacataagcttcaattcagttcgtattataattttatgttcattataatcaagtatgag
atcagatgcagtaagactctttatttcaataggttactttgatcgaatcttgtttattga
aatcggttaaaatgtccttttttacagTTCCGTATCGGTTATCGGCTGCATAACCAAACAG
GGTTAAATTAAGAATTTTCTTTATTCTAAACCATAGCCCAAGACTTACATGAAACGACAA
CGCAACGAATACACGACGACACCGCGCGGCACTCATGCTATCATAATCACTGAGTTGTGC
AAGAAGTTCCAGACAAGCAAGCGCGATACGCTAATTTCGGACAACTTGAACATGACGATC
AACAACAAGGAGATTACTGTCCTGCTGGGCCACAATGGAGCTGGAAAAACAACCATGATG
AACATGATAATGGgtagggactcaaactcaattcgcttcctcggccatccaatgcacatg

ttgattctctttcagGATTGGTACCAAAGGATTCGGGCAAGATAATTGTGTGCAGTGAGC
GCGATGTGGCCTCCTATCGCCACCTGATTGGATTCTGTCCGCAGCACAGCGTTTTCATGA
GCTACATGACATGTCACCAGCACTTGGAGTTCTTTGCCCAGCTGCGGGGAGCTTGCCGAT
CCGATGCACGCGATTGGGCAGATGAGAAACTTAAGAAGCTGGGACTTAGCGATAAGCGAA
ACGAATTCGGCAAGAATTTGTCTGGAGGCATGAAGAGGCGTTTATCACTGGGTATCGCCA
TTGCCGGTAACACCAAgtaaacttaagagatatattgcttaaagatattcggtttaaaaa
tctttgtttaatctcgcagAATCGTAATCCTTGACGAACCATCATCGGGATTGGACATTA
ACTCGCGTCGTGAGCTGTGGGACATCCTACTTAATCTACGCAAGGAGAAGGCCGTTCTGG
TCACCACGCACTACATGGAGGAGGCCGAGGTCCTTGGGGATACCATCTGCATATTGGCCA
ATGGAAAACTGCAGAGCATCGGGAGTCCTTTGGAATTAAAACGAAAATCGGGAATTGGTT
ATCGTCTCAAATTAGAGATCAACGATTTTACATCAAGAGAAGTGGAAATCATGGAAATAA
TCCATCACTTTGTGCCAACAGCCAGAGTCTTGgtaagtcattaataaatgaactttatat
aaggcgtgtgcataatatcctttaaacgttgaacagAATGTGGTGAATCCTACTGTGTAT
ATCTGCCTGCCGTATGCCTATAAAAATTGTTTCGCACAAATGCTTTATAGGCTGGAGACT
GAATCAAAGGAACTGGGCATACATACAATTTCCATGACCGACACTTCCCTGGAGGATGTT
TTCCTAAGgtagggattggaagatacattgtttattgttttgctttaatatcttatgtg
gtgttttagATGCGCAGGCGAACAGGATCAAGTGGATACCCCCGATGGTTCGCGCAATGA
TGCGCCGCTACTGGCACACTACAAAAGACTCCAAGACCATCCCCCTCATCGCGGACTTTT
TCAACTTTGGATGGCTGTGTTTTACAAAAAGTGGACCTTTATTTCCAATGAATGGTTATA
TACTCTGATAATGgtaagttgttagcaatttgtaggactttgctctgttgtataaacggc
gaaaacaactaaaactaaaacgaactaaaaacttttgtgctcccctctcgctagCTGTG
CATTCCCTTTGTATGCGTATTCGGGGCTATACTGGTGATGCACGCCATGTCCTTGGTGGA
GAACGAAGAGGCTCTGCCGCTGAAGCTCAGCCAGATGGGCAGTGGCGTTATATACGTTCA
CAATCCAACGGGCCATCACGCCCATTTGGAGCAGCAGCTGCGTCAACAGATCGAGCTGAA
TGGAATCACAGCGAAAACAATGCACCTGCGTGGGAGTAATGATGTGAAAAATGgtgagta
tgcgacgttgtgctaaacattttaatggctctatcaatacatgtgttctctagAATCCCT
TGACTTACAACGCGACAACTTGGCTGATTTCTTGGAGCAGGTGATTGGCATTATTGACAT
GTACGGAGGTGGGCGTGGCACCTCCGATACGCCCACCATTGAGATTTTTTACTCAGGCAA
TCGCTACCACAGCTCTGTGGAGCTTATCAACCTGGTGGACTCGGCAATGCTGAAGCTAGG
GCGTCCAGAGTCTGAAATTGATACGACTTACGTGCCAATTCGTCGATTTGTTAGCGACAT
AAGTCCATCGCGCCTCGAATACTATGCGGTCATCGTGCCGATCGGCATGTTCTTCTTCAT
GTTCTATTTCATCTCATTGCCGTTTCGGGAATATGCCAATGGATTCAAACAGCTGCAGAC
CATGTCGCGATTTACTTATTGGTTTGCGCATTTTACTTTTGATATGCTGATCCTGATCTT
CGTCTGCGTTGCCCTGTTCAGTCTGCAATCCTTGATGATGCCCTCGGAGCTGTATACAAC
GGCTGAACTTAAGGTCATTGTGTTAAGCATATTTTTCTACGGCTGCAGCTACCTGCCCAT
TCTATACGCCCTGGGAAACAACTTTAAGTCGATATCCACGATATCTACTTATTTGCTTTT
GATGCTGATTGTGTCCGgtaatattatttgattttataaccagtgacaacaattagaaaa
actataaaacccattttcttttagCCATTGCCCCACTTATCACCTCCAGCAATGCGGCGG
CCATGAAACTGCATGAGACCAAGATCGCCTTCCTCTGCTTCCTACCGGACTTCAATCTTA
ATCACCAGTTTCGCATCATCAATGAAAACTTTATAACCCGACGCCATCCGGCACTTATAA
AGGGTCTTATCAGCCAGGACACCTTCTTTGCCTATGCCACCGCCGTGGGTGTTATGGTCA
TGGCATTCTTTACCATAGTCCTGGAACACAAGTATCTGCGCAGACGAATTCATGATGGCA

TCTGGGAATGGGCATTCCAAAGAAAGAAATACAATTCGACAGGCACCCTTCCCAGTACTC
CGATCTCAGAAATTGATGATTGTGCAAGGGAGGAAAAACGGGTTACCGATCTGATAAAAG
ACCCATTGAACGACCATTCACTGATTGTGCACAATCTTCGCAAGCGATACGGCGATAAGC
TGGCTGTGGACGGAGTCAGCTTTGCGGCTGCCCAGGGTGAATGCTTTGGTCTGTTGGGTG
TTAACGGAGCGGGTAAGACAAGTACCTTTCAGATGATAGCGGCCAATTTGCCTCTAGATG
GTGGCACTATCCGCATCAAAGGCGCAGACATTCGCGAGCATGAGTTGAAATACCGGGAAT
ACTTTGGCTACTGCCCTCAGTACGATGCACTAAATAAATTCATGACCGCCGAGCAGTGCC
TATACTACATGGCATTGCTGCGCGGCCTGAGCCGCCGAAGGACCGATGGACCAGCCAGCT
GCAAGGAGCACGTGAAGTACTGGCTAGAGAAGATGCATTTGACCAAATATCAAAAGGTGC
AAGTGCGCCACTATTCGGGCGGCACGAAACGCAAGCTTCTGGCGGCAATGGCCATGATTG
GTGCACCCGCACTGGTGCTCCTGGACGAACCTACCACCGGTGTGGATCCCATCTCGAGAC
GATTTCTTTGGCAATGCATCAAGGATTTCCAGGGAAAGGATCGAACAGTGGTGCTCACAT
CACATAGgtaagcccaaaaaagtatatttccttttcaaacagattcaaaagtgtacacat
tctctacaaacagCATGGACGAGTGCGAAGAGCTGTGCAATCGCTTGGCCATCATGGCGC
ACGGAAAGTTCAAGTGTCTGAACAATATTTGCGCCCTTAAGCGATTAAGCGGCTTCACGA
TAAAACTGAAAATGAAGGCGGACACCGAAACGGAGATGAATGTGTCCACGATCACTGGCA
CGTTGAAGTCAGAGTTTCCTGGTCTGGAACTGCGCGAGAGCCATGCCGGCACACTCACCT
ACTTTGTTAGCACGCAGGAGAGTGTGGTCCTTTGGTCAAGTGTTTTCAAGATAGCTGAGG
AATATCTGGGCGATCGCTTAAGCGCTCTCGTGGCCGACTATTCGGTGAACGAGTGCACAC
TCGAGGATATTTTCCTCAAGTTCGAGAGAGAGGCGAAATCACAATCGACGTCACGTCAAA
CCTCCGTGCAACGCAGGCCGGAATGCAGCTACGTTTAGGCCAGATAGTCGGAGTGTCGGA
GTATCAAGTAAGATAAGCAGAAGACGGGCGTCGTACATTTCATTATTTCCCTCAAATATG
GAACTTTTATGAATCTCTATCCGGTGGGAATAATCTACTTAATGTATTTAGGGACTAATA
AAACCAAACAAACACCTTCGACATGGGTATATAAAACTAAAATATAAAAGTAAGATATAA
CTAGTACGACAAATAAATAATATTTTTTATTTATATTATAATAAATATTTCTACATAAT

CG31731 gene region. The *CG31731* gene extends from 13,784,084–13,790,562. The location of the insertions: *P{EPgy2}* at 13,784,172, *PBac* at 13,784,330, and *Mi{MIC}* at 13,784,705, are depicted (red line). The gene span (xxxx), RNA (XXXX), and coding exons (XXXX) are shown. (Sequence obtained from Flybase)

**Figure 3.5 *CG31731* gene map and transgenic constructs**

**A**

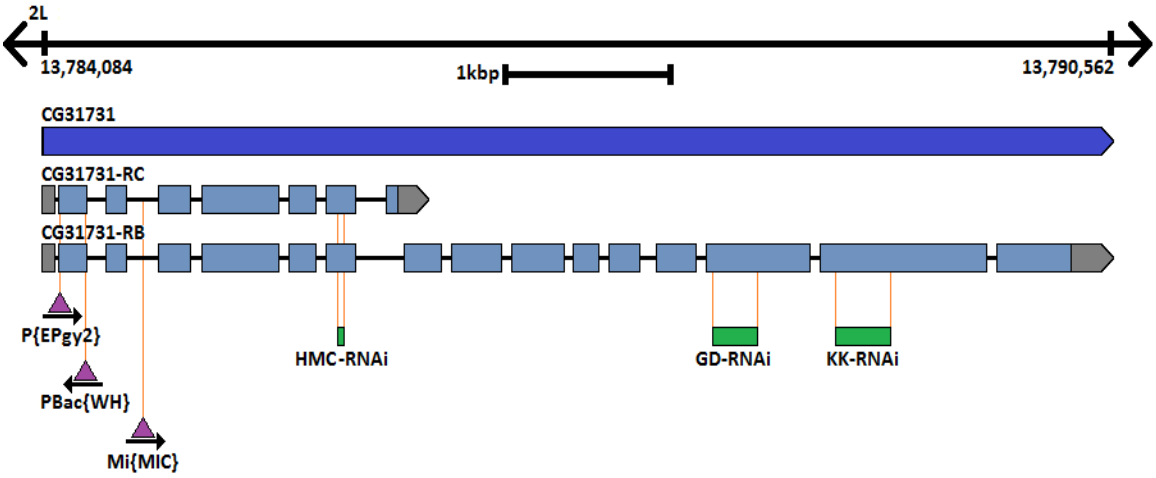


**B**

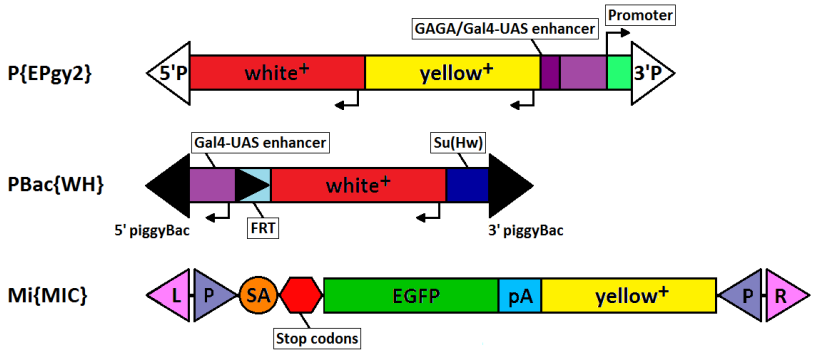


**(A)** Schematic of the *CG31731* gene region on chromosome 2L. The *CG31731* gene (dark blue) extends from 13,784,084–13,790,562. The translated regions (light blue) and untranslated regions (grey) in the 2 mRNA transcripts, *CG31731-RC* and *CG31731-RB*, and the locations of the transgenic insertions (purple) and RNAi target sites (green) are mapped. (Figure modified from Flybase)

**(B)** Structure of transgenic constructs. The **P{EPgy2}** construct carries two visible markers, the mini-white marker and the mini-yellow marker, and UAS binding sites for the GAL4 transcriptional regulator, adjacent to GAGA sites and upstream of the

promoter. The **PBac{WH}** construct carries the mini-white marker, Su(Hw) insulator sequences, a long (199-bp) FRT site for FLP-mediated recombination, and a terminal UAS site for GAL4-driven misexpression of adjacent genes. The **Mi{MIC}** construct is flanked by two *Minos* inverted repeats (L and R) and two inverted attP sites (P), and carries the mini-yellow marker, an EGFP coding sequence with a polyadenylation signal (pA), and a mutagenic gene-trap cassette consisting of a splice acceptor site (SA) followed by stop codons in all three reading frames. Elements are not drawn to scale and are meant only to indicate the components in each construct. Arrows indicate direction of transcription. (Figures modified from Bellen et al., 2011 and Venken et al., 2015)

**Figure 3.6 *CG1718* gene map**

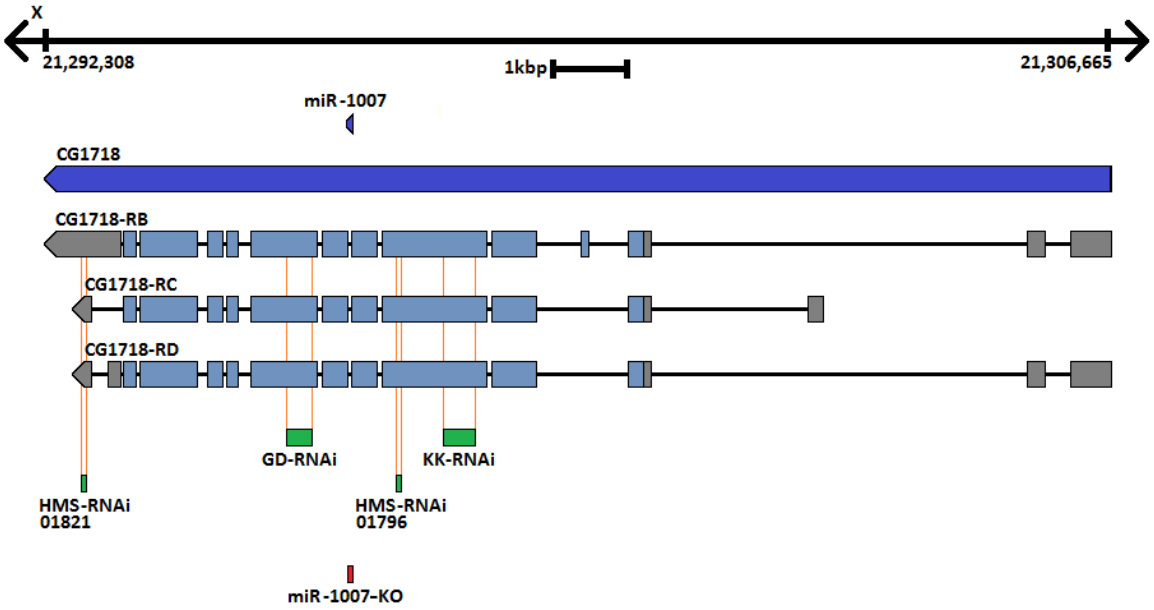


Schematic of the *CG1718* gene region on chromosome X. The *CG1718* gene (dark blue) extends from 21,292,308–21,306,665. The translated regions (light blue) and untranslated regions (grey) in the 3 mRNA transcripts, *CG1718-RB*, *CG1718-RC*, and *CG1718-RD*, and the locations of the RNAi target sites (green) are mapped. The *miR-1007* gene (dark blue) is also shown with the location of the *miR-1007* deletion (red) generated via targeted homologous recombination. (Figure modified from Flybase)

**Figure 3.7 *CG31731* insertional mutations, *CG31731*$^{PBac}$ and *CG31731*$^{Mi\{MIC\}}$, have persisting nurse cell nuclei**

**A**

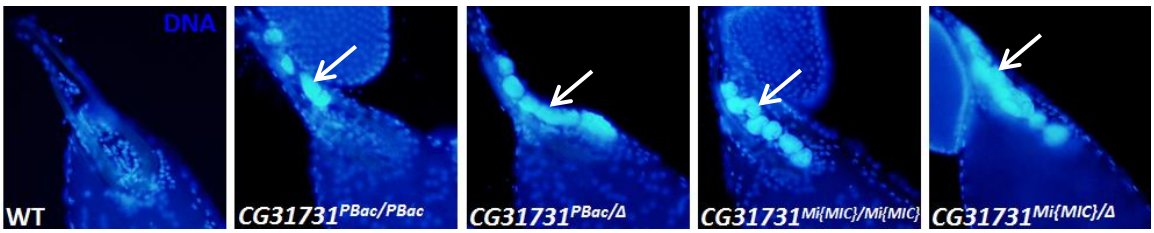


**B**

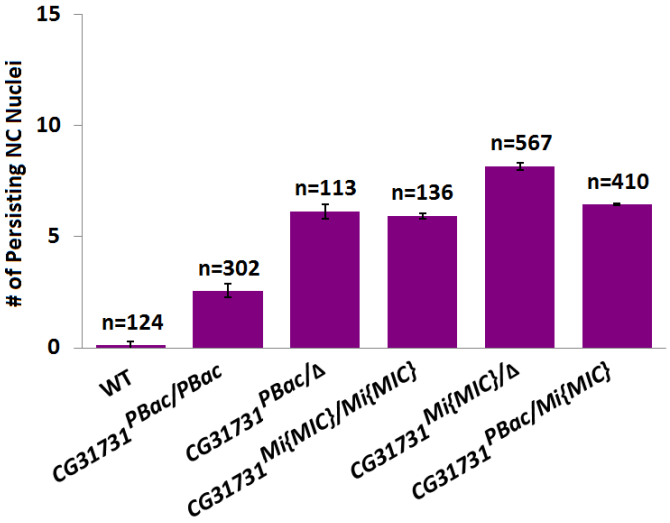


**C**

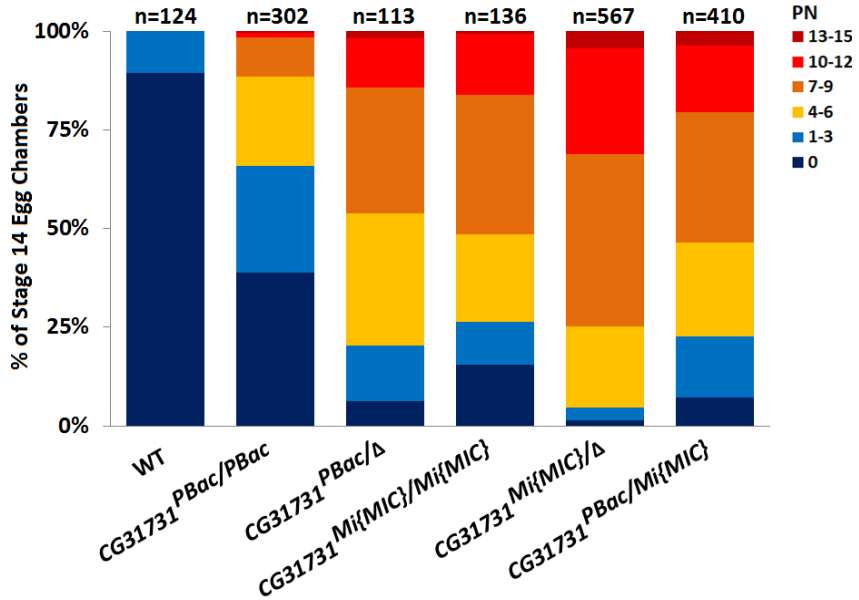

**(A)** Stage 14 egg chambers, stained with DAPI (blue) to label DNA, from wild-type (WT) or *CG31731* transgenic mutants. WT ($w^{1118}$) egg chambers successfully complete PCD and do not have persisting nurse cell nuclei. Homozygous $CG31731^{PBac/\,PBac}$ and $CG31731^{Mi\{MIC\}/\,Mi\{MIC\}}$ mutants, and hemizygotes in trans to a deficiency allele ($^{\Delta}$) have defects in nurse cell clearance and have persisting nuclei (arrows).

**(B)** The average number of persisting nuclei (PN) in stage 14 egg chambers from each genotype: WT ~0, $CG31731^{PBac/\,PBac}$ ~2-3, $CG31731^{PBac/-}$ ~6, $CG31731^{Mi\{MIC\}/\,Mi\{MIC\}}$ ~6, $CG31731^{Mi\{MIC\}/-}$ ~8, and $CG31731^{PBac/Mi\{MIC\}}$ ~6. Error bars indicate ±SEM.

**(C)** The percentage of stage 14 egg chambers exhibiting 0 PN, 1-3 PN, 4-6 PN, 7-9 PN, 10-12 PN, 13-15 PN, of all stage 14 egg chambers quantified per genotype.

**Figure 3.8 The *P{EPgy2}* insertional mutation does not disrupt *CG31731***

**A**

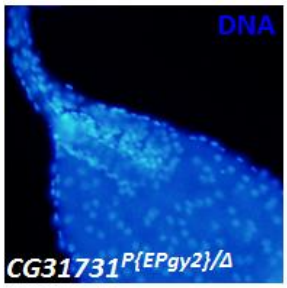


**B**

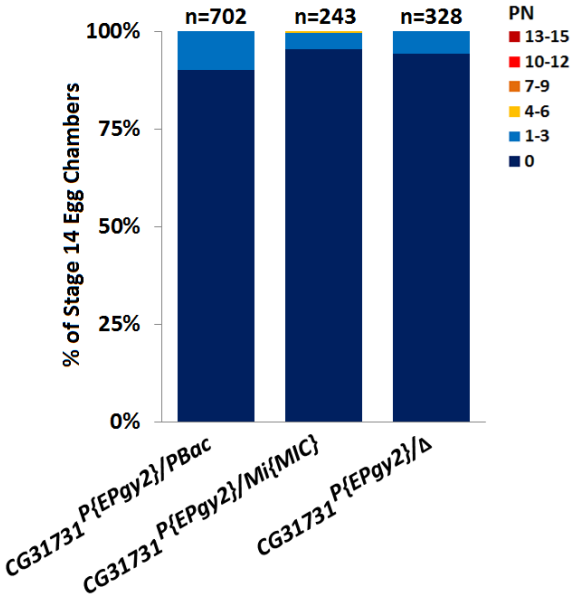


**(A)** Stage 14 egg chamber, stained with DAPI (blue) to label DNA, from a *CG31731*$^{P\{EPgy2\}/-}$ hemizygous mutant, does not exhibit persisting nurse cell nuclei. **(B)** Quantification of the persisting nuclei (PN) in *CG31731*$^{P\{EPgy2\}}$ heterozygous mutants in trans to a *CG31731*$^{PBac}$ or *CG31731*$^{Mi\{MIC\}}$ allele, and hemizygous mutants in trans to a a deficiency ($^{\Delta}$). None of these *CG31731*$^{P\{EPgy2\}}$ mutants appear to have defects in nurse cell clearance as stage 14 egg chambers do not exhibit a persisting nuclei phenotype. The percentage of stage 14 egg chambers exhibiting 0 PN, 1-3 PN, 4-6 PN, 7-9 PN, 10-12 PN, 13-15 PN, of all stage 14 egg chambers quantified per genotype is shown.

**Figure 3.9 Over-expression of *CG31731* with *P{EPgy2}* in the follicle cells, stretched follicle cells, or nurse cells, does not disrupt nurse cell clearance**

**A**

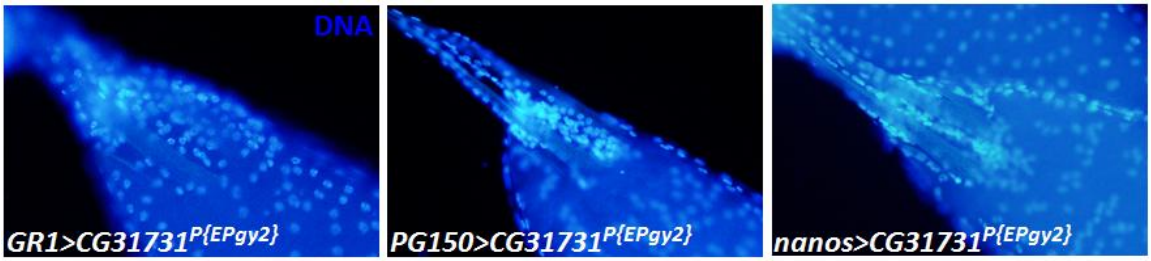


**B**

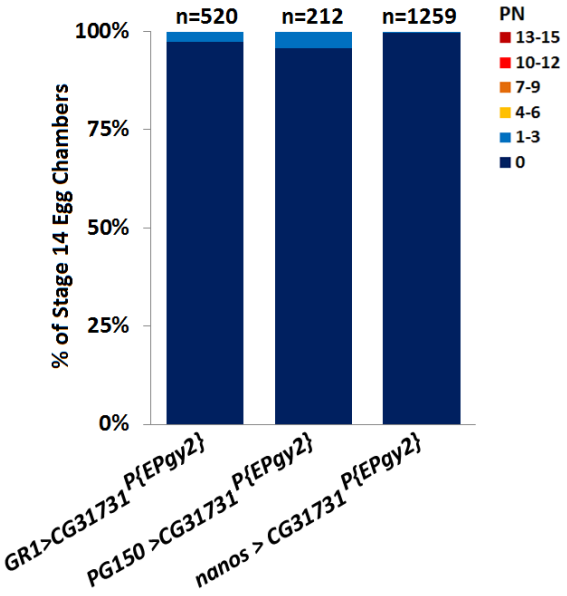


**(A)** Stage 14 egg chambers, stained with DAPI (blue) to label DNA, with GAL4 predicted to over-express *CG31731* specifically in the follicle cells (*GR1-GAL4/UAS-CG31731*$^{P\{EPgy2\}}$), stretched follicle cells (*PG150-GAL4/UAS-CG31731*$^{P\{EPgy2\}}$), or nurse cells (*nanos-GAL4/UAS-CG31731*$^{P\{EPgy2\}}$), do not have persisting nurse cell nuclei. **(B)** The percentage of stage 14 egg chambers exhibiting 0 PN, 1-3 PN, 4-6 PN, 7-9 PN, 10-12 PN, 13-15 PN, of all stage 14 egg chambers quantified per genotype.

**Figure 3.10 *CG31731* is not haploinsufficient**

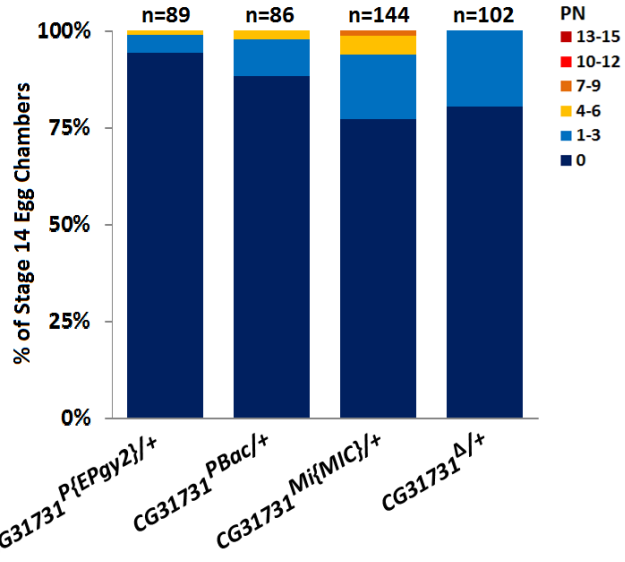


Quantification of the persisting nuclei in *CG31731* heterozygous transgenic or deficiency mutants in trans to a WT *CG31731* allele (*Cyo* balancer). None of these mutants appear to have defects in nurse cell clearance as stage 14 egg chambers do not have a persisting nuclei phenotype. The percentage of stage 14 egg chambers exhibiting 0 PN, 1-3 PN, 4-6 PN, 7-9 PN, 10-12 PN, 13-15 PN, of all stage 14 egg chambers quantified per genotype is shown.

**Figure 3.11 Knockdown of *CG31731* in the stretched follicle cells does not disrupt nurse cell clearance**

**A**

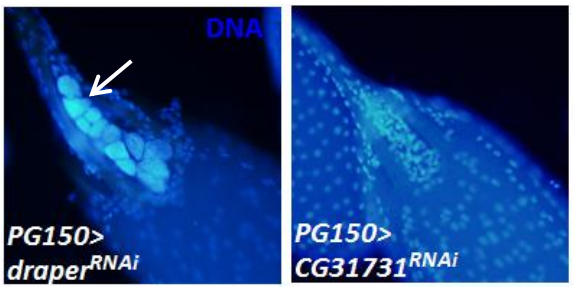


**B**

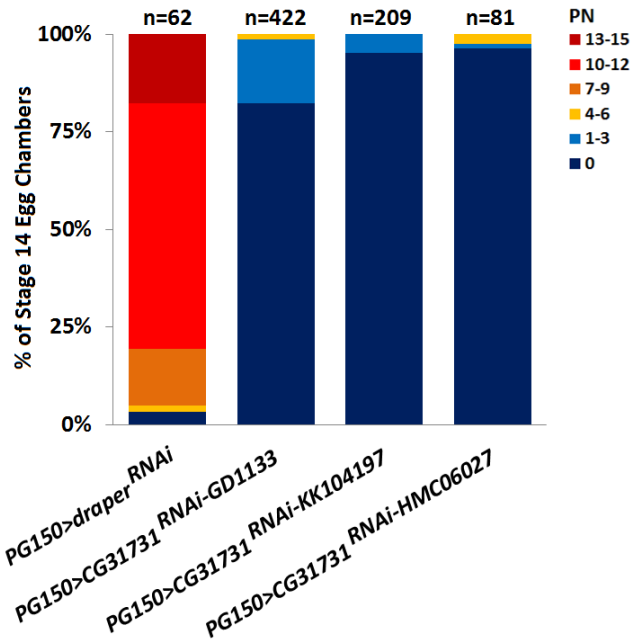


**(A)** Stage 14 egg chambers, stained with DAPI (blue) to label DNA, from *draper*$^{RNAi}$ or one of 3 different *CG31731*$^{RNAi}$ constructs (*GD*$^{1133}$, *KK*$^{104197}$, *HMC*$^{06027}$) expressed specifically in the stretched follicle cells (*PG150-GAL4/UAS-draper*$^{RNAi}$or *CG31731*$^{RNAi}$). Control *draper*$^{RNAi}$ expressing stage 14 egg chambers have persisting nuclei (arrow). *CG31731*$^{RNAi}$ expressing stage 14 egg chambers do not have persisting nuclei.
**(B)** The percentage of stage 14 egg chambers exhibiting 0 PN, 1-3 PN, 4-6 PN, 7-9 PN, 10-12 PN, 13-15 PN, of all stage 14 egg chambers quantified per genotype.

**Figure 3.12 *CG31731* is required in the follicle cells for nurse cell clearance**

**A**

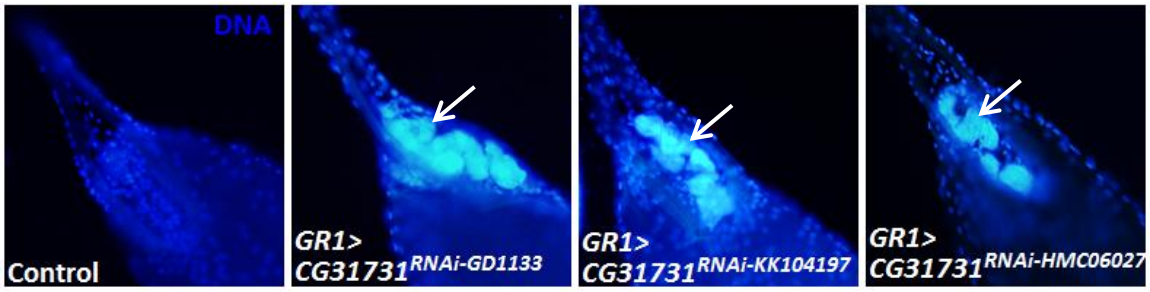


**B**

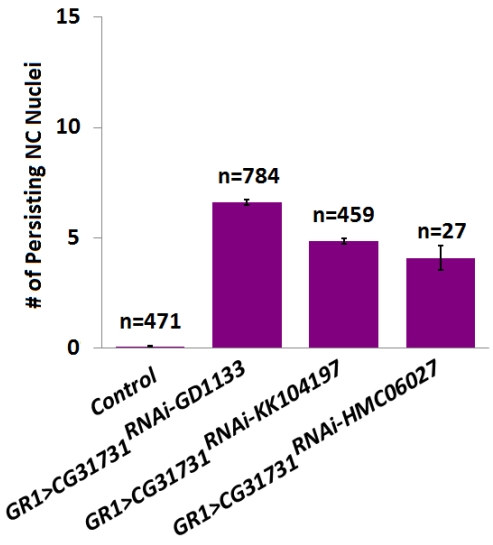


**C**

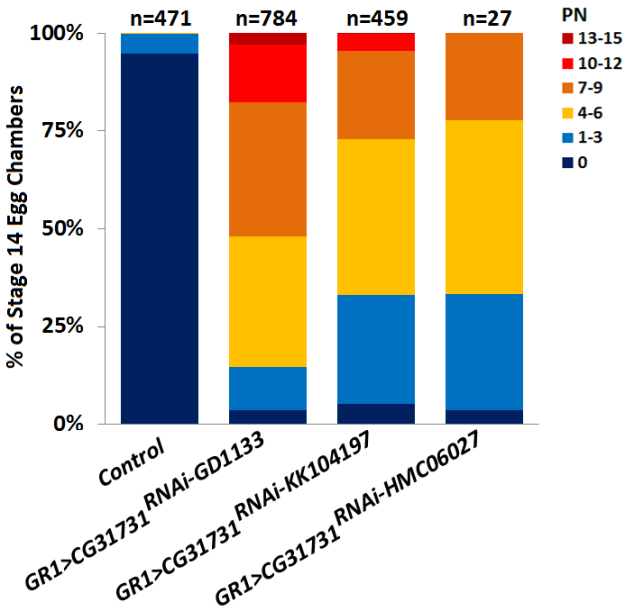

**(A)** Stage 14 egg chambers, stained with DAPI (blue) to label DNA, from control or one of 3 different *CG31731*$^{RNAi}$ constructs (*GD*$^{1133}$, *KK*$^{104197}$, *HMC*$^{06027}$) expressed specifically in the follicle cells (*GR1-GAL4 G89/UAS-CG31731*$^{RNAi}$). Sibling control (TM6B/*UAS-CG31731*$^{RNAi}$) egg chambers sucessfully complete PCD and do not have persisting nurse cell nuclei. RNAi-expressing egg chambers fail to complete PCD and have persisting nuclei (arrows).

**(B)** The average number of persisting nuclei (PN) in stage 14 egg chambers from each genotype: control ~0, *GR1>GD*$^{1133}$ ~7, *GR1>KK*$^{10419}$ ~5, *GR1>HMC*$^{06027}$ ~4-5. Error bars indicate ±SEM.

**(C)** The percentage of stage 14 egg chambers exhibiting 0 PN, 1-3 PN, 4-6 PN, 7-9 PN, 10-12 PN, 13-15 PN, of all stage 14 egg chambers quantified per genotype.

**Figure 3.13 Predicted over-expression of *CG31731* with *P{EPgy2}* does not rescue the defects in nurse clearance in egg chambers expressing *CG31731*$^{RNAi}$ specifically in the follicle cells**

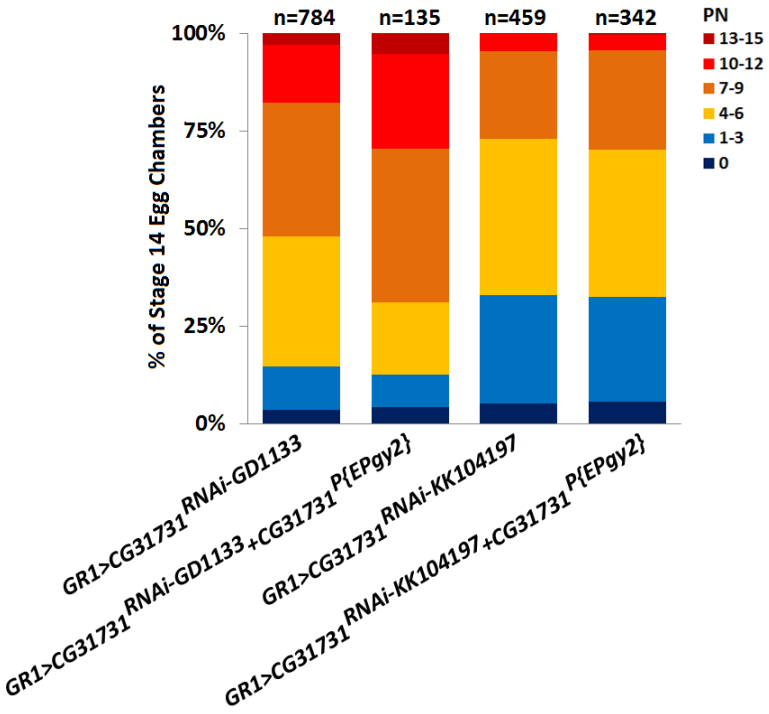


Quantification of the persisting nurse cell nuclei in egg chambers expressing one of 2 different *CG31731*$^{RNAi}$ constructs (*GD*$^{1133}$, *KK*$^{104197}$) specifically in the follicle cells (*GR1-GAL4 G89/UAS-CG31731*$^{RNAi}$) and simultaneously over-expressing *CG31731* specifically in the follicle cells (*GR1-GAL4 G89/UAS-CG31731*$^{P\{EPgy2\}}$). The simultaneous expression of *CG31731*$^{RNAi}$ and *CG31731*$^{P\{EPgy2\}}$ specifically in the follicle cells results in a similar engulfment defect observed in egg chambers only expressing *CG31731*$^{RNAi}$. The percentage of stage 14 egg chambers exhibiting 0 PN, 1-3 PN, 4-6 PN, 7-9 PN, 10-12 PN, 13-15 PN, of all stage 14 egg chambers quantified per genotype is shown.

**Figure 3.14 *CG31731* is not required in the nurse cells for their clearance**

**A**

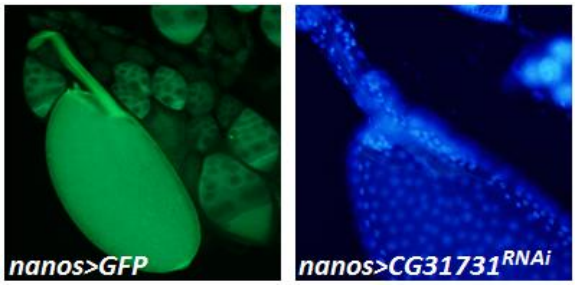


**B**

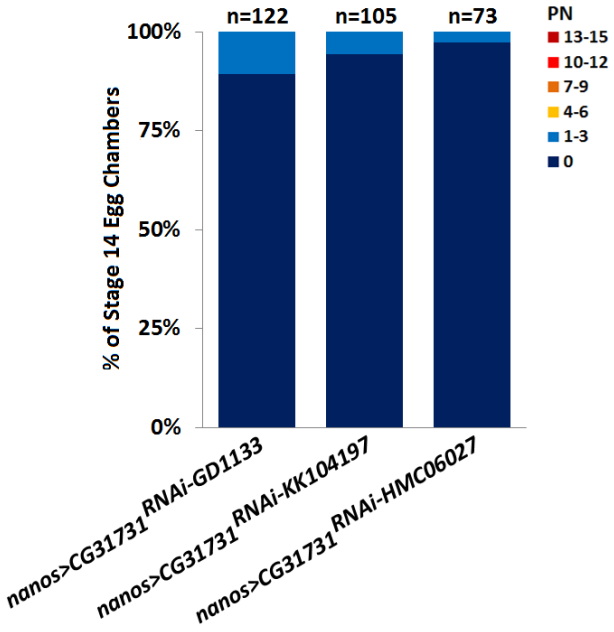


**(A)** Control egg chambers express GFP specifically in the nurse cells (*nanos-GAL4/UAS-GFP*). Stage 14 egg chamber, stained with DAPI (blue) to label DNA, from one of 3 different $CG31731^{RNAi}$ constructs ($GD^{1133}$, $KK^{104197}$, $HMC^{06027}$) expressed specifically in the nurse cells (*nanos-GAL4/UAS-*$CG31731^{RNAi}$) does not have persisting nuclei.
**(B)** The percentage of stage 14 egg chambers exhibiting 0 PN, 1-3 PN, 4-6 PN, 7-9 PN, 10-12 PN, 13-15 PN, of all stage 14 egg chambers quantified per genotype.

**Figure 3.15 *CG1718* is not required in the nurse cells for their clearance**

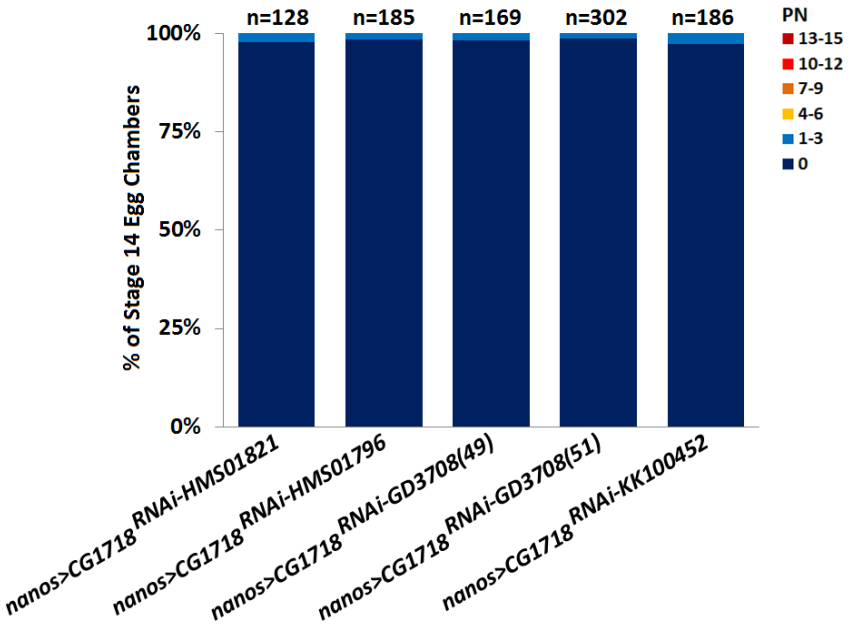


Quantification of the persisting nuclei in egg chambers expressing one of 5 different $CG1718^{RNAi}$ constructs ($HMS^{01821}$, $HMS^{01796}$, $GD^{3708}$(stock # 44449), $GD^{3708}$(stock # 44451), $KK^{100452}$) expressed specifically in the nurse cells (*nanos-Gal/UAS-*$CG1718^{RNAi}$). None of these knockdowns appear to have defects in nurse cell clearance as stage 14 egg chambers do not have a persisting nuclei phenotype. The percentage of stage 14 egg chambers exhibiting 0 PN, 1-3 PN, 4-6 PN, 7-9 PN, 10-12 PN, 13-15 PN, of all stage 14 egg chambers quantified per genotype is shown.

**Figure 3.16 *CG1718* may be required in the follicle cells for nurse cell clearance**

**A**

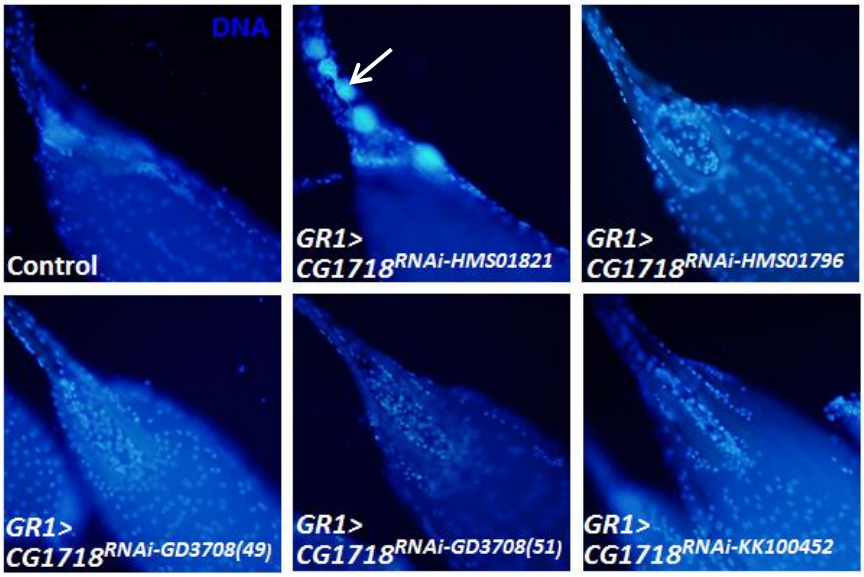


**B**

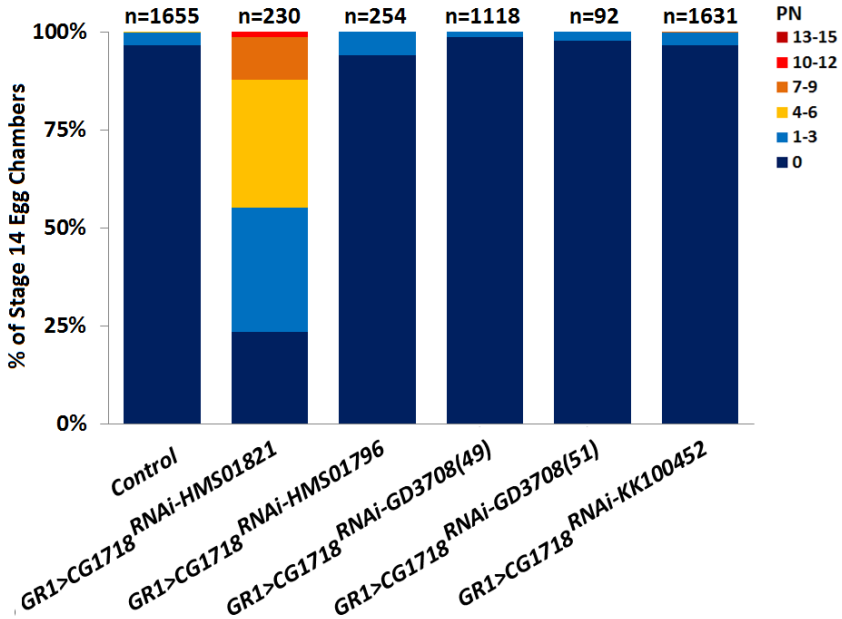

**(A)** Stage 14 egg chambers, stained with DAPI (blue) to label DNA, from control or one of 5 different *CG1718*$^{RNAi}$ constructs (*HMS*$^{01821}$, *HMS*$^{01796}$, *GD*$^{3708}$(stock # 44449), *GD*$^{3708}$(stock # 44451), *KK*$^{100452}$) expressed specifically in the follicle cells (*GR1-GAL4 G89/UAS-CG1718*$^{RNAi}$). Control (TM6B/*UAS-CG1718*$^{RNAi}$) stage 14 egg chambers sucessfully complete PCD and do not have persisting nuceli. Some *HMS*$^{01821}$ RNAi expressing egg chambers have persisting nuclei (arrow). Egg chambers expressing one of the other RNAi constructs do not have persisting nuclei.
**(B)** The percentage of stage 14 egg chambers exhibiting 0 PN, 1-3 PN, 4-6 PN, 7-9 PN, 10-12 PN, 13-15 PN, of all stage 14 egg chambers quantified per genotype

**Figure 3.17 Predicted over-expression of *CG31731* with *P{EPgy2}* does not rescue the defects in nurse clearance in egg chambers expressing *CG1718*$^{RNAi\text{-}HMS01821}$ specifically in the follicle cells**

**A**

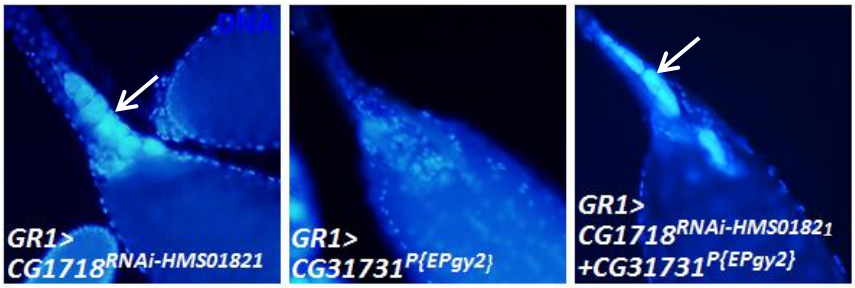


**B** **C**

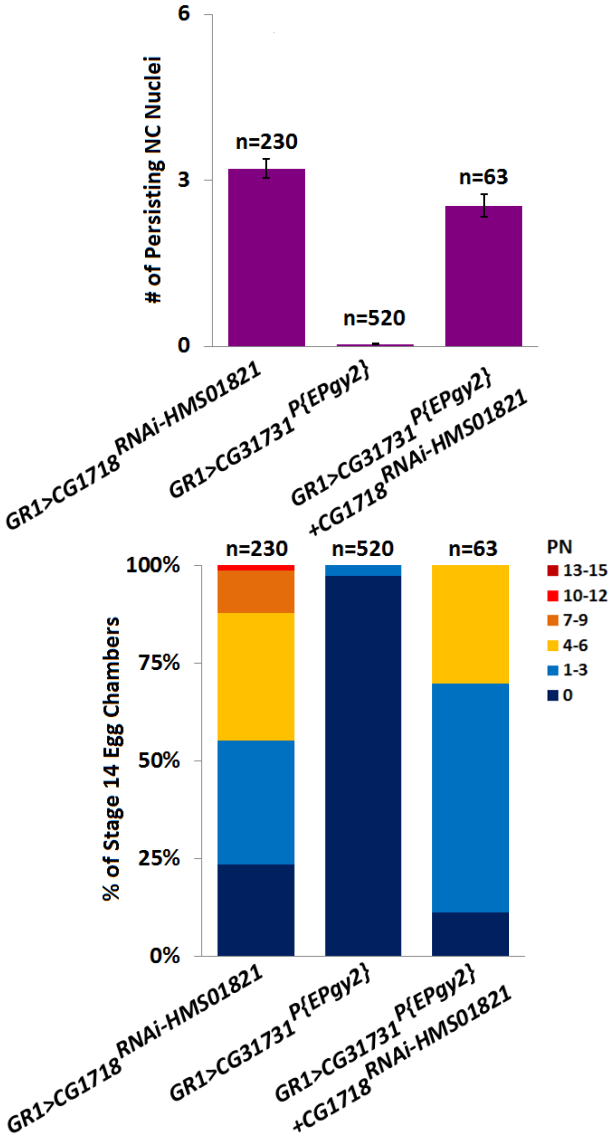


**(A)** Stage 14 egg chambers, stained with DAPI (blue) to label DNA, from *CG1718*$^{RNAi\text{-}HMS01821}$ expressed specifically in the follicle cells (*GR1-GAL4 G89/UAS-CG1718*$^{RNAi\text{-}HMS01821}$), *CG31731* predicted to be over-expressed specifically in the follicle cells (*GR1-*

*GAL4 G89/UAS-CG31731*$^{P\{EPgy2\}}$), or these double mutants. Persisting nuclei are indicated (arrows).

**(B)** The average number of persisting nuclei (PN) in stage 14 egg chambers from each genotype: *GR1> CG1718*$^{RNAi\text{-}HMS01821}$ ~3, *GR1>CG31731*$^{P\{EPgy2\}}$ ~0, *GR1> CG1718*$^{RNAi\text{-}HMS01821}$+*CG31731*$^{P\{EPgy2\}}$ ~2-3. Error bars indicate ±SEM

**(C)** The percentage of stage 14 egg chambers exhibiting 0 PN, 1-3 PN, 4-6 PN, 7-9 PN, 10-12 PN, 13-15 PN, of all stage 14 egg chambers quantified per genotype.

**Figure 3.18 *CG1718*$^{miR\text{-}1007\text{-}KO/\ miR\text{-}1007\text{-}KO}$+*CG31731*$^{PBac/\ PBac}$ double mutants have a more severe persisting nuclei phenotype than either *CG1718*$^{miR\text{-}1007\text{-}KO/\ miR\text{-}1007\text{-}KO}$ or *CG31731*$^{PBac/\ PBac}$ mutants alone**

**A**

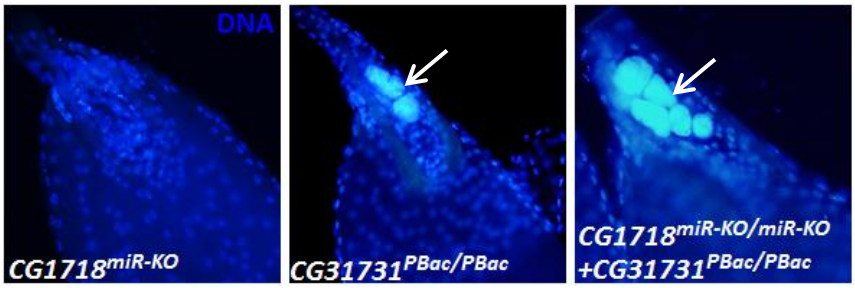


**B**

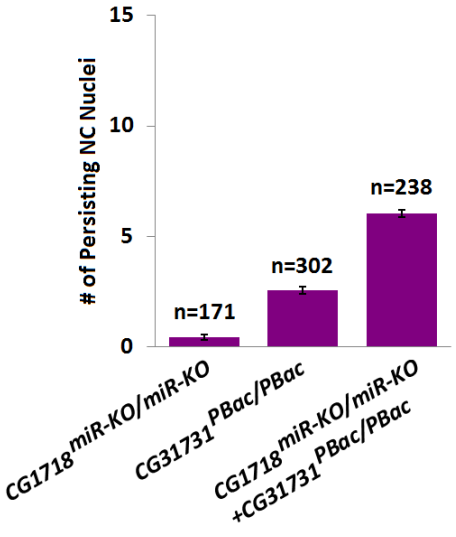


**C**

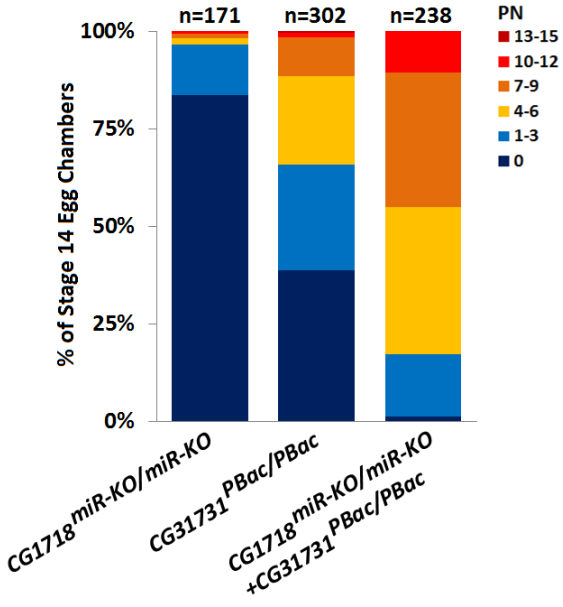

**(A)** Stage 14 egg chambers, stained with DAPI (blue) to label DNA, from *CG1718*$^{miR\text{-}1007\text{-}KO/miR\text{-}1007\text{-}KO}$ mutants, *CG31731*$^{PBac/\ PBac}$ mutants, or these double mutants. *CG1718*$^{miR\text{-}1007\text{-}KO/miR\text{-}1007\text{-}KO}$ egg chambers do not have persisting nurse cell nuclei. *CG31731*$^{PBac/\ PBac}$ and *CG1718*$^{miR\text{-}1007\text{-}KO/miR\text{-}1007\text{-}K+}$*CG31731*$^{PBac/\ PBac}$ double mutants have persisting nuclei (arrows).

**(B)** The average number of persisting nuclei (PN) in stage 14 egg chambers from each genotype: *CG1718*$^{miR\text{-}1007\text{-}KO/miR\text{-}1007\text{-}KO}$ ~0, *CG31731*$^{PBac/\ PBac}$ ~2-3, *CG1718*$^{miR\text{-}1007\text{-}KO/miR\text{-}1007\text{-}KO+}$*CG31731*$^{PBac/\ PBac}$ ~6. Error bars indicate ±SEM.

**(C)** The percentage of stage 14 egg chambers exhibiting 0 PN, 1-3 PN, 4-6 PN, 7-9 PN, 10-12 PN, 13-15 PN, of all stage 14 egg chambers quantified per genotype.

**Figure 3.19 *CG31731*$^{Mi\{MIC\}/Mi\{MIC\}}$*+GR1>Ced-12*$^{RNAi}$ double mutants have a more severe persisting nuclei phenotype than either *CG31731*$^{Mi\{MIC\}/Mi\{MIC\}}$ or *GR1>Ced-12*$^{RNAi}$ mutants alone**

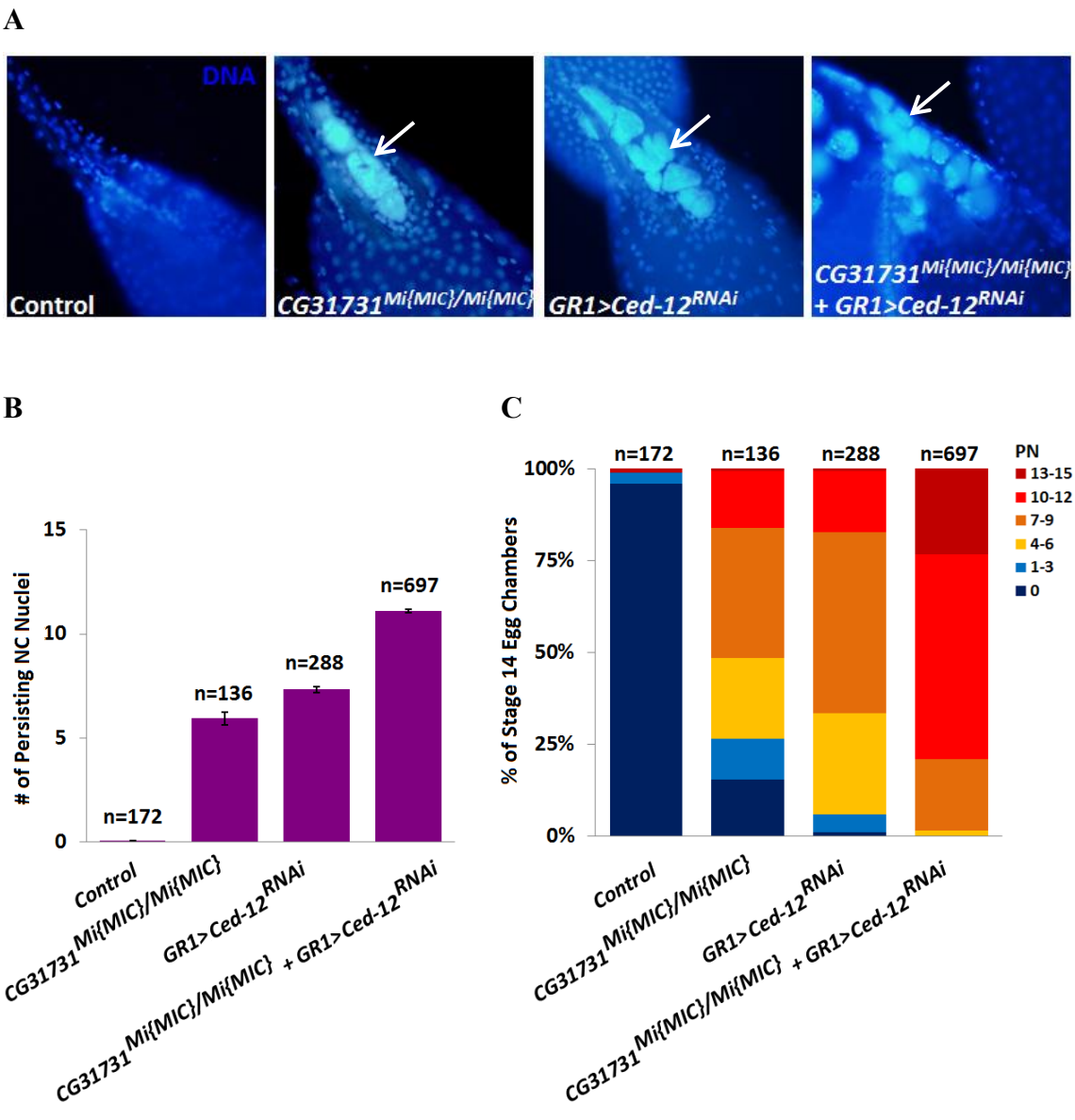

**(A)** Stage 14 egg chambers, stained with DAPI (blue) to label DNA, from control, *CG31731*$^{Mi\{MIC\}/Mi\{MIC\}}$ mutants, *Ced-12*$^{RNAi}$ expressed specifically in the follicle cells (*GR1-GAL4 G89/UAS-Ced-12*$^{RNAi}$), or these double mutants. Control (*TM6B/UAS-Ced-12*$^{RNAi}$) stage 14 egg chambers successfully complete PCD and do not have persisting nurse cell nuclei. The *CG31731*$^{Mi\{MIC\}/Mi\{MIC\}}$ and *Ced-12*$^{RNAi}$ expressing egg chambers chambers have persisting nuclei (arrows).

**(B)** The average number of persisting nuclei (PN) in stage 14 egg chambers from each genotype: control ~0, *CG31731*$^{Mi\{MIC\}/Mi\{MIC\}}$ ~6, *GR1>Ced-12*$^{RNAi}$ ~7, *CG31731*$^{Mi\{MIC\}/Mi\{MIC\}}$*+GR1>Ced-12*$^{RNAi}$ ~11. Error bars indicate ±SEM.

**(C)** The percentage of stage 14 egg chambers exhibiting 0 PN, 1-3 PN, 4-6 PN, 7-9 PN, 10-12 PN, 13-15 PN, of all stage 14 egg chambers quantified per genotype.

**Figure 3.20 *CG31731*$^{Mi\{MIC\}/Mi\{MIC\}}$ +*draper*$^{\Delta 5}$ double mutants have a similar persisting nuclei phenotype to *draper*$^{\Delta 5}$ mutants alone**

**A**

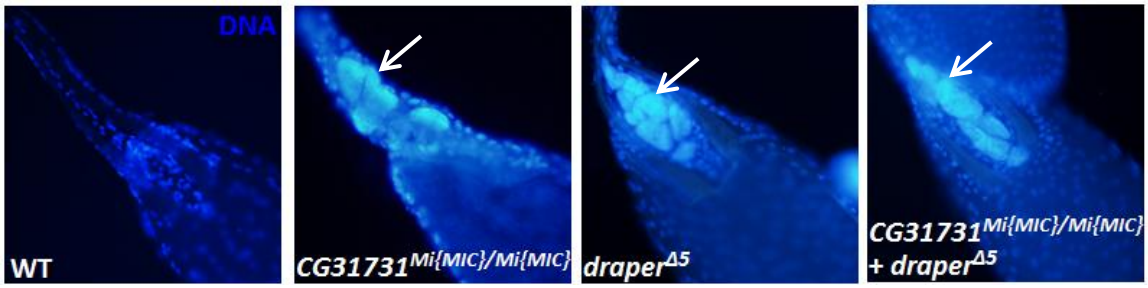


**B**

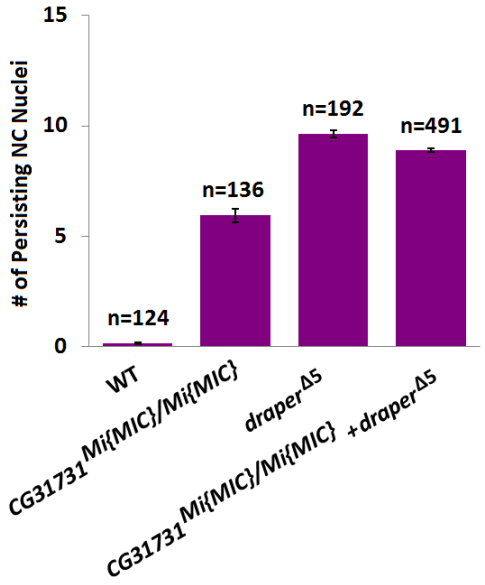


**C**

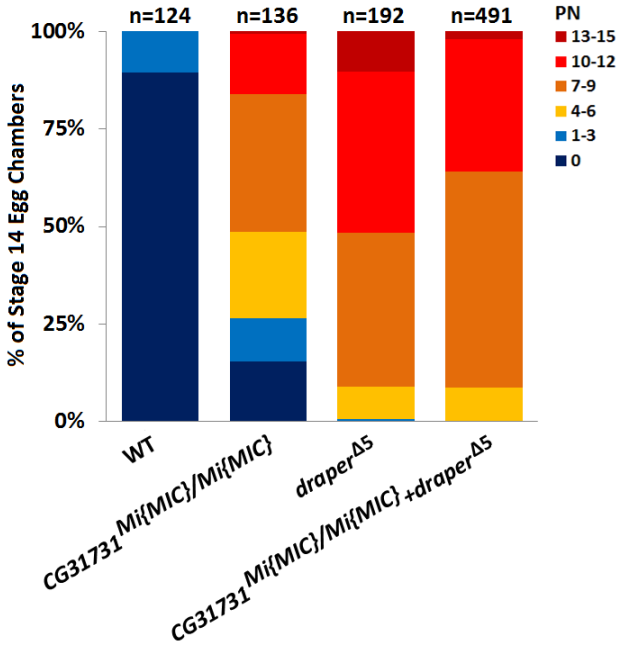

**(A)** Stage 14 egg chambers, stained with DAPI (blue) to label DNA, from wild-type (WT), *CG31731*$^{Mi\{MIC\}/Mi\{MIC\}}$ mutants, *draper*$^{\Delta 5}$mutants, or these double mutants. WT (*w*$^{1118}$) stage 14 egg chambers successfully complete PCD and do not have persistng nurse cell nuclei. *CG31731*$^{Mi\{MIC\}/Mi\{MIC\}}$ and *draper*$^{\Delta 5}$stage 14 egg chambers have persisting nuclei (arrows).

**(B)** The average number of persisting nuclei (PN) in stage 14 egg chambers from each genotype: WT ~0, homozygous *CG31731*$^{Mi\{MIC\}/Mi\{MIC\}}$ ~6, *draper*$^{\Delta 5}$~9-10, *CG31731*$^{Mi\{MIC\}}$+ *draper*$^{\Delta 5}$~9. Error bars indicate ±SEM.

**(C)** The percentage of stage 14 egg chambers exhibiting 0 PN, 1-3 PN, 4-6 PN, 7-9 PN, 10-12 PN, 13-15 PN, of all stage 14 egg chambers quantified per genotype.

**Figure 3.21 CG31731 promotes Draper enrichment surrounding the nurse cells**

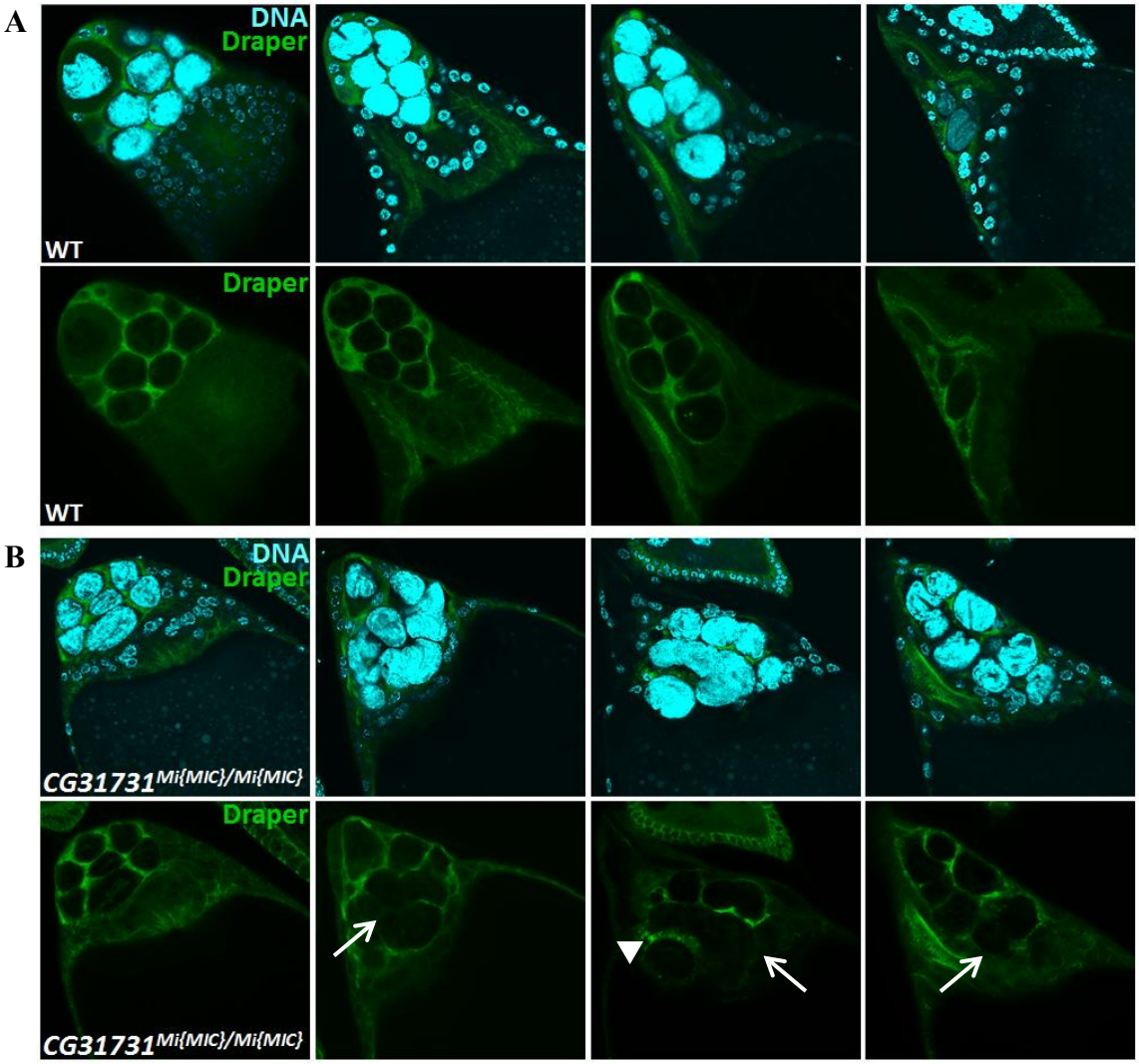


**(A-B)** Late-stage egg chambers, stained with anti-Draper antibody (green) to label Draper, and DAPI (cyan) to label DNA, from WT or *CG31731*$^{Mi\{MIC\}/Mi\{MIC\}}$ mutants.
**(A)** In WT ($w^{1118}$) late-stage egg chambers, Draper is evenly enriched in the stretched follicle cells and completely surrounds each nurse cell.
**(B)** In *CG31731*$^{Mi\{MIC\}/Mi\{MIC\}}$ late-stage egg chambers, Draper enrichment in the stretched follicle cell membranes is scattered (arrowhead). Draper staining does not completely surround the nurse cells and is sometimes absent around the nurse cells (arrows).

**Figure 3.22 CG31731 promotes acidification of the nurse cells**

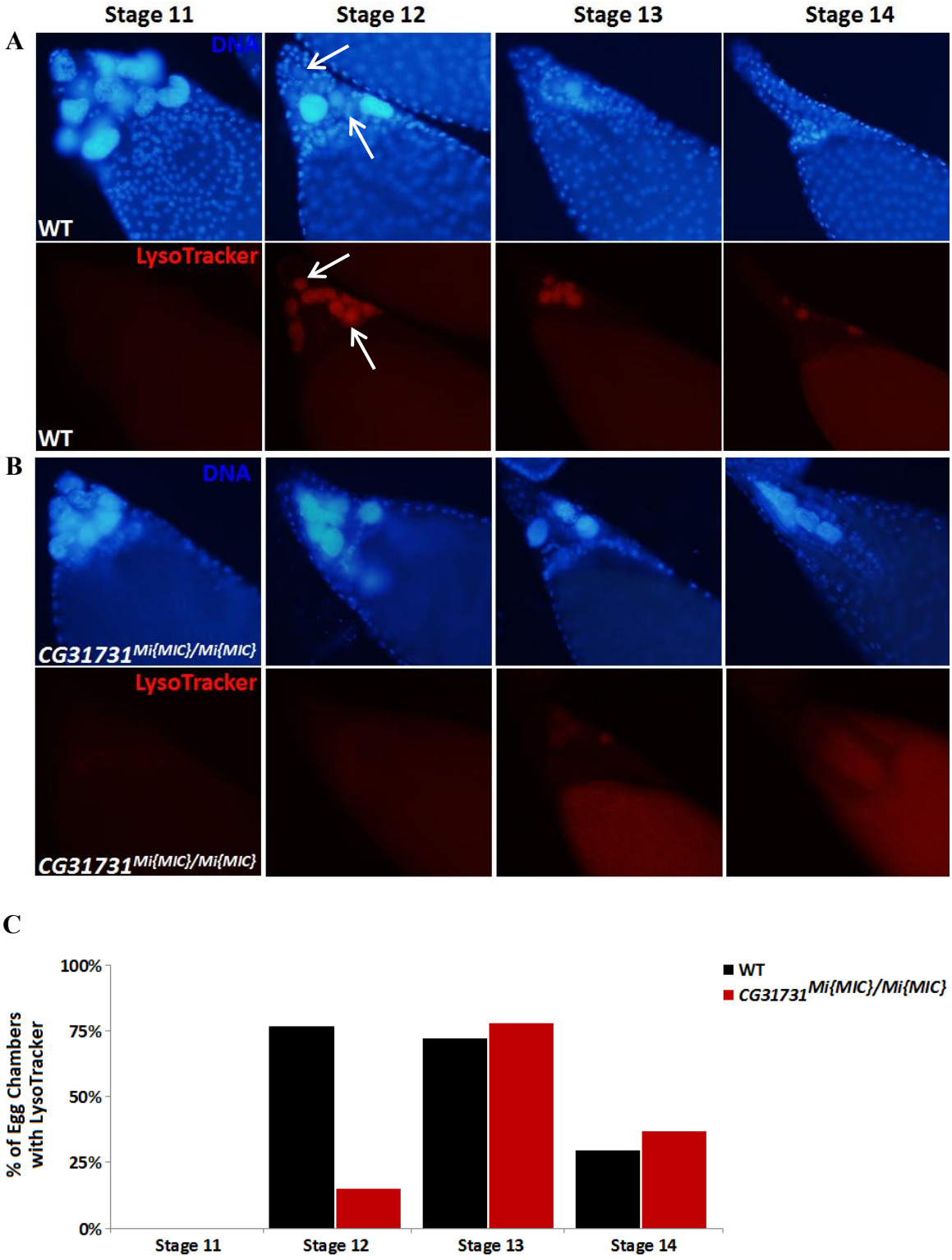

**(A-B)** Egg chambers, stained with LysoTracker (red) to label acidified compartments, and DAPI (blue) to label DNA, from WT or *CG31731*$^{Mi\{MIC\}/Mi\{MIC\}}$ mutants.
**(A)** WT (*w*$^{1118}$) developing egg chambers show acidified nurse cells beginning stage 12, after dumping has completed, when majority of the nurse cells become LysoTracker-positive. LysoTracker-positive staining of the nurse cell nuclei visibly corresponds to a reduction DAPI staining (arrows). By stage 13 when the dorsal appendages begin to form, only a few nurse cell nuclei stain with DAPI as almost all the nurse cells have been acidified. By stage 14, all the remaining nurse cells become LysoTracker-positive and no nurse cell nuclei can be detected in the DAPI channel.
**(B)** *CG31731*$^{Mi\{MIC\}/Mi\{MIC\}}$ stage 12-14 egg chambers exhibit a few nurse cells that are LysoTracker-positive. The stage 12 egg chamber does not show any LysoTracker-positive staining, while a few nurse cells in the stage 13 egg chamber are acidified. At stage 14, the persisting nurse cell nuclei are not LysoTracker-positive and can be detected in the DAPI channel.
**(C)** The percentage of egg chambers that exhibit nurse cells with LysoTracker-positive staining of all late stage egg chambers quantified per genotype. WT stage 11 (n=41), stage 12 (n=43), stage 13 (n=18), stage 14 (n=34), and *CG31731*$^{Mi\{MIC\}/Mi\{MIC\}}$ stage 11 (n=26), stage 12 (n=47), stage 13 (n=18), stage 14 (n=68).

**Figure 3.23 *CG31731* is required in the follicle cells for engulfment of the germline material during starvation-induced PCD**

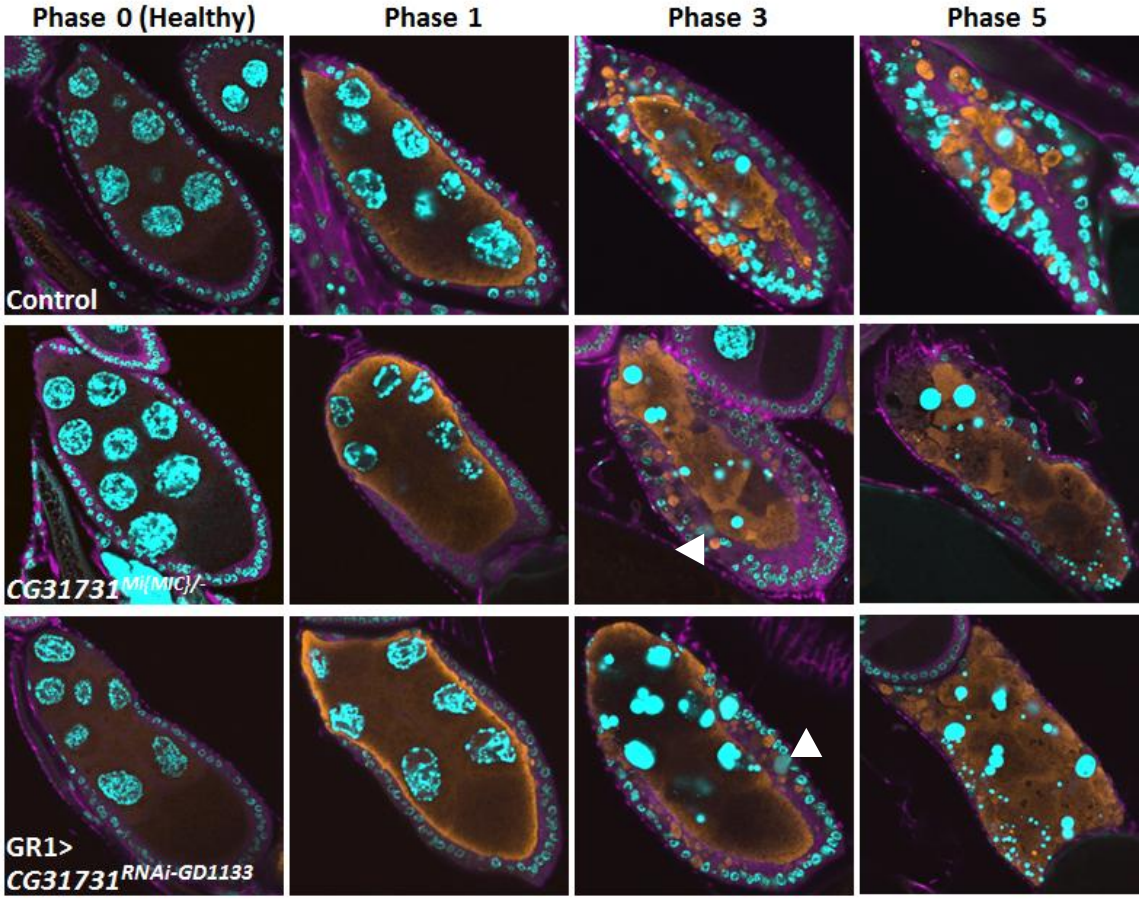


Healthy and dying egg chambers stained with anti-Dlg antibody (magenta) to label follicle cell membranes, anti-cleaved Dcp-1 antibody (orange) to label active caspases and apoptotic germline debris, and DAPI (cyan) to label DNA. In control (*TM6B/UAS-CG31731*$^{RNAi\text{-}GD1133}$) dying egg chambers, follicle cells normally enlarge from phase 1-5 and engulfed Dcp-1-positive vesicles can be seen inside the follicle cells. In *CG31731*$^{Mi\{MIC\}/-}$ mutants or when *CG31731*$^{RNAi\text{-}GD1133}$ is expressed specifically in the follicle cells (*GR1-GAL4 G89/UAS-CG31731*$^{RNAi\text{-}GD1133}$), late phase dying egg chambers show severe engulfment defects with fewer engulfed Dcp-1 vesicles in phase 3, completely unengulfed germline and follicle cells with pyknotic nuclei and no membrane markers in phase 5. Engulfed nurse cell nuclei are indicated (arrowheads).

**Figure 3.24 *CG31731*$^{Mi\{MIC\}/Mi\{MIC\}}$ mutants do not exhibit defects in neuronal cell clearance in the brain**

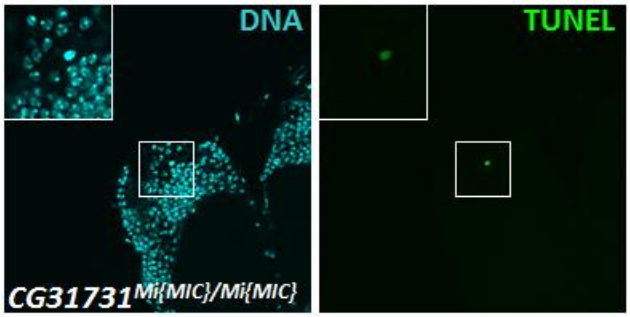


A brain from a *CG31731*$^{Mi\{MIC\}/Mi\{MIC\}}$ mutant stained with DAPI (cyan) to label DNA and TUNEL (green) to label fragmented DNA. DAPI staining shows predominantly neuronal nuclei with healthy dispersed chromatin and a single condensed, TUNEL-positive, nucleus (n= 12). (Images acquired by Johnny Elguero)

# CHAPTER 4: DISCUSSION AND FUTURE PERSPECTIVES

## 4.1 Engulfment during programmed cell death

The engulfment process is essential in a variety of tissues and organs to ensure the efficient removal of potentially deleterious dying and dead cells. In general, the removal process is performed by phagocytes which engulf the dead material. Extensive genetic studies in *C. elegans*, *Drosophila*, mice, and humans have illustrated a highly conserved engulfment mechanism regulated by two parallel signaling pathways, one involving *ced-1/-6/-7* and the other *ced-2/-5/-12*. Together, these components of the engulfment machinery promote vesicle delivery and cytoskeletal rearrangements for membrane extensions at the phagocytic cup. Currently, the orthologs for each of these core engulfment genes have been identified in each respective species, except for *ced-7* in *Drosophila*. The work presented in this thesis characterizes the role of novel gene, *CG31731*, which appears to play a *ced-7*-like role in engulfment during PCD in the *Drosophila* ovary.

## 4.2 CED-7/ABCA1

The *C. elegans ced-7* gene, and its mammalian homolog *ABCA1,* encode proteins of the ABCA class of transporters. Sequence analyses of *ced-7/ABCA* indicate they each possess 2 TMDs which can localize to membranes, and 2 NBDs which can hydrolyze ATP to translocate substrates across the membrane. Interestingly, while in ABCA1 the function of both NBDs is equally important (Luciani and Chimini, 1996), in CED-7 the first NBD appears to be more important than the second (Wu and Horvitz, 1998). To

date, the precise mechanism of transport in CED-7/ABCA1 remains elusive. The lack of collective data between these functionally equivalent ABC transporters has made it difficult to determine their precise roles during engulfment during PCD.

Some studies in *C. elegans* suggest CED-7 promotes CED-10- mediated cytoskeletal rearrangements (Kinchen et al., 2005). How this may be achieved is unclear and this model is controversial (Mangahas and Zhou, 2005). Other studies in mammalian cell culture have demonstrated a requirement for ABCA1 in PtdSer exposure following an apoptotic stimulus (Hamon et al., 2000). Whether ABCA1 is expressed in dying cells *in vivo,* remains unknown. While CED-7 is reported to be required in both the phagocyte and the dying cell for efficient engulfment (Wu and Horvitz, 1998), it is not required for PtdSer exposure in dying cells *in vivo* (Mapes et al., 2012).

With more consistency, CED-7/ABCA1 have both been shown to be required for CED-1/MEGF10 clustering at the phagocytic cup (Zhou et al., 2001; Hamon et al., 2006), which in *C. elegans* allows for the recognition of PtdSer on the surface of dying cells by CED-1 (Wang et al., 2010). Recently, CED-7 was also shown to promote the shuttling of vesicles, possibly containing engulfment recognition signals, from dying cells to phagocytic cells (Mapes et al., 2012), which correlates with the known role of ABCA1 and also ABCA7 in mediating cholesterol and lipid efflux from the plasma membrane (Hamon et al., 2000; Wang et al., 2003). Furthermore, CED-7/ABCA1 have also been implicated in vesicle trafficking with DYN-1/Dynamin to deliver vesicles to the growing phagocytic cup (Yu et al., 2006), and to promote phagosome maturation and subsequent degradation of the cell corpse (Yu et al., 2008). All taken into consideration, these

observations suggest that CED-7/ABCA1 likely contributes several roles during engulfment and may have a role in cell corpse degradation.

Most of the proposed activities of CED-7/ABCA1 involve the trafficking of lipids, suggesting they may act as lipid transporters. Indeed, ABCA transporters share a functional relation in lipid transport (Vasiliou et al., 2009). However, where exactly these unique transporters act to transport lipids, whether they export or import lipids across the membrane, and which types of lipids they transport during engulfment, remains unclear.

**4.3 CG31731 discussion and future perspectives**

To our knowledge, prior to this study there have been no reports of a *Drosophila* functional equivalent for CED-7/ABCA. In this work, we show that *CG31731* encodes an ABCA transporter similar to CED-7/ABCA1 that is required for engulfment during PCD. Sequence analyses of *CG31731* indicates that the gene encodes an ABC transporter of the ABCA family that contains 2 membrane-spanning TMDs and 2 ATP-binding NBDs. Alignment of the predicted amino acid sequence of *CG31731* with that of *ced-7* and the mammalian counterpart *ABCA1* found a substantial amount of similarity and identity between the polypeptides, especially in the catalytic NBD regions. Although *CG1718* showed a higher similarity and identity with *ced-7* and *ABCA1*, suggesting that the gene is evolutionarily closer to *ced-7* and *ABCA1*, we did not find an independent role for *CG1718* during nurse cell clearance in the ovary, and a separate group similarly did not observe a role for *CG1718* during neuronal corpse clearance in the brain (Ziegenfuss, 2012). Instead, our experiments show that CG31731 is functionally more similar to CED-7/ABCA1 during engulfment during PCD in the *Drosophila* ovary.

We found that *CG31731* mutants exhibit engulfment defects during developmental PCD in the ovary, as indicated by the persistence of uncleared nurse cell corpses in stage 14 egg chambers. Our genetic analyses show that *CG31731* is required in the follicle cells for clearance of the nurse cells. Intriguingly, RNAi-mediated gene silencing of *CG31731* specifically in the phagocytic stretched follicle cells did not disrupt clearance of the nurse cells, suggesting *CG31731* is expressed earlier before the stretched follicle cells differentiate from the follicle cells after stage 8. While additional expression of *CG31731* is not required in these specialized follicle cells, the CG31731 protein is likely present and required for the stretched follicle cell phagocytic function. In the future, to verify exactly in which cell types *CG31731* is present, we hope to detect the protein via an antibody or endogenous tag.

In *C. elegans*, CED-7 was reported to be required in both the phagocytic cell and in the dying cell for efficient corpse clearance (Wu and Horvitz, 1998). Our studies in the *Drosophila* ovary observed a requirement for CG31731 in the phagocytic follicle cells, but not in the dying nurse cells. We knocked down *CG31731* expression specifically in the germline and did not notice any apparent engulfment defects. Of the 3 available RNAi constructs, 2 encode long hairpin RNAs which are typically ineffective in the germline (Ni et al., 2011). 1 expresses short hairpin RNAs, which should efficiently facilitate knockdown in the nurse cells, however it is still possible that the knockdown was unsuccessful. Thus, we are currently generating homozygous *CG31731* germline clones using the FLP/FRT $ovo^{D}$ system (Chou and Perrimon, 1996). The results from

these germline clones will reliably determine whether *CG31731* also has a role in the dying nurse cells for their clearance.

In several experiments, we also attempted to over-express *CG31731* using the *P{EPgy2}* UAS-enhancer construct. Unfortunately, our results from these experiments were often inconclusive and did not corroborate with our other findings. We speculate that the $CG31731^{P\{EPgy2\}}$ allele may not actually over-express the *CG31731* gene. We have extracted RNA from the ovaries of $GR1>CG31731^{P\{EPgy2\}}$ mutants and plan to perform qRT-PCR to check the expression levels of *CG31731* in these mutants compared to in WT ovaries. We also plan to perform qRT-PCR with RNA extracted from the ovaries of $CG31731^{PBac/PBac}$, $CG31731^{Mi\{MIC\}/Mi\{MIC\}}$, and $CG31731^{Mi\{MIC\}/-}$ mutants. Our data suggest the $CG31731^{PBac/PBac}$ mutant is a weak hypomorph while the $CG31731^{Mi\{MIC\}/Mi\{MIC\}}$ mutant is a strong hypomorph. In theory the *Mi{MIC}* insertion should generate a null mutation in the gene. We hope to validate the expression of *CG31731* in these mutants via qRT-PCR. If we find that the $CG31731^{Mi\{MIC\}/Mi\{MIC\}}$ mutant is a null, this would suggest that other genes affected in the deficiency allele are contributing to the more severe engulfment defect in $CG31731^{Mi\{MIC\}/-}$ mutants. In such a case, it would be interesting to pursue other genes missing in the deficiency and perhaps identify other novel components of the engulfment machinery.

Core components of the engulfment machinery identified in *Drosophila* include Draper/Ced-6 and Crk/MBC/Ced-12. Our double mutant analyses of $CG31731^{Mi\{MIC\}/Mi\{MIC\}}$ with $draper^{\Delta 5}$ or $Ced\text{-}12^{RNAi}$, demonstrate that *CG31731* likely acts in the same pathway as *draper* and in parallel to *Ced-12*. Indeed, in *C. elegans* and

mammals CED-7/ABCA1 is known to act in the same pathway as CED-1/MEGF10 and parallel to CED-12/ELMO (Mangahas and Zhou, 2005; Hamon et al., 2006). These results suggest *CG31731* may serve as the functional equivalent for CED-7/ABCA1 in the Draper pathway. We also found a role for *CG1718* when *CG31731* is disrupted. Our data show evidence of a compensatory relationship between *CG1718* and *CG31731* during removal of the nurse cells in developmental PCD. Since both genes encode ABC transporters of the same ABCA family, which are known to share a functional relationship in lipid trafficking, it may not be too surprising that the proteins may be able to compensate for one another. In mammals, ABCA1 and ABCA7 have been observed to provide homologous functions, especially in lipid homeostasis (Hamon et al., 2000; Wang et al., 2003). Therefore, we speculate that in the lack of *CG31731*, *CG1718* may provide a *CG31731*-like function during nurse cell clearance in the ovary.

Curiously, the $CG1718^{miR\text{-}1007\text{-}KO/miR\text{-}1007\text{-}KO}$ mutant, which provided evidence of genetic redundancy between *CG1718* and *CG31731*, specifically carries a null mutation in the *miR-1007* gene, and microRNAs are known to also influence lipid metabolism and cell death (Ambros, 2003). It is not obvious whether the engulfment defect we observed identifies a role for *CG1718* or for *miR-1007*. Additional experiments are needed to clarify this dilemma. A relatively straightforward experiment would be to simultaneously silence *CG1718* and *CG31731* gene expression without affecting *miR-1007* expression. Conveniently, there are several *CG1718* RNAi constructs readily available to specifically knockdown only the *CG1718* transcripts. The results from these experiments would

provide additional evidence as to whether *CG1718* can genetically compensate for the lack of *CG31731* in nurse cell clearance.

Multiple investigations in *C. elegans* and mammals have repeatedly observed a role for CED-7/ABCA1 in lipid transport (Hamon et al., 2000; Wang et al., 2010; Mapes et al., 2012). Attractively, *CG1718* was previously implicated in lipid metabolism and speculated to play a similar role to ABCA1 in lipid efflux (Bujold et al., 2010). While we did not find an independent role for *CG1718* in nurse cell clearance, our data suggest a genetic redundancy for *CG31731*, supporting a hypothetical role for CG31731 in lipid transport. Thus by analogy, CG31731 may function as a lipid transporter. In support of this hypothesis, *CG31731* is expressed at very high levels in the larval fat bodies (Flybase). Additionally, in *CG31731* mutant egg chambers, follicle cells fail to properly extend their membranes, perhaps because the delivery of vesicles containing lipids to the growing follicle cell membrane is disrupted, resulting in insufficient membrane extensions. Indeed, CED-7 has been implicated in intracellular vesicle delivery to the phagocytic cup (Yu et al., 2006), and ABCA1 has been demonstrated to shuttle lipids albeit to extracellular HDLs (Hamon et al., 2000). To further investigate a potential role for CG31731 in lipid transport, it would be useful to determine the membranes to which CG31731 localizes, possibly with an antibody or an endogenous tag, and observe any changes in lipid distribution across these membranes. It would also be interesting to visualize the abundance of lipid vesicles, perhaps with Oil Red O staining, in WT versus *CG31731* mutant egg chambers. The data from these experiments may provide more concrete evidence to determine a role for CG31731 in lipid trafficking.

An equally important question concerns the specific substrates – if lipids, then what type of lipids, are transported by CED-7/ABCA1 and CG31731? *In vitro* mouse cell culture experiments have suggested that ABCA1 may act as a floppase to transport PtdSer from the inner leaflet to the outer leaflet in apoptotically dying cells (Hamon et al., 2000). However, PtdSer exposure on the surface of dying cells *in vivo* does not require CED-7 in *C. elegans* (Mapes et al., 2012). Perhaps a different approach to determine the substrate would be to define the direction of transport, specifically whether these proteins function as exporters or importers. While not ideal, these experiments may be more easily carried out *in vitro* in cell culture. Since more is known about the distribution of lipids across healthy versus dying cells, if these ABC transporters are transporting lipids, knowing which direction they may be transporting lipids would provide a clue to its specific lipid substrate, and thereby how their activity contributes to PCD.

CED-7/ABCA1 has been demonstrated to promote CED-1/MEGF10 clustering at the phagocytic cup (Zhou et al., 2001; Hamon et al., 2006). Similarly, we observed a requirement for *CG31731* in Draper enrichment and accumulation around the dying nurse cells. Draper staining in egg chambers from $CG31731^{Mi\{MIC\}/Mi\{MIC\}}$ mutants showed a lack of Draper enrichment in the stretched follicle cells, scattered Draper staining around some nurse cell nuclei, and absent Draper staining around other nuclei. We wonder whether in these mutants Draper fails to cluster at the phagocytic cup or the stretched follicle cells fail to extend and surround all the nurse cells. In other engulfment defective mutants we have previously characterized, the stretched follicle cells can fail to surround

some nurse cells (Timmons et al., 2016). Moving forward, we plan to express an endogenous mCD8-GFP marker specifically in the stretched follicle cells, to observe the location of the stretched follicle cells in *CG31731*$^{Mi\{MIC\}/Mi\{MIC\}}$ mutants.

Previous work from our lab has shown that in *draper*$^{\Delta 5}$mutants, acidification of the nurse cells is dramatically blocked (Timmons et al., 2016). We deduced that since Draper enrichment is depressed in *CG31731*$^{Mi\{MIC\}/Mi\{MIC\}}$ mutants, perhaps nurse cell acidification may also be disrupted. Indeed, LysoTracker staining of late stage egg chambers from *CG31731*$^{Mi\{MIC\}/Mi\{MIC\}}$ mutants indicate that while acidification is not blocked, it is delayed in developing egg chambers. Attractively, a similar defect is observed in *C. elegans* wherein null mutations in the pathway not only delay and block the engulfment of some corpses, but also delay the degradation of engulfed apoptotic material. The same studies also demonstrate a role for CED-7 in intracellular endosome trafficking and RAB-7 enrichment on the surface of phagosomes (Yu et al., 2006; Yu et al., 2008). Thus, perhaps in *CG31731*$^{Mi\{MIC\}/Mi\{MIC\}}$ mutants, trafficking of the lysosomal machinery for acidification of the nurse cells is disrupted. Consistent with this hypothesis, ABCA1 is observed to localize to the Golgi stacks, plasma membrane, and endolysosomal vesicles (Hamon et al., 2000), dynamic compartments which are involved in both engulfment and lysosomal degradation events. How the nurse cells become acidified and subsequently degraded is currently under investigation in our lab. It would be interesting to also pursue how the lysosomal machinery is disrupted in *CG31731* mutant follicle cells. Future experiments to elucidate this question could involve

monitoring the activity of proteins involved in lysosomal acidification events, including V-ATPases, LAMP, Shibire, Rab5 and Rab7, in *CG31731*$^{Mi\{MIC\}/Mi\{MIC\}}$ egg chambers.

In *C. elegans*, CED-7 has been shown to have a role during engulfment in multiple PCD systems *in vivo*. We wondered whether *CG31731* may also be involved in other PCD systems in *Drosophila*. Conveniently, a distinct PCD modality from developmental PCD in late oogenesis can be easily induced via protein starvation in mid-oogenesis. While in late stage developmental PCD the nurse cells die via phagoptosis (Timmons et al., 2016), in mid-stage starvation-induced PCD the nurse cells die via apoptotic and autophagic cell death pathways (Jenkins et al., 2013). Engulfment of the nurse cells in both PCD systems are regulated similarly by components of the *draper* and *Ced-12* pathways (Timmons, 2015). From our studies in late oogenesis, we selected the *CG31731* mutants which exhibited the most severe phenotypes and looked for engulfment defects in mid-oogenesis. As we anticipated, mid-stage dying egg chambers from *CG31731*$^{Mi\{MIC\}/-}$ mutants exhibited engulfment defects in follicle cells that fail to enlarge normally and die prematurely, leaving behind egg chambers with unengulfed germline debris. We observed a similar phenotype when *CG31731*$^{RNAi\text{-}GD1133}$ was expressed specifically in the follicle cells, but not when *CG31731*$^{RNAi\text{-}GD1133}$ or *CG31731*$^{RNAi\text{-}HMC06027}$ was expressed specifically in the nurse cells. These observations are similar to our data in late oogenesis, in which *CG31731* appears to primarily act in the engulfing follicle cells to regulate clearance of the dying nurse cells.

Of specific personal interest is the manner by which the follicle cells disappear in engulfment defective mid-oogenesis mutants. In WT mid-stage dying egg chambers, once

the follicle cells have completed engulfment of the germline debris, they similarly lose membrane markers, display pyknotic nuclei, and eventually disappear. Over-expression of the *Drosophila* inhibitor of apoptosis (Diap1) or the p35 caspase inhibitor specifically in the follicle cells does not prevent the follicle cell nuclei from becoming pyknotic, indicating the follicle cells do not die via apoptotic mechanisms (Etchegaray et al., 2012). There is evidence to suggest that the follicle cells die via autophagic cell death pathways, for example under starved conditions, the follicle cells upregulate autophagy machinery (Barth et al., 2011). Moreover, the lack of ATG genes, including in $atg7^{d14/d77}$ mutants, results in dying egg chambers which exhibit a significant quantity of uncleared pyknotic follicle cells (unpublished observation, Jeanne Peterson). These observations suggest that the autophagic cell death pathway may have a role in the clearance of follicle cell corpses. From these pieces of data, we postulate that perhaps in starvation-induced mid-stage dying egg chambers, as a result of insufficient nutrients the follicle cells normally uptake the dying germline in an attempt to recycle its degraded material. However, in engulfment defective mutants, the follicle cells do not efficiently uptake the germline and therefore prematurely activate autonomous autophagic cell death mechanisms as an adaptive response. At this time, these hypotheses remain highly speculative. What exactly regulates the death and clearance of the follicle cells has not been well studied.

We also looked for a role for *CG31731* outside the ovary, specifically in the *Drosophila* brain where engulfing glia are responsible for neuronal corpse clearance. Our observations in $CG31731^{Mi\{MIC\}/Mi\{MIC\}}$ mutants did not observe any accumulation of uncleared neuronal corpses in the brain, suggesting CG31731 does not play a prominent

role during engulfment in the brain. We speculate that perhaps there is another *ABCA* gene that provides a *ced-7-/ABCA1*-like role in engulfing glia. Nevertheless, we are still exploring potential roles for *CG31731* in other PCD systems. Fascinatingly, *CG31731* is expressed highest in the white prepupal salivary glands (Flybase), which undergo massive cell death during development. It was found that in *E93* mutants, which exhibit salivary glands that fail to undergo PCD, *CG31731* expression is downregulated (Dutta, 2008). These pieces of information suggest a role for *CG31731* in PCD of the salivary glands, thus we are currently investigating this hypothesis.

To date, the precise molecular mechanism by which CED-7/ABCA1 promotes engulfment during PCD has yet to be determined. Several other questions, including why the catalytic function of each NBD appears to be differentially important between CED-7 and ABCA1, despite these transporters contributing homologous roles in engulfment, and how ATP is used to catalyze the conformational changes that allow transport, remain unanswered. In general, the mechanism of transport in ABC transporters is controversial. Our characterization of CG31731 provides another ABC transporter to elucidate not only the molecular mechanisms of its *C. elegans* and mammalian counterparts, CED-7/ABCA1 in engulfment, but also that of ABCA transporters in general.

In conclusion, the results and discussions outlined in this thesis provide insight into the molecular activities that occur during engulfment in PCD, with specific attention to the role of ABCA transporters. We have identified *CG31731*, a *ced-7/ABCA1*-like ABCA transporter gene that is required during engulfment in the *Drosophila* ovary. Moreover, we have evidence of some genetic redundancy with another ABCA transporter

gene, *CG1718*. To our knowledge, this is the first reporting of a role for ABCA transporters in PCD in *Drosophila*. We hope that our identification of at least one putative *ced-7/ABCA1* homolog in the *Drosophila* will advance the study to elucidate the functions and molecular mechanisms of this unique class of transporters during PCD *in vivo*.

# BIBLIOGRAPHY

Albert, M. L., Kim, J. I. and Birge, R. B. (2000). alphavbeta5 integrin recruits the CrkII-Dock180-rac1 complex for phagocytosis of apoptotic cells. *Nature Cell Biology* 2, 899–905.

Ambros, V. (2003). MicroRNA pathways in flies and worms: Growth, death, fat, stress, and timing. *Cell* 113, 673–676.

Awasaki, T., Tatsumi, R., Takahashi, K., Arai, K., Nakanishi, Y., Ueda, R. and Ito, K. (2006). Essential Role of the Apoptotic Cell Engulfment Genes draper and ced-6 in Programmed Axon Pruning during *Drosophila* Metamorphosis. *Neuron* 50, 855–867.

Bastock, R. and St Johnston, D. (2008). *Drosophila* oogenesis. *Current Biology* 18, 1082–1087.

Bellen, H. J., Levis, R. W., He, Y., Carlson, J. W., Evans-Holm, M., Bae, E., Kim, J., Metaxakis, A., Savakis, C., Schulze, K. L. et al. (2011). The *Drosophila* gene disruption project: Progress using transposons with distinctive site specificities. *Genetics* 188, 731–743.

Bellen, H. J., Levis, R. W., Liao, G., He, Y., Carlson, J. W., Tsang, G., Evans-Holm, M., Hiesinger, P. R., Schulze, K. L., Rubin, G. M. et al. (2004). The BDGP gene disruption project: Single transposon insertions associated with 40% of *Drosophila* genes. *Genetics* 167, 761–781.

Brown, G. C. and Neher, J. J. (2012). Eaten alive! Cell death by primary phagocytosis: "Phagoptosis." *Trends in Biochemical Sciences* 37, 325–332.

Brugnera, E., Haney, L., Grimsley, C., Lu, M., Walk, S. F., Tosello-Trampont, A.-C., Macara, I. G., Madhani, H., Fink, G. R. and Ravichandran, K. S. (2002). Unconventional Rac-GEF activity is mediated through the Dock180-ELMO complex. *Nature Cell Biology* 4, 574–582.

Bujold, M., Gopalakrishnan, A., Nally, E. and King-Jones, K. (2010). Nuclear receptor DHR96 acts as a sentinel for low cholesterol concentrations in *Drosophila melanogaster*. *Molecular and Cellular Biology* 30, 793–805.

Chen, Y. W., Song, S., Weng, R., Verma, P., Kugler, J. M., Buescher, M., Rouam, S. and Cohen, S. (2014). Systematic study of *Drosophila* MicroRNA functions using a collection of targeted knockout mutations. *Developmental Cell* 31, 784–800.

Chimini, G. and Chavrier, P. (2000). Function of Rho family proteins in actin dynamics during phagocytosis and engulfment. *Nature Cell Biology* 2, E191-6.

Chou, T. B. and Perrimon, N. (1996). The autosomal FLP-DFS technique for generating germline mosaics in *Drosophila melanogaster*. *Genetics* 144, 1673–1679.

Côté, J.-F., Motoyama, A. B., Bush, J. a and Vuori, K. (2005). A novel and evolutionarily conserved PtdIns(3,4,5)P3-binding domain is necessary for DOCK180 signalling. *Nature Cell Biology* 7, 797–807.

Daleke, D. L. (2003). Regulation of transbilayer plasma membrane phospholipid asymmetry. *Journal of Lipid Research* 44, 233–242.

Darland-Ransom, M., Wang, X., Sun, C., Mapes, J., Gengyo-ando, K., Mitani, S. and Xue, D. (2008). Role of *C. elegans* TAT-1 Protein in Maintaining Plasma Membrane Phosphatidylserine Asymmetry. *Science* 320(5875): 528-531.

Dermauw, W., Osborne, E. J., Clark, R. M., Grbić, M., Tirry, L. and Van Leeuwen, T. (2013). A burst of ABC genes in the genome of the polyphagous spider mite Tetranychus urticae. *BMC genomics* 14:317.

Dermauw, W. and Van Leeuwen, T. (2014). The ABC gene family in arthropods: Comparative genomics and role ininsecticide transport and resistance. *Insect Biochemistry and Molecular Biology* 45, 89–110.

Dobens, L. L. and Raftery, L. A. (2000). Integration of Epithelial Patterning and Morphogenesis in *Drosophila* Ovarian Follicle Cells. *Developmental Dynamics* 218, 80–93.

Dutta, S. (2008). Genetic regulation of autophagic cell death in *Drosophila melanogaster.*

Elliott, M. R. and Ravichandran, K. S. (2010). Clearance of apoptotic cells: Implications in health and disease. *Journal of Cell Biology* 189, 1059–1070.

Ellis, R. E., Jacobson, D. M. and Horvitz, H. R. (1991). Genes required for the engulfment of cell corpses during programmed cell death in *Caenorhabditis elegans*. *Genetics* 129, 79–94.

Etchegaray, J. I., Elguero, E. J., Tran, J. A., Sinatra, V., Feany, M. B. and McCall, K. (2016). Defective Phagocytic Corpse Processing Results in Neurodegeneration and Can Be Rescued by TORC1 Activation. *Journal of Neuroscience* 36, 3170–3183.

Etchegaray, J. I., Timmons, A. K., Klein, A. P., Pritchett, T. L., Welch, E., Meehan, T. L., Li, C. and McCall, K. (2012). Draper acts through the JNK pathway to control

synchronous engulfment of dying germline cells by follicular epithelial cells. *Development* 139, 4029–39.

Fuchs, Y. and Steller, H. (2011). Programmed cell death in animal development and disease. *Cell* 147, 742–758.

Fuchs, Y. and Steller, H. (2015). Live to die another way: modes of programmed cell death and the signals emanating from dying cells. *Nature Reviews. Molecular Cell Biology* 16, 329–344.

Fullard, J. F., Kale, A. and Baker, N. E. (2009). Clearance of apoptotic corpses. *Apoptosis* 14, 1029–1037.

Geisbrecht, E. R., Haralalka, S., Swanson, S. K., Florens, L., Washburn, M. P. and Abmayr, S. M. (2008). *Drosophila* ELMO/CED-12 interacts with Myoblast city to direct myoblast fusion and ommatidial organization. *Developmental Biology* 314, 137–149.

Gumienny, T. L., Brugnera, E., Kinchen, J. M., Haney, L. B., Nishiwaki, K., Walk, S. F., Nemergut, M. E., Macara, I. G., Francis, R., Schedl, T. et al. (2001). CED-12 / ELMO , a Novel Member of the CrkII / Dock180 / Rac Pathway , Is Required for Phagocytosis and Cell Migration. *Cell* 107, 27–41.

Hamon, Y., Broccardo, C., Chambenoit, O., Luciani, M. F., Toti, F., Chaslin, S., Freyssinet, J. M., Devaux, P. F., McNeish, J., Marguet, D. et al. (2000). ABC1 promotes engulfment of apoptotic cells and transbilayer redistribution of phosphatidylserine. *Nature Cell Biology* 2, 399–406.

Hamon, Y., Trompier, D., Ma, Z., Venegas, V., Pophillat, M., Mignotte, V., Zhou, Z. and Chimini, G. (2006). Cooperation between engulfment receptors: The case of ABCA1 and MEGF10. *PLoS One* 1(1): e120.

Hengartner, M. O. (2001). Apoptosis: Corralling the corpses. *Cell* 104, 325–328.

Hsu, T. Y. and Wu, Y. C. (2010). Engulfment of Apoptotic Cells in *C. elegans* Is Mediated by Integrin α/SRC Signaling. *Current Biology* 20, 477–486.

Jacobson, M., Weil, M. and Raff, M. (1997). Programmed cell death in animal development. *Cell* 88, 347–354.

Jenkins, V. K., Timmons, A. K. and McCall, K. (2013). Diversity of cell death pathways: Insight from the fly ovary. *Trends in Cell Biology* 23, 567–574.

Kinchen, J. M., Cabello, J., Klingele, D., Wong, K., Feichtinger, R., Schnabel, H., Schnabel, R. and Hengartner, M. O. (2005). Two pathways converge at CED-10 to mediate actin rearrangement and corpse removal in *C. elegans*. *Nature* 434, 93–99.

Kinchen, J. M. and Ravichandran, K. S. (2007). Journey to the grave: signaling events regulating removal of apoptotic cells. *Journal of Cell Science* 120, 2143–2149.

Kroemer, G., Galluzzi, L., Vandenabeele, P., Abrams, J., Alnemri, E. S., Baehrecke, E. H., Blagosklonny, M. V, El-Deiry, W. S., Golstein, P., Green, D. R. et al. (2009). Classification of cell death: recommendations of the Nomenclature Committee on Cell Death 2009. *Cell Death and Differentiation* 16, 3–11.

Kuraishi, T., Nakagawa, Y., Nagaosa, K., Hashimoto, Y., Ishimoto, T., Moki, T., Fujita, Y., Nakayama, H., Dohmae, N., Shiratsuchi, A. et al. (2009). Pretaporter, a *Drosophila* protein serving as a ligand for Draper in the phagocytosis of apoptotic cells. *EMBO Journal* 28, 3868–3878.

Kurant, E., Axelrod, S., Leaman, D. and Gaul, U. (2008). Six-Microns-Under Acts Upstream of Draper in the Glial Phagocytosis of Apoptotic Neurons. *Cell* 133, 498–509.

Lai, C. F., Chen, C. Y. and Au, L. C. (2013). Comparison between the repression potency of siRNA targeting the coding region and the 3'-untranslated region of mRNA. *BioMed Research International* 2013, 3–8.

Li, F. (2015). Characterization of ATP-binding Cassette Transporter Genes in Silkworm, Bombyx Mori. *American Journal of Bioscience and Bioengineering* 3, 123.

Liu, Q. A. and Hengartner, M. O. (1998). Candidate adaptor protein CED-6 promotes the engulfment of apoptotic cells in *C. elegans*. *Cell* 93, 961–972.

Locher, K. P. (2004). Structure and mechanism of ABC transporters. *Current Opinion in Structural Biology* 14, 426–431.

Lu, M., Kinchen, J. M., Rossman, K. L., Grimsley, C., deBakker, C., Brugnera, E., Tosello-Trampont, A.-C., Haney, L. B., Klingele, D., Sondek, J. et al. (2004). PH domain of ELMO functions in trans to regulate Rac activation via Dock180. *Nature Structural & Molecular Biology* 11, 756–762.

Lu, T.-Y., Doherty, J. and Freeman, M. R. (2014). DRK/DOS/SOS converge with Crk/Mbc/dCed-12 to activate Rac1 during glial engulfment of axonal debris. *Proceedings of the National Academy of Sciences of the United States of America* 111, 12544–9.

Lu, T.-Y., MacDonald, J. M., Neukomm, L. J., Sheehan, A. E., Bradshaw, R., Logan, M. A. and Freeman, M. R. (2017). Axon degeneration induces glial responses through Draper-TRAF4-JNK signalling. *Nature Communications* 8, 14355.

Luciani, M. F. and Chimini, G. (1996). The ATP binding cassette transporter ABC1, is required for the engulfment of corpses generated by apoptotic cell death. *The EMBO Journal* 15, 226–35.

MacDonald, J. M., Beach, M. G., Porpiglia, E., Sheehan, A. E., Watts, R. J. and Freeman, M. R. (2006). The *Drosophila* Cell Corpse Engulfment Receptor Draper Mediates Glial Clearance of Severed Axons. *Neuron* 50, 869–881.

Manaka, J., Kuraishi, T., Shiratsuchi, A., Nakai, Y., Higashida, H., Henson, P. and Nakanishi, Y. (2004). Draper-mediated and phosphatidylserine-independent phagocytosis of apoptotic cells by *Drosophila* hemocytes/macrophages. *Journal of Biological Chemistry* 279, 48466–48476.

Mangahas, P. M. and Zhou, Z. (2005). Clearance of apoptotic cells in *Caenorhabditis elegans*. *Seminars in Cell and Developmental Biology* 16, 295–306.

Mapes, J., Chen, Y. Z., Kim, A., Mitani, S., Kang, B. H. and Xue, D. (2012). CED-1, CED-7, and TTR-52 regulate surface phosphatidylserine expression on apoptotic and phagocytic cells. *Current Biology* 22, 1267–1275.

Meehan, T. L., Joudi, T. F., Timmons, A. K., Taylor, J. D., Habib, C. S., Peterson, J. S., Emmanuel, S., Franc, N. C. and McCall, K. (2016). Components of the engulfment machinery have distinct roles in corpse processing. *PLoS One* 11, 1–22.

Mizushima, N. and Komatsu, M. (2011). Autophagy: Renovation of cells and tissues. *Cell* 147, 728–741.

Nelson, C. and Baehrecke, E. H. (2014). Eaten to death. *FEBS Journal* 281, 5411–5417.

Neukomm, L. J., Nicot, A.-S., Kinchen, J. M., Almendinger, J., Pinto, S. M., Zeng, S., Doukoumetzidis, K., Tronchère, H., Payrastre, B., Laporte, J. F. et al. (2011). The phosphoinositide phosphatase MTM-1 regulates apoptotic cell corpse clearance through CED-5-CED-12 in *C. elegans*. *Development (Cambridge, England)* 138, 2003–14.

Ni, J., Zhou, R., Czech, B., Liu, L.-P., Holderbaum, L., Yang-Zhou, D., Shim, S., Handler, D., Karpowicz, P., Binari, R. et al. (2011). A genome-scale shRNA resource for transgenic RNAi in *Drosophila*. *Nature Methods* 8, 405–7.

Paredes, J. C., Herren, J. K., Sch??pfer, F. and Lemaitre, B. (2016). The role of lipid competition for endosymbiont-mediated protection against parasitoid wasps in *Drosophila*. *mBio* 7, 1–8.

Ravichandran, K. S. (2010). Find-me and eat-me signals in apoptotic cell clearance: progress and conundrums. *The Journal of Experimental Medicine* 207, 1807–1817.

Reddien, P. and Horvitz, H. (2000). CED-2/CrkII and CED-10/Rac control phagocytosis and cell migration in *Caenorhabditis elegans*. *Nature Cell Biology* 2, 131–136.

Rees, D. C., Johnson, E. and Lewinson, O. (2009). ABC transporters: the power to change. *Nature Reviews. Molecular Cell Biology* 10, 218–227.

Scheib, J. L., Sullivan, C. S. and Carter, B. D. (2012). Jedi-1 and MEGF10 signal engulfment of apoptotic neurons through the tyrosine kinase Syk. *The Journal of neuroscience : the official journal of the Society for Neuroscience* 32, 13022–31.

Stroschein-Stevenson, S. L., Foley, E., O'Farrell, P. H. and Johnson, A. D. (2006). Identification of *Drosophila* gene products required for phagocytosis of Candida albicans. *PLoS Biology* 4, 0087–0099.

Sturm, A., Cunningham, P. and Dean, M. (2009). The ABC transporter gene family of Daphnia pulex. *BMC Genomics* 10, 170.

Su, H. P., Nakada-Tsukui, K., Tosello-Trampont, A. C., Li, Y., Bu, G., Henson, P. M. and Ravichandran, K. S. (2002). Interaction of CED-6/GULP, an adapter protein involved in engulfment of apoptotic cells with CED-1 and CD91/low density lipoprotein receptor-related protein (LRP). *Journal of Biological Chemistry* 277, 11772–11779.

ter Beek, J., Guskov, A. and Slotboom, D. J. (2014). Structural diversity of ABC transporters. *The Journal of General Physiology* 143, 419–35.

Timmons, A. K., Mondragon, A. a, Schenkel, C. E., Yalonetskaya, A., Taylor, J. D., Moynihan, K. E., Etchegaray, J. I., Meehan, T. L. and McCall, K. (2016). Phagocytosis genes nonautonomously promote developmental cell death in the *Drosophila* ovary. *Proceedings of the National Academy of Sciences of the United States of America* 113, E1246-55.

Tung, T. T., Nagaosa, K., Fujita, Y., Kita, A., Mori, H., Okada, R., Nonaka, S. and Nakanishi, Y. (2013). Phosphatidylserine recognition and induction of apoptotic cell clearance by *Drosophila* engulfment receptor Draper. *Journal of Biochemistry* 153, 483–491.

Vasiliou, V., Vasiliou, K. and Nebert, D. W. (2009). Human ATP-binding cassette (ABC) transporter family. *Human Genomics* 3, 281–90.

Venken, K. J. T., Schulze, K. L., Haelterman, N. a, Pan, H., He, Y., Evans-Holm, M., Carlson, J. W., Levis, R. W., Spradling, A. C., Hoskins, R. a et al. (2011). MiMIC: a highly versatile transposon insertion resource for engineering *Drosophila melanogaster* genes. *Nature Methods* 8, 737–743.

Wang, N., Lan, D., Gerbod-Giannone, M., Linsel-Nitschke, P., Jehle, A. W., Chen, W., Martinez, L. O. and Tall, A. R. (2003). ATP-binding Cassette Transporter A7 (ABCA7) Binds Apolipoprotein A-I and Mediates Cellular Phospholipid but Not Cholesterol Efflux. *Journal of Biological Chemistry* 278, 42906–42912.

Wang, X. (2003). Cell Corpse Engulfment Mediated by *C. elegans* Phosphatidylserine Receptor Through CED-5 and CED-12. *Science* 302, 1563–1566.

Wang, X., Li, W., Zhao, D., Liu, B., Shi, Y., Chen, B., Yang, H., Guo, P., Geng, X., Shang, Z. et al. (2010). *Caenorhabditis elegans* transthyretin-like protein TTR-52 mediates recognition of apoptotic cells by the CED-1 phagocyte receptor. *Nature Cell Biology* 12, 655–64.

White, P. M., Serbus, L. R., Debec, A., Codina, A., Bray, W., Guichet, A., Lokey, R. S. and Sullivan, W. (2017). Reliance of Wolbachia on High Rates of Host Proteolysis Revealed by a Genome-Wide RNAi Screen of *Drosophila* Cells. *Genetics* 205, 1473–1488.

William S. Hummers, J. and Offeman, R. E. (1958). Preparation of Graphitic Oxide. *Journal of the American Chemical Society* 80, 1339.

Wu, X., Tanwar, P. S. and Raftery, L. A. (2008). *Drosophila* follicle cells: Morphogenesis in an eggshell. *Seminars in Cell and Developmental Biology* 19, 271–282.

Wu, Y. C. and Horvitz, H. R. (1998). The *C. elegans* cell corpse engulfment gene ced-7 encodes a protein similar to ABC transporters. *Cell* 93, 951–960.

Yu, X., Lu, N. and Zhou, Z. (2008). Phagocytic receptor CED-1 initiates a signaling pathway for degrading engulfed apoptotic cells. *PLoS Biology* 6, 0581–0600.

Yu, X., Odera, S., Chuang, C. H., Lu, N. and Zhou, Z. (2006). *C. elegans* Dynamin Mediates the Signaling of Phagocytic Receptor CED-1 for the Engulfment and Degradation of Apoptotic Cells. *Developmental Cell* 10, 743–757.

Zhou, Z., Caron, E., Hartwieg, E., Hall, A. and Horvitz, H. R. (2001). The *C. elegans* PH Domain Protein CED-12 Regulates Cytoskeletal Reorganization via a Rho/Rac GTPase Signaling Pathway. *Developmental Cell* 1, 477–489.

Zhou, Z., Hartwieg, E. and Horvitz, H. R. (2001). CED-1 is a transmembrane receptor that mediates cell corpse engulfment in *C. elegans*. *Cell* 104, 43–56.

Ziegenfuss, J. S. (2012). Eaters of the Dead: How Glial Cells Respond to and Engulf Degenerating Axons in the CNS: A Dissertation. University of Massachusetts.

Ziegenfuss, J. S., Biswas, R., Avery, M. A., Hong, K., Sheehan, A. E., Yeung, Y.-G., Stanley, E. R. and Freeman, M. R. (2008). Draper-dependent glial phagocytic activity is mediated by Src and Syk family kinase signalling. *Nature* 453, 935–9.

Ziegenfuss, J. S., Doherty, J. and Freeman, M. R. (2012). Distinct molecular pathways mediate glial activation and engulfment of axonal debris after axotomy. *Nature Neuroscience* 15, 979–987.

# CURRICULUM VITAE